



CERN-PH-EP-2014-233

Submitted to: JHEP

Measurement of the charge asymmetry in dileptonic decays of top quark pairs in pp collisions at $\sqrt{s} = 7$ TeV using the ATLAS detector

The ATLAS Collaboration

Abstract

A measurement of the top–antitop ($t\bar{t}$) charge asymmetry is presented using data corresponding to an integrated luminosity of 4.6 fb^{-1} of LHC pp collisions at a centre-of-mass energy of 7 TeV collected by the ATLAS detector. Events with two charged leptons, at least two jets and large missing transverse momentum are selected. Two observables are studied: $A_C^{\ell\ell}$ based on the identified charged leptons, and $A_C^{t\bar{t}}$, based on the reconstructed $t\bar{t}$ final state. The asymmetries are measured to be

$$A_C^{\ell\ell} = 0.024 \pm 0.015 \text{ (stat.)} \pm 0.009 \text{ (syst.)},$$

$$A_C^{t\bar{t}} = 0.021 \pm 0.025 \text{ (stat.)} \pm 0.017 \text{ (syst.)}.$$

The measured values are in agreement with the Standard Model predictions.

Measurement of the charge asymmetry in dileptonic decays of top quark pairs in pp collisions at $\sqrt{s} = 7$ TeV using the ATLAS detector

The ATLAS collaboration

ABSTRACT: A measurement of the top–antitop ($t\bar{t}$) charge asymmetry is presented using data corresponding to an integrated luminosity of 4.6 fb^{-1} of LHC pp collisions at a centre-of-mass energy of 7 TeV collected by the ATLAS detector. Events with two charged leptons, at least two jets and large missing transverse momentum are selected. Two observables are studied: $A_C^{\ell\ell}$ based on the identified charged leptons, and $A_C^{t\bar{t}}$, based on the reconstructed $t\bar{t}$ final state. The asymmetries are measured to be

$$A_C^{\ell\ell} = 0.024 \pm 0.015 \text{ (stat.)} \pm 0.009 \text{ (syst.)},$$

$$A_C^{t\bar{t}} = 0.021 \pm 0.025 \text{ (stat.)} \pm 0.017 \text{ (syst.)}.$$

The measured values are in agreement with the Standard Model predictions.

Contents

1	Introduction	1
2	The ATLAS detector	3
3	Simulated samples	4
4	Object and event selection	5
5	Kinematic reconstruction	7
6	Corrections	14
6.1	Correction of the lepton-based asymmetry	14
6.2	Unfolding of the $t\bar{t}$ asymmetry	15
7	Systematic uncertainties	17
8	Results	20
9	Conclusion	24
A	Additional tables	32

1 Introduction

The top quark is the heaviest elementary particle known to date. It was discovered in 1995 at the Tevatron proton–antiproton ($p\bar{p}$) collider by the CDF and D0 collaborations [1, 2]. It is the only quark in the Standard Model (SM) that decays before hadronization occurs, and the only quark with Yukawa coupling to the Higgs boson close to unity. A precise study of top quark properties could shed light on possible physics models beyond the SM [3–9].

This analysis uses a data set corresponding to an integrated luminosity of 4.6 fb^{-1} of Large Hadron Collider (LHC) proton–proton (pp) collisions at a centre-of-mass energy of 7 TeV collected by the ATLAS detector. It is performed in the dilepton channel of the $t\bar{t}$ pair decay, realized when both W bosons decay to a charged lepton and a neutrino. The measured observables are the lepton-based charge asymmetry $A_C^{\ell\ell}$ and the $t\bar{t}$ charge asymmetry $A_C^{t\bar{t}}$. The observable $A_C^{\ell\ell}$ is defined as an asymmetry between positively and negatively charged leptons (electrons and muons) in the dilepton decays of the $t\bar{t}$ pairs,

$$A_C^{\ell\ell} = \frac{N(\Delta|\eta| > 0) - N(\Delta|\eta| < 0)}{N(\Delta|\eta| > 0) + N(\Delta|\eta| < 0)}, \quad (1.1)$$

where

$$\Delta|\eta| = |\eta_{\ell+}| - |\eta_{\ell-}|, \quad (1.2)$$

$\eta_{\ell+}$ ($\eta_{\ell-}$) is the pseudorapidity¹ of the positively (negatively) charged lepton and N is the number of events with positive or negative $\Delta|\eta|$. While $A_C^{\ell\ell}$ is defined in eq. (1.1) as an asymmetry between positively and negatively charged lepton pseudorapidities, $A_C^{t\bar{t}}$ corresponds to the asymmetry in top quark and antitop quark rapidities²,

$$A_C^{t\bar{t}} = \frac{N(\Delta|y| > 0) - N(\Delta|y| < 0)}{N(\Delta|y| > 0) + N(\Delta|y| < 0)}, \quad (1.3)$$

where

$$\Delta|y| = |y_t| - |y_{\bar{t}}|, \quad (1.4)$$

y_t ($y_{\bar{t}}$) is the rapidity of the top (antitop) quark, and N is the number of events with positive or negative $\Delta|y|$.

In SM $t\bar{t}$ production, the asymmetry is absent at leading-order (LO) in Quantum Chromodynamics (QCD) and is introduced by the next-to-leading-order (NLO) QCD contributions to the $t\bar{t}$ differential cross-sections, which are odd with respect to the exchange of t and \bar{t} . At the LHC, the contributions to the asymmetries defined in eq. (1.1) and eq. (1.3) are predominantly from $q\bar{q}$ -initiated $t\bar{t}$ production, and gg -initiated production also has a non-negligible contribution. The gg -initiated processes are symmetric [10]. The asymmetry predicted in the SM is slightly positive, implying that the top quark is preferentially emitted in the direction of the quark in the initial state. In $q\bar{q}$ interactions at the LHC, the quark is in most cases a valence quark whereas the antiquark is from the sea. The asymmetry translates to a higher boost along the beam direction for the t -quark than for the \bar{t} -quark. The rapidity distribution of the t is thus slightly broader than the one of the \bar{t} .

The SM predictions of $A_C^{t\bar{t}}$ and $A_C^{\ell\ell}$ computed at NLO in QCD and including electroweak corrections (NLO QCD+EW) are [10]

$$A_C^{t\bar{t}} = 0.0123 \pm 0.0005 \text{ (scale)}, \quad (1.5)$$

$$A_C^{\ell\ell} = 0.0070 \pm 0.0003 \text{ (scale)}. \quad (1.6)$$

These asymmetries are evaluated without acceptance cuts. The uncertainties are due to scale variations, estimated by simultaneous variation of the renormalization and factorization scale by a factor of half or two with respect to the reference scale value, which is set to the top quark mass. Recent next-to-next-to-leading order (NNLO) calculations of the forward-backward asymmetry for the Tevatron suggest that varying these scales significantly underestimates the uncertainty due to higher order corrections [11], but no NNLO calculation has yet been published for pp interactions at the LHC energies. There is however a recent calculation obtained with the Principle of Maximum Conformality [12] which gives a consistent value of $A_C^{t\bar{t}} = 0.0115_{-0.0003}^{+0.0001}$ (scale). The predicted value of $A_C^{\ell\ell}$ is smaller than

¹The pseudorapidity is defined in terms of the polar angle θ as $\eta = -\ln \tan(\theta/2)$.

²The rapidity is defined as $y = \frac{1}{2} \ln \frac{E+p_z}{E-p_z}$ where E is the energy of the particle and p_z is the component of the momentum along the LHC beam axis.

the prediction for $A_{\text{C}}^{t\bar{t}}$, since the directions of the leptons do not fully follow the direction of the parent t and \bar{t} quarks. However, $A_{\text{C}}^{\ell\ell}$ can be measured more precisely, since it is determined without the need for a full reconstruction of t and \bar{t} kinematics, which involves the use of jets and missing transverse momentum that are reconstructed with less precision than the kinematic variables of the leptons. The values of $A_{\text{C}}^{\ell\ell}$ and $A_{\text{C}}^{t\bar{t}}$ as well as their correlation can be sensitive to new physics arising in top quark pair production [13–17].

The asymmetry $A_{\text{C}}^{t\bar{t}}$ has been measured in the single-lepton decay channel by the ATLAS [18] and CMS [19] collaborations at $\sqrt{s} = 7$ TeV. The CMS collaboration has reported measurements of $A_{\text{C}}^{\ell\ell}$ and $A_{\text{C}}^{t\bar{t}}$ in the dilepton decay channel at $\sqrt{s} = 7$ TeV [20]. The measured asymmetry values as well as those from a combination of ATLAS and CMS $A_{\text{C}}^{t\bar{t}}$ results in the single-lepton decay channel [21] are consistent with the SM predictions.

At the Tevatron collider, $t\bar{t}$ production has a forward-backward asymmetry with respect to the direction of the proton and antiproton beams. The asymmetry based on t and \bar{t} quarks, $A_{\text{FB}}^{t\bar{t}}$, is defined as

$$A_{\text{FB}}^{t\bar{t}} = \frac{N(\Delta y > 0) - N(\Delta y < 0)}{N(\Delta y > 0) + N(\Delta y < 0)}, \quad (1.7)$$

where

$$\Delta y = y_t - y_{\bar{t}}, \quad (1.8)$$

y_t ($y_{\bar{t}}$) is the rapidity of the t (\bar{t}) quark and N is the number of events with positive or negative Δy . An analogously defined lepton-based forward-backward asymmetry in $t\bar{t}$ production has been studied as well. At the Tevatron, $t\bar{t}$ events are predominantly produced by $q\bar{q}$ annihilation, thus the predicted asymmetries are typically larger than at the LHC, where gg -initiated production dominates. The Tevatron experiments have reported deviations of forward-backward asymmetries from the SM predictions [22, 23], which have motivated a number of further asymmetry measurements. Comparing the results with the latest NNLO calculations available at the Tevatron [11], the deviations reported by the CDF collaboration [24–26] are reduced, while the latest measurements by the D0 collaboration [27, 28] are now in good agreement with the predictions.

This paper is organized as follows. In section 2 the main components of the ATLAS detector relevant for this measurement are summarized. In section 3 the simulated samples used for the analysis are presented. In section 4 the object and event selection are described. In section 5 the kinematic reconstruction used for the $A_{\text{C}}^{t\bar{t}}$ measurement is detailed. For comparison with theory prediction, the measurements are corrected for detector resolution and acceptance effects, as presented in section 6. Sections 7 and 8 describe the systematic uncertainties and the measurement results, respectively. Finally, the conclusions are given in section 9.

2 The ATLAS detector

The ATLAS detector [29] at the LHC covers nearly the entire solid angle around the collision point.³ It consists of an inner tracking detector surrounded by a thin superconducting

³ATLAS uses a right-handed coordinate system with its origin at the nominal interaction point (IP) in the centre of the detector and the z -axis along the beam pipe. The x -axis points from the IP to the centre

solenoid, electromagnetic and hadronic calorimeters, and a muon spectrometer incorporating three large superconducting toroid magnets. The inner-detector system is immersed in a 2 T axial magnetic field and provides charged-particle-tracking in the range $|\eta| < 2.5$.

A high-granularity silicon pixel detector covers the interaction region and typically provides three measurements per track. It is surrounded by a silicon microstrip tracker designed to provide four two-dimensional measurement points per track. These silicon detectors are complemented by a transition radiation tracker, which enables radially extended track reconstruction up to $|\eta| = 2.0$. The transition radiation tracker also provides electron identification information based on the fraction of hits (typically 30 in total) exceeding an energy-deposit threshold corresponding to transition radiation.

The calorimeter system covers the pseudorapidity range $|\eta| < 4.9$. Within the region $|\eta| < 3.2$, electromagnetic calorimetry is provided by barrel and end-cap high-granularity lead/liquid-argon (LAr) electromagnetic calorimeters, with an additional thin LAr presampler covering $|\eta| < 1.8$ to correct for energy loss in the material upstream of the calorimeters. Hadronic calorimetry is provided by a steel/scintillator-tile calorimeter, segmented into three barrel structures within $|\eta| < 1.7$, and two copper/LAr hadronic endcap calorimeters. The solid angle coverage is completed with forward copper/LAr and tungsten/LAr calorimeters used for electromagnetic and hadronic measurements.

The muon spectrometer comprises separate trigger and high-precision tracking chambers measuring the deflection of muons in a magnetic field generated by superconducting air-core toroids. The precision chamber system covers the region $|\eta| < 2.7$ with three layers of monitored drift tube chambers, complemented by cathode strip chambers in the forward region. The muon trigger system covers the range $|\eta| < 2.4$ with resistive plate chambers in the barrel, and thin gap chambers in the endcap regions.

A three-level trigger system is used to select interesting events. The Level-1 trigger is implemented in hardware and uses a subset of detector information to reduce the event rate to a design value of at most 75 kHz. This is followed by two software-based trigger levels, which together reduce the event rate to about 300 Hz.

3 Simulated samples

Several Monte Carlo (MC) simulated samples are used in the analysis to model the signal and background processes. The total background, estimated partly from these simulated samples, is subtracted from the data at a later stage of the analysis. The signal sample is used to correct the background subtracted data for detector, resolution and acceptance effects. The MC samples are also used to evaluate the systematic uncertainties of the measurement.

The nominal simulated $t\bar{t}$ sample is generated using the POWHEG-hvq [30–32] (patch4) generator with the CT10 [33] parton distribution function (PDF) set. The NLO QCD matrix element is used for the $t\bar{t}$ hard-scattering process. The parton showers (PS) and the underlying event are simulated using PYTHIA6 [34] (v6.425) with the CTEQ6L1 [35] PDF

of the LHC ring, and the y -axis points upward. Cylindrical coordinates (r, ϕ) are used in the transverse plane, ϕ being the azimuthal angle around the beam pipe.

and the corresponding Perugia 2011C set of tunable parameters (tune) [36] intended to be used with this PDF. The hard-scattering process renormalization and factorization scales are fixed at the generator default value Q that is defined by

$$Q = \sqrt{m_t^2 + p_T^2}, \quad (3.1)$$

where m_t and p_T are the top quark mass and the top quark transverse momentum, evaluated for the underlying Born configuration (i.e. before radiation). Additional $t\bar{t}$ samples used to evaluate signal modelling uncertainties are described in section 7. Signal samples are normalized to a reference value of $\sigma_{t\bar{t}} = 177_{-11}^{+10}$ pb for a top quark mass of $m_t = 172.5$ GeV. The cross-section has been calculated at next-to-next-to-leading-order (NNLO) in QCD including resummation of next-to-next-to-leading logarithmic (NNLL) soft gluon terms [37–42] with top++2.0 [43]. The PDF and strong coupling (α_s) uncertainties were calculated using the PDF4LHC prescription [44] with the MSTW2008 68% CL NNLO [45, 46], CT10 NNLO [33, 47] and NNPDF2.3 5f FFN [48] PDF sets, and added in quadrature to the scale uncertainty. The NNLO+NNLL cross-section value is about 3% larger than the exact NNLO prediction, as implemented in Hathor 1.5 [49].

The MC generators which are utilized to estimate the backgrounds are as follows. Single-top processes in the Wt channel are generated with the MC@NLO event generator (v4.01) [50, 51] with the CT10 PDF. The parton showers, hadronization and the underlying event are modelled using the HERWIG (v6.520) [52, 53] and JIMMY (v4.31) [54] generators. The CT10 PDF with the corresponding ATLAS AUET2 tune [55] is used for parton shower and hadronization settings. For Z/γ^* +jets and diboson events (WW , WZ and ZZ), ALPGEN (v2.13) [56] interfaced to HERWIG and JIMMY is used. The CTEQ6L1 PDF and the corresponding ATLAS AUET2 tune is used for the matrix element and parton shower settings. The Wt background process is normalized to the reference NLO+NNLL QCD [57] prediction. Diboson production is normalized to the reference NLO QCD prediction obtained using MCFM [58] and MC@NLO generators with the MSTW2008 NLO PDF [45]. The $Z/\gamma^* \rightarrow ee/\mu\mu$ +jets cross-section is normalized using a control region in data as detailed in section 4. The $Z/\gamma^* \rightarrow \tau\tau$ +jets events are normalized to a NNLO reference cross-section using the FEWZ [59] and ZWPROD [60] programs with the MSTW2008 NNLO PDF.

To realistically model the data, the simulated samples are generated with an average of eight additional inelastic pp interactions from the same bunch crossing (referred to as pileup) overlaid on the hard-scatter event. Simulated samples are processed through ATLAS detector simulation. For the majority of the samples, a full detector simulation [61] based on GEANT4 [62] is used. Some of the samples used for assessment of generator modelling uncertainties are obtained using a faster detector simulation program that relies on parameterized showers in the calorimeters [61, 63]. Simulated events are then processed using the same reconstruction algorithms and analysis chain as the data.

4 Object and event selection

The data sample collected by the ATLAS detector in 2011 at a centre-of-mass energy of 7 TeV is used for the analysis. The integrated luminosity of the sample is 4.6 fb^{-1} with an

overall uncertainty of 1.8% [64]. The analysis makes use of reconstructed electrons, muons, jets and missing transverse momentum in the detector. Electrons are reconstructed as clusters of energy deposits in the electromagnetic calorimeter, matched to a track in the inner detector. They are required to pass a set of tight selection criteria [65]. The selected electrons have to satisfy a requirement on their transverse energy (E_T) and the pseudorapidity of the associated calorimeter cluster ($|\eta_{\text{cluster}}|$): $E_T > 25 \text{ GeV}$ and $|\eta_{\text{cluster}}| < 2.47$. The electrons in the region $1.37 < |\eta_{\text{cluster}}| < 1.52$, which corresponds to a transition between the barrel and endcap electromagnetic calorimeters, are excluded. Electrons are required to be isolated, using the requirements described as follows (excluding calorimeter deposits and tracks from the electrons). The E_T within a cone of size $\Delta R = \sqrt{(\Delta\eta)^2 + (\Delta\phi)^2} = 0.2$ and the scalar sum of track p_T within a cone of $\Delta R = 0.3$ around the electron are required to be below E_T - and η -dependent thresholds. The efficiency of this isolation requirement on electrons is 90%, and its goal is to reduce the contribution from hadrons mimicking lepton signatures, as well as leptons produced in heavy-hadron decays or photon conversion. These are referred to as fake and non-prompt leptons (NP) in the following.

Muons are reconstructed by matching a track in the inner detector to a track segment in the muon spectrometer. They are required to pass tight selections [66]. The selected muons are required to have $p_T > 20 \text{ GeV}$ and $|\eta| < 2.5$. To reject fake and non-prompt muons, the following isolation requirements are imposed: the calorimeter transverse energy within a cone of $\Delta R = 0.2$ around the muon is required to be less than 4 GeV and the scalar sum of track p_T within a cone of $\Delta R = 0.3$ is required to be less than 2.5 GeV (excluding the calorimeter deposits and tracks from the muons).

Jets are reconstructed from energy deposits in the calorimeter, using the anti- k_t algorithm with a distance parameter $R = 0.4$ [67]. The energy of the input clusters [68] is corrected to the level of stable particles using calibration factors derived from simulation and data [69]. The jets are required to have a p_T of at least 25 GeV and $|\eta| < 2.5$. To suppress the contribution from low- p_T jets originating from pileup interactions, tracks associated with the jet and emerging from the primary vertex are required to account for at least 75% of the scalar sum of the p_T of all tracks associated with the jet. A primary vertex, originating from pp interactions, is a reconstructed vertex required to have at least five associated tracks with $p_T > 0.4 \text{ GeV}$. In the cases where more than one primary vertex is reconstructed, the vertex with the highest $\sum_{\text{trk}} p_T^2$ is chosen and assumed to be associated with the hard-process, and the sum runs over all associated tracks.

The missing transverse momentum (E_T^{miss}) is a measure of transverse momentum imbalance due to the presence of neutrinos. It is reconstructed from the transverse momenta of jets in the kinematic range of $p_T > 20 \text{ GeV}$ and $|\eta| < 4.5$, electrons, muons, and calorimeter clusters not associated with any of the reconstructed objects, as detailed in ref. [70].

Using the objects reconstructed as above, an event selection optimized for signatures corresponding to $t\bar{t}$ events in which both W bosons from the t and \bar{t} quarks decay to leptons is performed. Events are required to have been selected by a single-electron trigger with a threshold of 20 or 22 GeV (depending on the data-taking period), or a single-muon trigger with a threshold of 18 GeV. They are required to have exactly two isolated, oppositely charged, leptons. Depending on the lepton flavours, the sample is divided into three analysis

channels referred to as ee , $e\mu$ and $\mu\mu$. To reduce the Drell–Yan production of Z/γ^* +jets background, the invariant mass of the two leptons ($m_{\ell\ell}$) is required to be above a threshold used to suppress $\gamma^* \rightarrow \ell\ell$ production background and outside a Z boson mass window in the ee and $\mu\mu$ channel events. The following requirements are used: $m_{\ell\ell} > 15$ GeV and $|m_{\ell\ell} - m_Z| > 10$ GeV. In the ee and $\mu\mu$ channels the Drell–Yan and diboson backgrounds are further reduced using a requirement on the missing transverse momentum, $E_T^{\text{miss}} > 60$ GeV. In the $e\mu$ channel the Z/γ^* +jets background is smaller and suppressed by requiring the scalar sum of the p_T of the two leading jets and leptons (H_T) to be larger than 130 GeV.

The background contributions are estimated using a combination of techniques using data and Monte Carlo events. In the case of single-top and diboson processes, both the shape and normalization of the distributions are taken from the simulation. For $Z/\gamma^* \rightarrow ee/\mu\mu$ +jets events, simulated MC events are used to model the shape of the distributions, but a data control region is used for normalization. Drell–Yan events with $E_T^{\text{miss}} > 60$ GeV are affected by energy mismeasurements, that are difficult to model in simulation. A control region with events with $m_{\ell\ell}$ in the Z -mass region is defined to study the effect of mismeasured E_T^{miss} . The relative E_T^{miss} , defined as the projection of the missing transverse momentum onto the direction of the jet or charged lepton with closest ϕ , is used to identify the events with mismeasured objects. Events with energy mismeasurements are characterized by high values of relative E_T^{miss} . A cut is applied to the relative E_T^{miss} , and data and simulation are then compared to derive a normalization correction factor which is applied to the simulated sample. The $Z/\gamma^* \rightarrow \tau\tau$ contribution is estimated from MC simulation. The background stemming from events with at least one non-prompt or fake lepton is estimated from the data, since the lepton misidentification rates are difficult to model in MC simulation. A matrix method technique is used [71]. It consists of selecting data samples dominated either by real leptons or by fake leptons, and estimating the efficiencies for a real or fake lepton to satisfy the isolation criteria.

After the final selection, the data sample contains more than 8000 events, with an expected signal-to-background ratio of approximately six. The number of events in data and simulation, including statistical and systematic uncertainties, are compared in table 1. After selection, the largest number of events is observed in the $e\mu$ channel, which has the highest branching ratio and the loosest background suppression cuts. The ee channel has the lowest number of events because of the stringent requirements on lepton kinematics. Figure 1 shows good agreement between the data and the SM predictions for the jet multiplicity, lepton p_T and lepton pseudorapidity distributions. The $\Delta|\eta|$ distributions are shown in figure 2 for the three channels separately.

5 Kinematic reconstruction

For the measurement of the $t\bar{t}$ charge asymmetry, the direction of the top and antitop quarks needs to be determined. The four-momenta of top quarks in selected events are computed with a kinematic reconstruction using the objects observed in the detector. The reconstruction is based on solving the kinematic equations obtained when imposing energy–momentum conservation at each of the decay vertices of the process. In the dilepton channel, at least

Channel	ee			$e\mu$			$\mu\mu$		
$t\bar{t}$	621	± 5	± 59	4670	± 10	± 325	1780	± 10	± 120
Single top	31.6	± 1.7	± 3.8	230	± 5	± 21	83.9	± 2.7	± 8.3
Diboson	22.8	± 0.9	± 2.6	177	± 3	± 16	61.5	± 1.5	± 6.1
$Z \rightarrow ee$ (DD)	20.8	± 1.7	± 1.4	—			—		
$Z \rightarrow \mu\mu$ (DD)	—			2.1	± 0.5	± 0.7	77	± 4	± 12
$Z \rightarrow \tau\tau$	18.6	± 1.8	± 7.0	170	± 6	± 60	67	± 4	± 25
NP & fake (DD)	19	± 4	± 19	99	± 10	± 63	26.8	± 5.1	± 1.9
Total expected	734	± 8	± 63	5350	± 20	± 340	2100	± 10	± 130
Data	740			5328			2057		

Table 1: Observed number of data events in comparison to the expected number of signal events and all relevant background contributions after the event selection. The backgrounds are estimated from the MC simulation or from the data-driven methods (DD) described in section 4. Events with one or more non-prompt or fake leptons are referred to as "NP & fake". The first uncertainty is statistical, the second corresponds to systematic uncertainties on background normalization and detector modelling described in section 7. The values labeled with "—" are estimated to be smaller than 0.5.

two neutrinos are produced and escape undetected. Consequently, the system is underconstrained and its kinematics cannot be fully determined without further assumptions (for example on the W boson and top quark masses, and the pseudorapidities of the neutrinos from the W boson decays). Moreover, several ambiguities have to be resolved to find the correct solution. For example, the lepton and jet from the same decay chain have to be associated. In an event with two leptons and two jets, this leads to two possible associations. In this analysis, the neutrino weighting technique [72] is used. This procedure steps through different hypotheses for the pseudorapidity of the two neutrinos in the final state. These hypotheses are made independently for the two neutrinos. For each hypothesis, the algorithm calculates the full event kinematics, assuming the W boson and the top quark masses. It then assigns a weight to the resulting solution based on the level of agreement between the calculated and measured missing transverse momentum. The weight is defined as

$$w = \prod_{d=x,y} \exp \left(\frac{-(E_d^{\text{miss,calc}} - E_d^{\text{miss,obs}})^2}{2(\sigma_{E_T^{\text{miss}}})^2} \right), \quad (5.1)$$

with $E_d^{\text{miss,obs}}$ being the projection of the measured missing transverse momentum along the axes defining the transverse plane ($d = x, y$) and $E_d^{\text{miss,calc}}$ the projection calculated with the assumed η values of the neutrino pair. The resolution on the missing transverse momentum is denoted $\sigma_{E_T^{\text{miss}}}$, and defined as $\sigma_{E_T^{\text{miss}}} = 0.5\sqrt{\sum E_T}$ GeV [70]. The total transverse energy, $\sum E_T$ is defined as $\sum E_T = \sum_{i=1}^{N_{\text{cell}}} E_i \sin \theta_i$ where E_i and θ_i are the energy and the polar angle of calorimeter cells associated with clusters. All possible lepton–jet associations are considered and jet energy mismeasurements are accounted for by random shifts of the jet energies within their resolutions. The solution corresponding to the maximum weight is

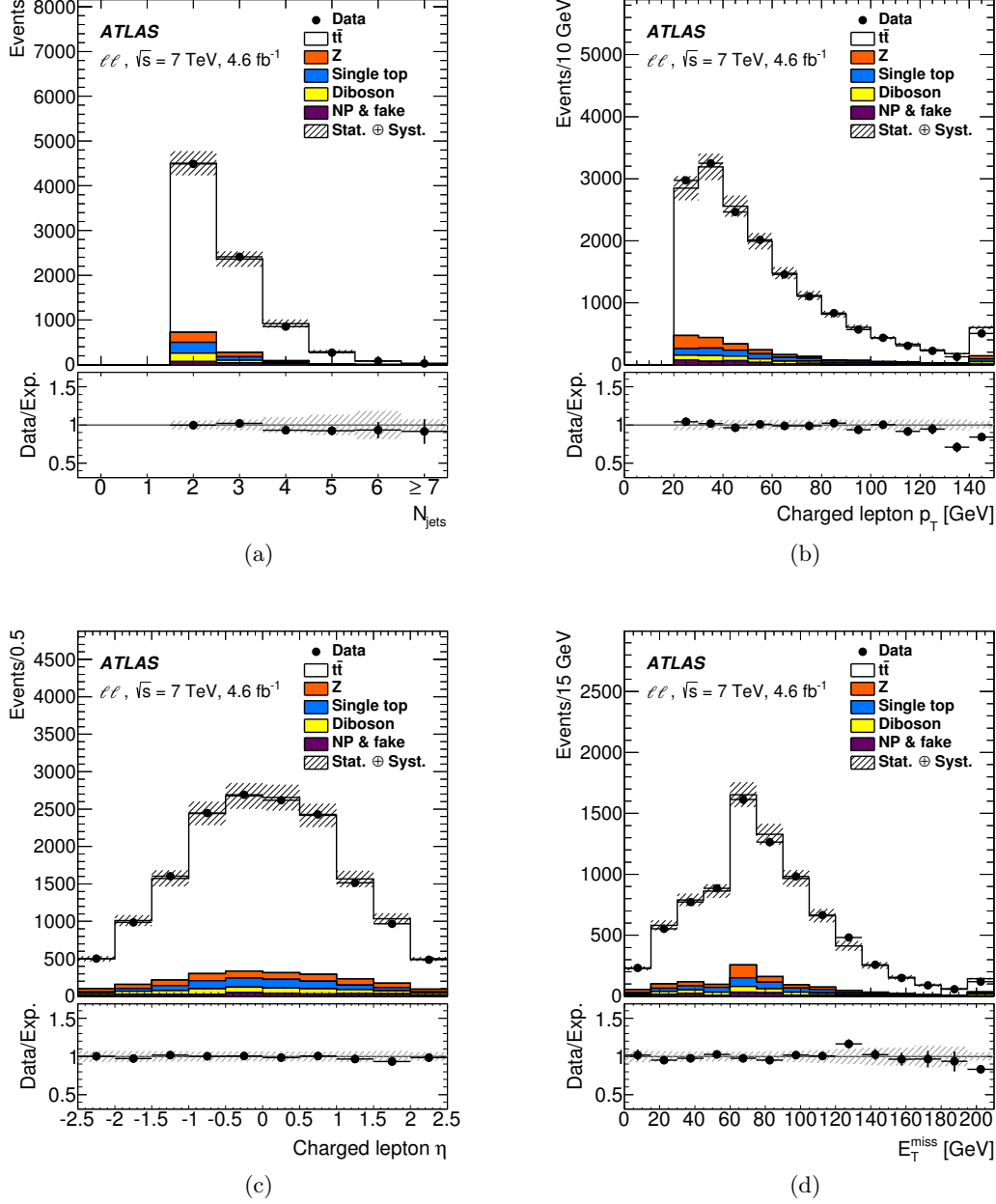


Figure 1: Comparison of the expected and observed distributions of (a) the jet multiplicity, (b) the lepton transverse momentum p_T , (c) the lepton pseudorapidity η and (d) the missing transverse momentum E_T^{miss} , shown for the combined ee , $e\mu$ and $\mu\mu$ channels. Events beyond the range of the horizontal axis of (a), (b) and (d) are included in the last bin. The hatched area corresponds to the combined statistical and systematic uncertainties. Events with one or more non-prompt or fake leptons are referred to as "NP & fake".

selected to represent the event.

As a result of the scan over neutrino pseudorapidities and jet energy values, the recon-

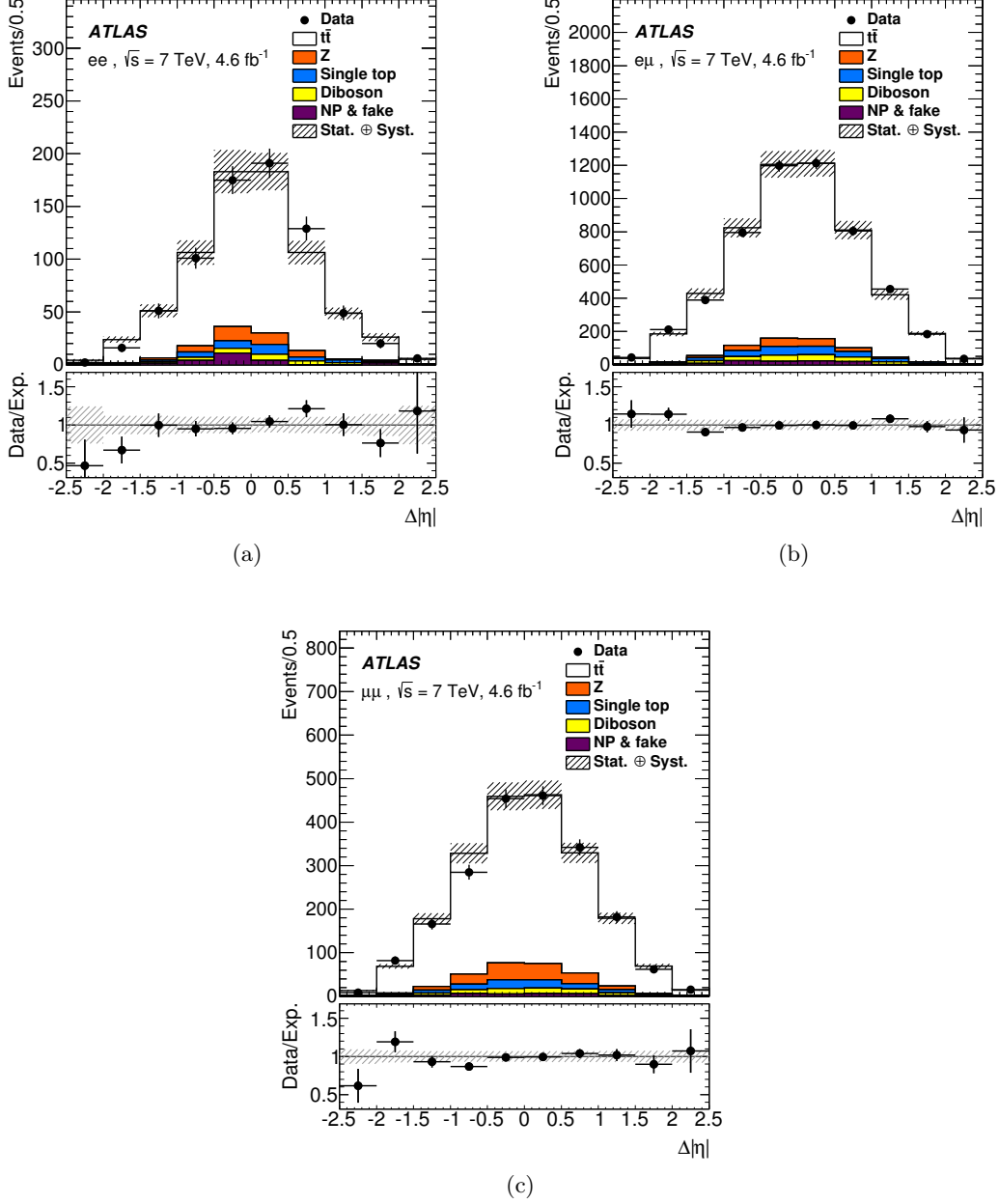


Figure 2: Comparison of the expected and observed distributions of the $\Delta|\eta|$ variable for the (a) ee , (b) $e\mu$ and (c) $\mu\mu$ channels. The hatched area corresponds to the combined statistical and systematic uncertainties. Events with one or more non-prompt or fake leptons are referred to as "NP & fake".

reconstruction efficiency, corresponding to the fraction of events in which solutions for t and \bar{t} four-momenta are found, is estimated to be about 80% in the data. In the other 20% of events, no solution to the system of the kinematic equations could be found, and the events are not used for the measurement of $A_C^{t\bar{t}}$. The performance of the reconstruction algorithm

for key variables, such as the top quark rapidities and $\Delta|y|$, is evaluated using the nominal $t\bar{t}$ simulated sample. The fraction of reconstructed MC events where the sign of $\Delta|y|$ is determined correctly is about 70%. In the simulated samples, the correct combination of the charged leptons and two jets from $b(\bar{b})$ -quarks is found in approximately 80% of the events with exactly two reconstructed jets, both of which are matched to the $b(\bar{b})$ -quarks. In case all events passing the event selection are considered, the correct combination is found in approximately 47% of the events.

In figure 3 the distributions of the top quark transverse momentum, top quark rapidity and the $t\bar{t}$ invariant mass are shown for the combined ee , $e\mu$ and $\mu\mu$ channels. In figure 4 the $\Delta|y|$ distribution is shown separately for each of the ee , $e\mu$ and $\mu\mu$ channels. Good agreement between the observed and expected distributions is found.

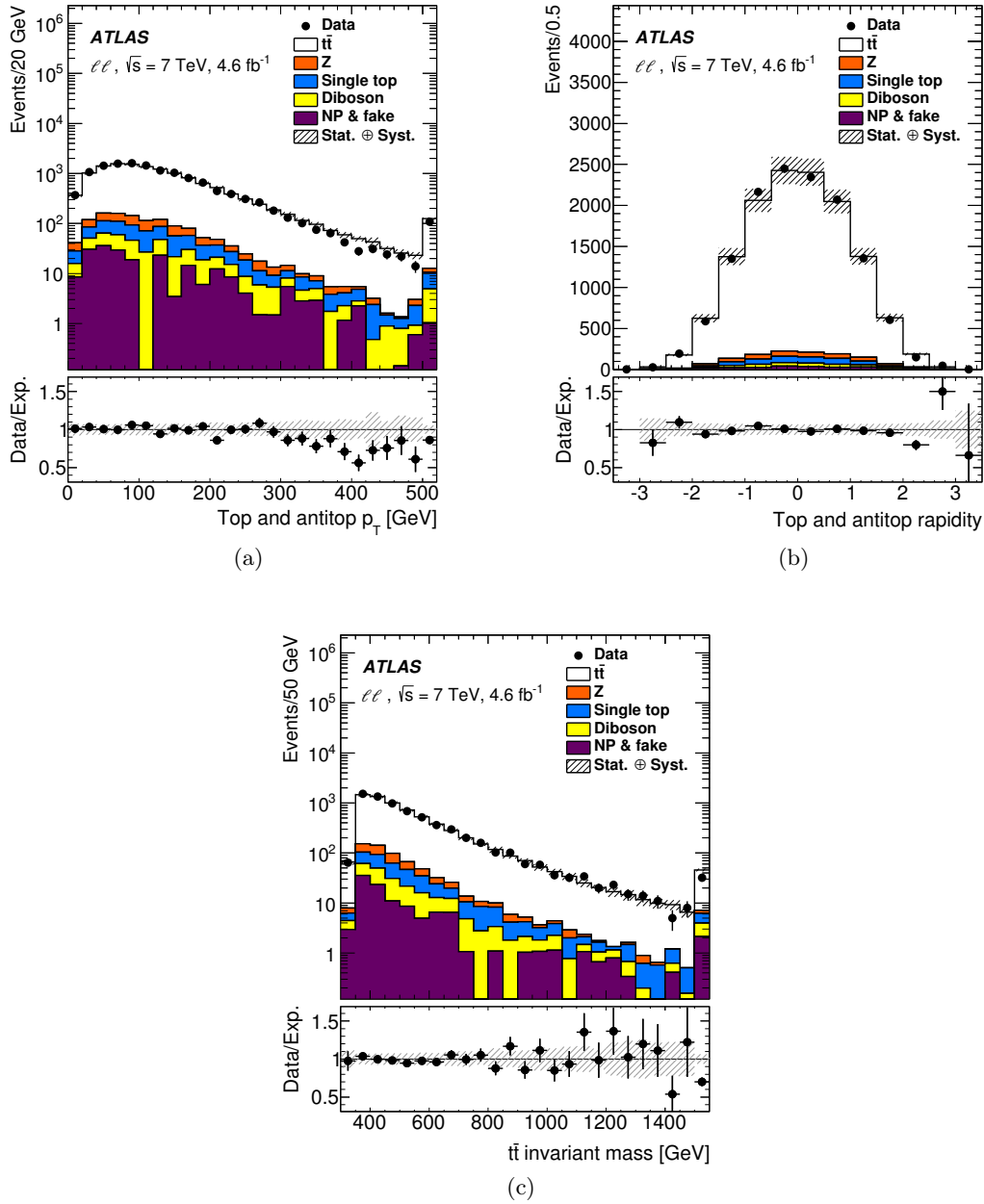


Figure 3: Comparison of the expected and observed distributions of (a) the top and antitop quark transverse momentum p_T , (b) top and antitop quark rapidity and (c) the $t\bar{t}$ invariant mass, shown for the combined ee , $e\mu$ and $\mu\mu$ channels. The hatched area corresponds to the combined statistical and systematic uncertainties. Events with one or more non-prompt or fake leptons are referred to as "NP & fake".

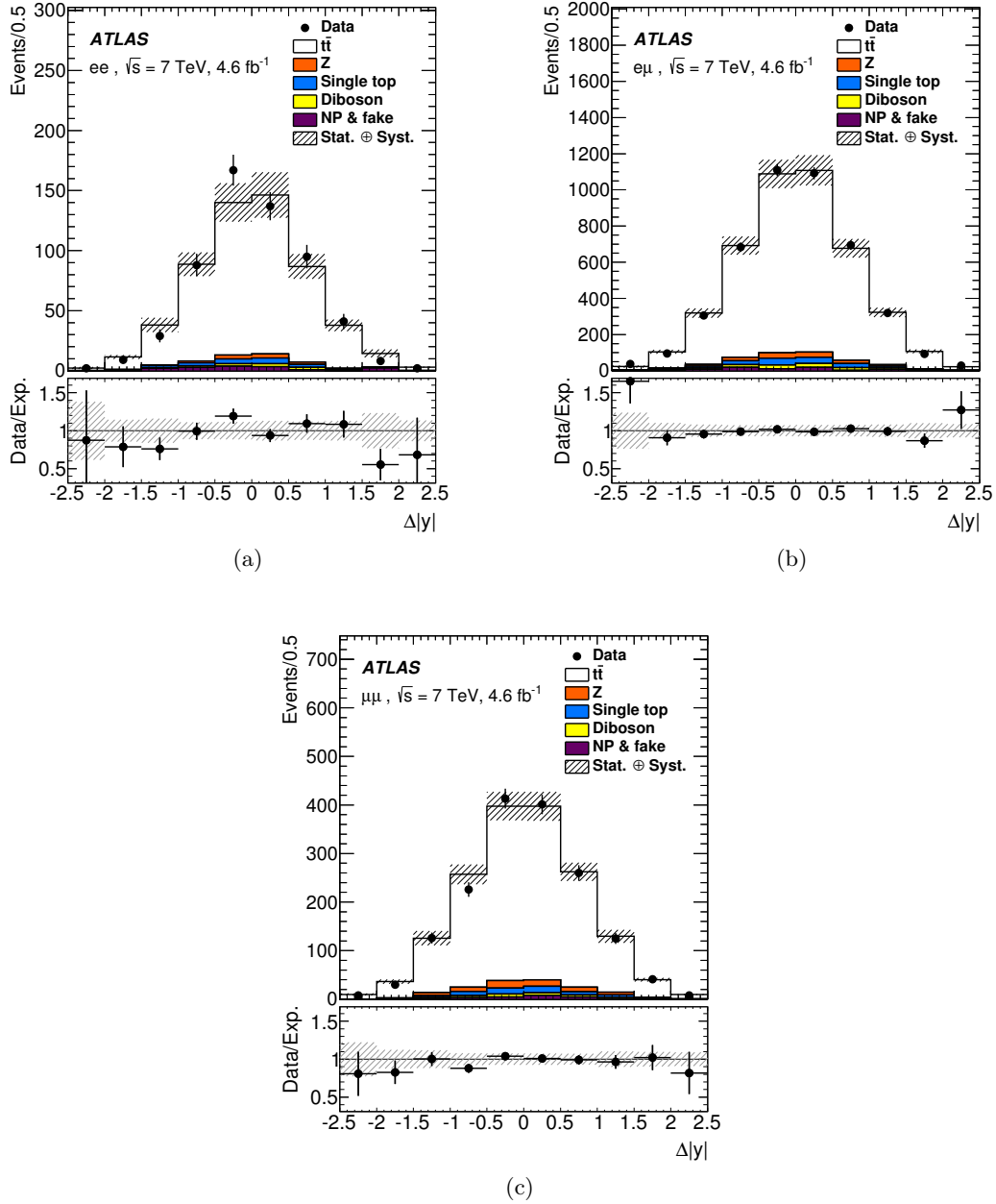


Figure 4: Comparison of the expected and observed distributions of the $\Delta|y|$ variable for the (a) ee , (b) $e\mu$ and (c) $\mu\mu$ channels. The hatched area corresponds to the combined statistical and systematic uncertainties. Events with one or more non-prompt or fake leptons are referred to as "NP & fake".

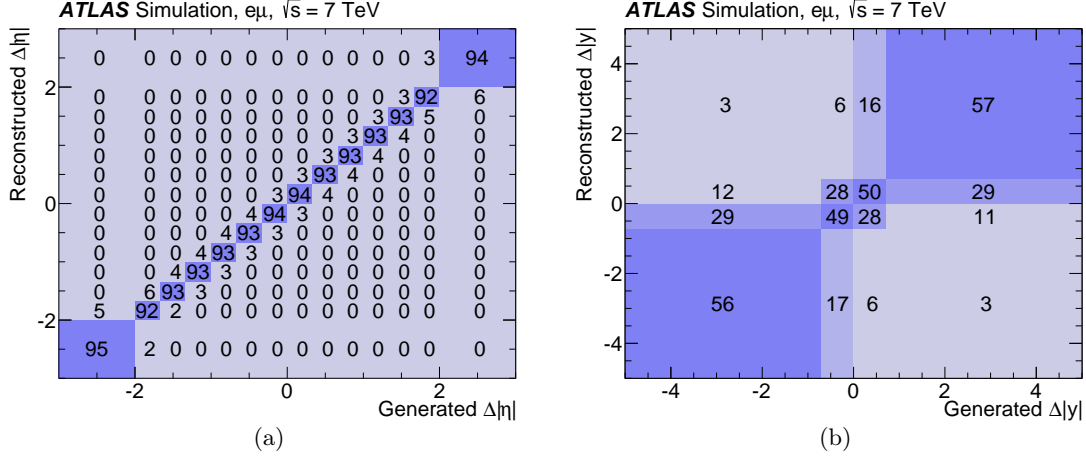


Figure 5: Response matrices for (a) the lepton $\Delta|\eta|$ and (b) $t\bar{t}$ $\Delta|y|$ observables in the $e\mu$ channel. Each column of the matrices is normalized to unity and values are reported as percentage (%) units. Values smaller than 0.5% are rounded to 0%.

6 Corrections

For comparison with theoretical calculations, the measurements are corrected for detector resolution and acceptance effects. The corrections are applied to the observed $\Delta|\eta|$ and $\Delta|y|$ spectra. Apart from the corrected inclusive asymmetry values, particle- or parton-level $\Delta|\eta|$ and $\Delta|y|$ distributions are obtained and presented as normalized differential cross-sections in section 8. Acceptance corrections are included, thus all the results correspond to an extrapolation to the full phase-space for $t\bar{t}$ production.

In case of the $A_C^{\ell\ell}$, the resolution of the measured lepton $\Delta|\eta|$ is very good. Figure 5(a) shows, for the $e\mu$ channel, the probability of an event with a generated value $\Delta|\eta|$ in the j -th bin to be reconstructed in the i -th bin of the corresponding distribution. This probability distribution is defined to be the response matrix for the observable $\Delta|\eta|$. The diagonal bins of the response matrix account for more than 90% of the events. The acceptance and the small migrations are accounted for by the bin-by-bin correction described in subsection 6.1.

In case of the $A_C^{t\bar{t}}$, the top quark direction, which is necessary to determine the $t\bar{t}$ asymmetry, is evaluated using the kinematic reconstruction of the events, described in section 5. In addition to lepton directions and energies measured with very good resolution, jet four-momenta and E_T^{miss} measured with worse resolution are used in reconstructing the t and \bar{t} four-momenta. The resolution of $t\bar{t}$ $\Delta|y|$ (figure 5(b)) is thus much worse than that for the lepton $\Delta|\eta|$. In order to correct for detector resolution and acceptance effects in $A_C^{t\bar{t}}$, the fully Bayesian unfolding (FBU) technique [73] described in subsection 6.2 is used.

6.1 Correction of the lepton-based asymmetry

For $A_C^{\ell\ell}$, bin-by-bin correction factors that also extrapolate to the full acceptance for the $t\bar{t}$ production are used. The goal of this procedure is to find an estimate of the true distribution, given an observed distribution and an expected background distribution. For

the lepton-based results, true distributions are obtained at particle level using leptons before Quantum Electrodynamics (QED) final-state radiation⁴. The following notation is used: $\boldsymbol{\mu}$ and $\hat{\boldsymbol{\mu}}$ are vectors of true distribution values and its estimate, respectively. An observed distribution is denoted by \boldsymbol{n} and its expected value from simulation by $\boldsymbol{\nu}^{\text{MC}}$. An expected background distribution is denoted by $\boldsymbol{\beta}$. For the i -th bin of the asymmetry distribution, the estimate of the true value is obtained by applying a correction factor C_i to the difference between the observed number of events and the expected number of background events,

$$\hat{\mu}_i = C_i(n_i - \beta_i) . \quad (6.1)$$

The C_i are estimated using the $t\bar{t}$ MC simulated sample as

$$C_i = \frac{\mu_i^{\text{MC}}}{\nu_i^{\text{MC}}} , \quad (6.2)$$

where μ_i^{MC} and ν_i^{MC} are the predictions for the number of events in the i -th bin of the true and reconstruction-level distributions.

The bin-by-bin correction of $A_C^{\ell\ell}$ is tested on simulation samples reweighted such that different levels of asymmetry $\Delta|\eta|$ are introduced. Samples are reweighted according to a linear function of $\Delta|\eta|$ with a slope between -6% and 6% in steps of 2% . Corrected values obtained from reweighted distributions are found to be in good agreement with the input value, following a linear relationship. The choice of the binning is done by optimizing the linearity of the method and the expected statistical uncertainty of the asymmetry. The results in section 8 are obtained with $\Delta|\eta|$ distribution binned in 14 bins in the interval between -3 and 3 .

The correction factors depend strongly on the channel and the bin, with the outer bins receiving larger fractional corrections. The ee channel has the lowest acceptance and thus the highest correction factors, reaching values of 500 in the outer bins, in which the events are mostly outside the detector fiducial acceptance. The $e\mu$ channel has a much higher acceptance, and the correction factors vary between 10 and 60. The dependence of the correction factors on the MC model and PDF is small, up to approximately 5%.

6.2 Unfolding of the $t\bar{t}$ asymmetry

In case of sizeable migrations across the bins of the considered distribution, the migrations need to be taken into account without introducing a significant bias during the correction procedure. Unfolding is better suited for the purpose than the bin-by-bin correction factors described in subsection 6.1. Using the response matrix (\mathbf{R}), the true distribution ($\boldsymbol{\mu}$) is related to the expected reconstruction-level distribution ($\boldsymbol{\nu}$) and the expected background ($\boldsymbol{\beta}$) by

$$\boldsymbol{\nu} = \mathbf{R}\boldsymbol{\mu} + \boldsymbol{\beta} . \quad (6.3)$$

⁴The particle-level definition uses status-code 3 for PYTHIA6 for electrons and muons produced in W boson decays. In addition, electrons and muons produced from status-code 3 τ leptons are used. These particles are used both for the unfolding and for the predictions of the MC generators.

In the FBU technique, the maximum likelihood estimator of $\boldsymbol{\mu}$, $L(\boldsymbol{\mu})$, is given by

$$\log L(\boldsymbol{\mu}) = \sum_{i=1}^N \log P(n_i; \nu_i) - \alpha S(\boldsymbol{\mu}) ; \quad p(\boldsymbol{\mu}) \propto L(\boldsymbol{\mu}) , \quad (6.4)$$

with P the Poisson distribution, \mathbf{n} the observed distribution, S a regularization function and α a regularization parameter. The sum in i runs over all N bins of the distributions. The probability density of the unfolded spectra $p(\boldsymbol{\mu})$ is proportional to $L(\boldsymbol{\mu})$. The regularization function S is selected such that the spectra with a desired quality, such as smoothness, are preferred. The regularization parameter α controls the relative strength of the regularization when evaluating the likelihood. The unfolded spectrum and its associated uncertainty are extracted from the probability density $p(\boldsymbol{\mu})$. The statistical uncertainty corresponds to the width of the shortest interval covering 68% probability, and the unfolded spectrum corresponds to the middle of that interval.

The response matrix is obtained using information from the nominal $t\bar{t}$ simulated sample and, in particular, using the top quarks before their decay (parton level) and after QCD radiation⁵.

As explained for the lepton-based asymmetry, the correction is done at the level of true dilepton events (where the two top quarks decay to electrons or muons, either from a direct W boson decay or through an intermediate τ lepton decay).

Using the vector of the true distribution's estimated values $\hat{\boldsymbol{\mu}}$, the regularization function is defined based on the curvature $S(\boldsymbol{\mu}) = |C(\boldsymbol{\mu}) - C(\hat{\boldsymbol{\mu}})|$, with

$$C(\boldsymbol{\mu}) = \sum_{i=2}^{N-1} (\Delta_{i+1,i} - \Delta_{i,i-1})^2, \quad \text{and} \quad \Delta_{i+1,i} = \mu_{i+1} - \mu_i. \quad (6.5)$$

As in the case of the lepton-based asymmetry, linearity tests are performed. A given asymmetry value is introduced by reweighting the samples according to a linear function of $t\bar{t}$ $\Delta|y|$ with a slope between -6% and 6% in steps of 2%. Unfolded values obtained from reweighted distributions are observed to be in good agreement with the injected values of $A_C^{t\bar{t}}$, following a linear relationship. This linearity test is performed with and without regularization and yields similar performance. The binning used for the $\Delta|y|$ distribution as well as the regularization parameter are optimized simultaneously to minimise the expected statistical uncertainty while achieving good linearity. The results in section 8 are obtained with a regularization parameter $\alpha = 10^{-7}$. The $\Delta|y|$ distribution is binned in 4 bins in the interval between -5 and 5 . For this binning choice, at least 50% of the events populate the response matrix diagonal bins for each of the ee , $e\mu$ and $\mu\mu$ channels (figure 5(b)).

The overall correction which is applied to the distribution varies between factors of 10 and 100, depending on the channel and the bin. As shown in figure 5 the bins used for the $t\bar{t}$ $\Delta|y|$ distribution are wider than the bins used for the lepton $\Delta|\eta|$ distribution. The acceptance correction applied to the outer bins of $\Delta|y|$ is thus smaller than the correction obtained for the outer bins of $\Delta|\eta|$ distribution.

⁵The parton-level definition uses status-code 155 for HERWIG and 3 for PYTHIA6 for both the unfolding and for the predictions of the MC generators.

	ee	$e\mu$	$\mu\mu$	comb.
Measured value	0.101	0.009	0.047	0.024
Statistical uncertainty	± 0.052	± 0.019	± 0.030	± 0.015
Lepton reconstruction	± 0.011	± 0.008	± 0.009	± 0.008
Jet reconstruction	± 0.006	± 0.001	± 0.004	± 0.001
$E_{\text{T}}^{\text{miss}}$	± 0.001	< 0.001	± 0.002	< 0.001
Signal modelling	± 0.004	± 0.003	± 0.003	± 0.003
PDF	± 0.004	< 0.001	< 0.001	< 0.001
NP & fake	± 0.016	± 0.001	± 0.001	± 0.001
Background	± 0.003	± 0.002	< 0.001	± 0.001
Total sys.	± 0.021	± 0.009	± 0.012	± 0.009

Table 2: Measured value and uncertainties for the lepton-based asymmetry $A_{\text{C}}^{\ell\ell}$. Uncertainties with absolute value below 0.001 are considered negligible for the total uncertainty.

7 Systematic uncertainties

The uncertainties of the $A_{\text{C}}^{\ell\ell}$ corrections and $A_{\text{C}}^{t\bar{t}}$ unfolding method are estimated from the non-closure in the linearity test described in section 6. For $A_{\text{C}}^{\ell\ell}$ the uncertainties are -0.002 in ee channel and negligible (< 0.001) in the $e\mu$ and $\mu\mu$ channels. For $A_{\text{C}}^{t\bar{t}}$ the uncertainties are 0.002 in the ee channel and negligible (< 0.001) in the $e\mu$ and $\mu\mu$ channels. For both $A_{\text{C}}^{\ell\ell}$ and $A_{\text{C}}^{t\bar{t}}$ the uncertainties have a negligible contribution to the measurement uncertainty and are not considered for the evaluation of the total systematic uncertainty of the results.

The systematic uncertainties considered in this analysis are classified into three categories: detector modelling uncertainties, signal modelling uncertainties and uncertainties related to the estimation of the backgrounds. The contributions of these sources of uncertainty are summarized in table 2 for the lepton-based asymmetry $A_{\text{C}}^{\ell\ell}$ and in table 3 for the $t\bar{t}$ asymmetry $A_{\text{C}}^{t\bar{t}}$. The resulting variations are assumed to be of the same size in both directions and are therefore symmetrized. Apart from one-sided uncertainties, as in the case of the comparison of different MC models, the symmetrization does not notably modify the uncertainty values.

Detector modelling uncertainties are evaluated by performing corrections for detector effects for $A_{\text{C}}^{\ell\ell}$ and $A_{\text{C}}^{t\bar{t}}$, with the response matrices corresponding to the systematic variations. Effects of detector modelling uncertainties on the background are included by subtracting the background, varied accordingly, from the data. The following sources are considered.

- **Lepton reconstruction**

The uncertainty due to lepton reconstruction includes several sources. Lepton momentum scale and resolution modelling correction factors and associated uncertainties are derived from comparisons of data and simulation in $Z \rightarrow \ell\ell$ events [65, 66]. Uncer-

	ee	$e\mu$	$\mu\mu$	comb.
Measured value	0.025	0.007	0.043	0.021
Statistical uncertainty	± 0.069	± 0.032	± 0.045	± 0.025
Lepton reconstruction	± 0.008	± 0.008	± 0.004	± 0.007
Jet reconstruction	± 0.015	± 0.009	± 0.006	± 0.009
E_T^{miss}	± 0.015	± 0.005	± 0.008	± 0.007
Signal modelling	± 0.004	± 0.004	± 0.003	± 0.003
PDF	± 0.004	± 0.005	± 0.004	± 0.005
NP & fake	± 0.013	± 0.011	± 0.003	± 0.008
Background	± 0.003	± 0.002	± 0.004	± 0.003
Total sys.	± 0.027	± 0.018	± 0.013	± 0.017

Table 3: Measured value and uncertainties for the $t\bar{t}$ asymmetry $A_C^{t\bar{t}}$.

tainties in the modelling of trigger, reconstruction and lepton identification efficiencies are also included. Data-to-simulation efficiency corrections, and their uncertainties, are derived from $J/\psi \rightarrow \ell\ell$, $Z \rightarrow \ell\ell$ and $W \rightarrow e\nu$ events.

- **Jet reconstruction**

The effects include the jet energy scale and jet resolution uncertainties. Jet energy scale uncertainty is derived using information from test-beam data, LHC collision data and simulation [69]. It includes uncertainties in the flavour composition of the samples and mismeasurements due to close-by jets and pileup effects. Jet energy resolution and reconstruction efficiency uncertainties are obtained using minimum bias and QCD dijet events [69, 74].

- E_T^{miss}

The uncertainties from the energy scale and resolution corrections for leptons and jets are propagated to the E_T^{miss} . The category accounts for uncertainties in the energies of calorimeter cells not associated with the reconstructed objects and the uncertainties from cells associated with low- p_T jets ($7 \text{ GeV} < p_T < 20 \text{ GeV}$) [70] as well as the dependence of their energy on the number of pileup interactions.

The uncertainties due to the modelling of the signal $t\bar{t}$ distributions are evaluated by performing the linearity test for signal model samples generated with various assumptions. The following sources are quoted.

- **Signal modelling**

The uncertainty is evaluated by adding in quadrature the MC generator uncertainties, initial- and final-state radiation (ISR and FSR), underlying event (UE) and colour reconnection (CR) uncertainties described in the following. The systematic uncertainty related to the choice of a MC generator includes the difference between the nominal sample generated with POWHEG-hvq + PYTHIA6 and samples generated with

MC@NLO + HERWIG, POWHEG-hvq + HERWIG and ALPGEN + HERWIG. The effects of renormalization and factorization scale choice are evaluated with a dedicated pair of samples generated with MC@NLO + HERWIG. In these samples renormalization and factorization scales are varied simultaneously by a factor of two with respect to the reference scale. The reference scale is fixed at the MC@NLO generator default, which is defined as the average of the t and the \bar{t} transverse masses, $Q = \sqrt{1/2(p_{T_t}^2 + p_{T_{\bar{t}}}^2) + m_t^2}$, where $p_{T_{t(\bar{t})}}$ corresponds to the transverse momentum of the t or \bar{t} . Since the effects covered by generator comparisons and scale variations partially overlap, only the largest contribution from all comparisons is used. For the lepton-based asymmetry the dominant contribution was found to stem from the difference between the nominal sample and the sample generated with ALPGEN + HERWIG. For the $t\bar{t}$ asymmetry the contributions of the comparison of the baseline sample result to the results obtained with each of MC@NLO + HERWIG, POWHEG-hvq + HERWIG and ALPGEN + HERWIG samples are of comparable size and significantly larger than the contribution of the renormalization and factorization scale uncertainty. The amount of ISR and FSR are treated as an additional source of signal modelling uncertainty. It is evaluated using samples generated with ALPGEN + PYTHIA6 with variations of parameters controlling the renormalization scale used in ALPGEN and in the PYTHIA6 parton shower. The renormalization scale is varied by factors of 0.5 and 2. The PYTHIA6 settings correspond to Perugia radLO and radHi tunes [36]. Apart from this, the UE and CR uncertainties are evaluated by comparing samples generated with POWHEG-hvq + PYTHIA6, using Perugia2011, Perugia2011 mpiHi and Perugia2011 noCR tunes [36]. For $A_C^{\ell\ell}$, the contributions from the choice of MC generator and from ISR and FSR exceed the non-perturbative UE and CR contributions. For $A_C^{t\bar{t}}$, the contributions from the choice of MC generator and from radiation and non-perturbative modelling uncertainties are comparable.

- **PDF uncertainty**

The uncertainty due to the PDF is evaluated by performing linearity tests with samples obtained from the nominal signal sample, generated with CT10 PDF, reweighted to other PDFs. The CT10 error set as well as MSTW2008 68% CL NLO [45] and NNPDF2.3 NLO ($\alpha_s = 0.118$) [48] central predictions are used. For each asymmetry value, the largest value of the three sources is quoted as uncertainty.

The uncertainties on the modelling of the SM backgrounds are divided into two categories described below.

- **NP & fake**

This source corresponds to the uncertainty in the estimation of processes fulfilling the event selection due to non-prompt or misidentified leptons. The uncertainties are obtained by varying the efficiencies for a real or fake lepton to pass the tight selection, and are affecting both the normalization of the background and its shape.

- **Background**

The uncertainties in the modelling of diboson, Z +jets and single-top SM processes are

quoted in the background category. They are evaluated by varying the normalization of each of these processes by the uncertainty on its cross-section. The uncertainty on the overall luminosity of 1.8% is also entering this category [64].

For both the lepton-based asymmetry $A_C^{\ell\ell}$ and the $t\bar{t}$ asymmetry $A_C^{t\bar{t}}$, the statistical uncertainty is larger than the total systematic uncertainty. The $A_C^{\ell\ell}$ measurement has a combined statistical uncertainty of 1.5%, whereas the combined systematic uncertainty is 0.9%. The largest source of $A_C^{\ell\ell}$ systematic uncertainty is the lepton reconstruction uncertainty, which accounts for approximately 90% of the total systematic uncertainty. The uncertainty on the asymmetry $A_C^{\ell\ell}$ measured in the ee channel receives a sizeable contribution from the NP & fake leptons category (1.6%). This, however, does not significantly impact the combined systematic uncertainty since the ee channel receives a small weight in the combination, as detailed in section 8. The $t\bar{t}$ asymmetry $A_C^{t\bar{t}}$ has a combined statistical uncertainty of 2.5% and a combined systematic uncertainty of 1.7%. The detector modelling uncertainties account for approximately 80% of the combined systematic uncertainty, with comparable large contributions from the lepton reconstruction, the E_T^{miss} (0.7%) and the jet reconstruction uncertainty (0.9%). The NP & fake contribution to the $A_C^{t\bar{t}}$ systematic uncertainty is also sizeable (0.8%).

The uncertainties related to detector and background modelling are evaluated in each bin of the corrected distributions and presented in section 8.

8 Results

After the event selection and reconstruction but before the correction described in section 6 the inclusive lepton and $t\bar{t}$ asymmetries measured in the data are $A_C^{\ell\ell} = 0.021 \pm 0.011$ (stat.) and $A_C^{t\bar{t}} = 0.003 \pm 0.012$ (stat.), respectively for the combination of the $ee, e\mu$ and $\mu\mu$ channels. After the subtraction of the background contribution, the measured data asymmetries are $A_C^{\ell\ell} = 0.029 \pm 0.013$ (stat.) and $A_C^{t\bar{t}} = 0.006 \pm 0.014$ (stat.). The corresponding asymmetry predictions in the nominal simulated $t\bar{t}$ sample are $A_C^{\ell\ell} = 0.005 \pm 0.003$ (stat.) and $A_C^{t\bar{t}} = 0.008 \pm 0.003$ (stat.). This sample is generated with the POWHEG-hvq + PYTHIA6 generator with a particle-level lepton asymmetry of $A_C^{\ell\ell} = 0.0045 \pm 0.0009$ (stat.) and a parton-level $t\bar{t}$ asymmetry of $A_C^{t\bar{t}} = 0.0071 \pm 0.0009$ (stat.), evaluated in the full phase-space.

After the correction for detector, resolution and acceptance effects, the normalized differential cross-sections corrected to particle and parton level are obtained for $\Delta|\eta|$ and $\Delta|y|$ separately for the three channels. From these distributions, the inclusive asymmetry values can be extracted. The inclusive results obtained in the $ee, e\mu$ and $\mu\mu$ channels (see tables 2 and 3) are then combined using the best linear unbiased estimator (BLUE) method [75, 76]. All systematic uncertainties are assumed to be 100% correlated, except for the uncertainties on electrons and muons and on the NP & fake lepton background.

The normalized differential cross-sections for $\Delta|\eta|$ and $\Delta|y|$ are presented in figure 6 for the $e\mu$ channel. Good agreement is observed between the measured distributions and the ones predicted by POWHEG-hvq + PYTHIA6. The normalized differential cross-sections

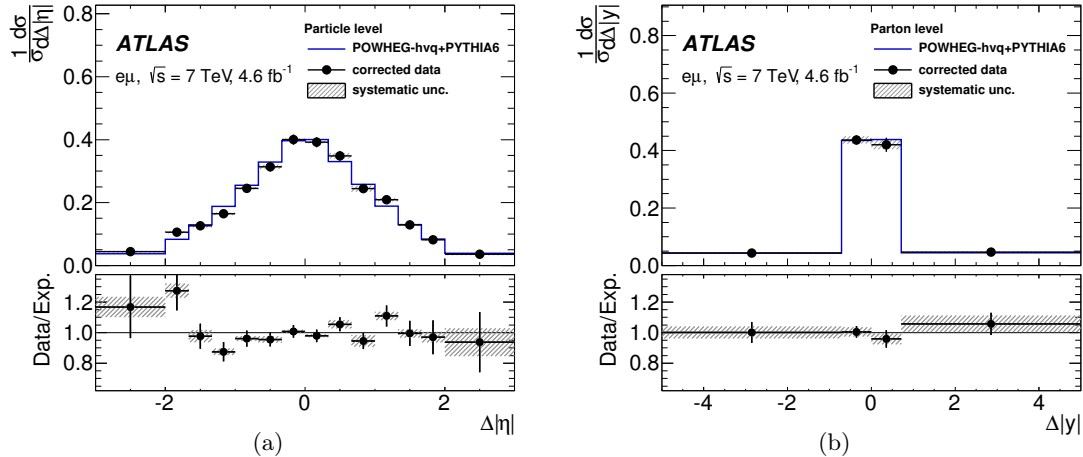


Figure 6: Normalized differential cross-sections for (a) lepton $\Delta|\eta|$ and (b) $t\bar{t}$ $\Delta|y|$ in the $e\mu$ channel after correcting for detector effects. The distributions predicted by POWHEG-hvq + PYTHIA6 are compared to the data in the top panels. The bottom panels show the ratio of the corrected data to the predictions. The error bars correspond to the statistical uncertainties and the hatched area to the systematic uncertainties.

in that channel are also presented with statistical and systematic uncertainties in tables 4 and 5. The systematic uncertainties for the differential distributions do not include the signal modelling uncertainties, which could not be evaluated with sufficient precision due to the limited statistics of the simulated samples. For both distributions, the statistical uncertainty is somewhat larger than the systematic uncertainty. In appendix A the contributions from each source of systematic uncertainty, described in section 7, to the total systematic uncertainty in each bin of the $\Delta|\eta|$ and $\Delta|y|$ distributions are provided. The statistical correlations between the different bins of the distributions are also given.

The results for the inclusive lepton-based asymmetry $A_C^{\ell\ell}$ and the $t\bar{t}$ asymmetry $A_C^{t\bar{t}}$ after corrections for detector and resolution effects are shown in table 6. The values in the ee , $e\mu$ and $\mu\mu$ channels as well as for their combination are presented, together with statistical and systematic uncertainties.

Detailed information about the combination of the inclusive values is given in table 7. The combination probabilities are 21% and 81% for $A_C^{\ell\ell}$ and $A_C^{t\bar{t}}$ respectively, demonstrating the compatibility of the measurements in the three channels (ee , $e\mu$ and $\mu\mu$). The weight of each channel in the combination is also reported in table 7. The $e\mu$ channel dominates the combination, reflecting the larger data statistics compared to that of the ee and $\mu\mu$ channels.

The inclusive measurements after the detector and resolution effects corrections can be compared with the state-of-the-art theoretical predictions calculated at NLO QCD, including the electromagnetic and weak-interaction corrections [10]: $A_C^{\ell\ell} = 0.0070 \pm 0.0003$ (scale) and $A_C^{t\bar{t}} = 0.0123 \pm 0.0005$ (scale). In figure 7 the measured values of $A_C^{\ell\ell}$ and $A_C^{t\bar{t}}$ are compared to these predictions and POWHEG-hvq + PYTHIA6 predictions. In the figure, el-

Bin of $\Delta \eta $	$\frac{1}{\sigma} \frac{d\sigma}{d\Delta \eta }$ (\pm stat. \pm syst.)		
$[-3.00, -2.00]$	0.0440	± 0.0077	± 0.0025
$[-2.00, -1.67]$	0.106	± 0.011	± 0.004
$[-1.67, -1.33]$	0.126	± 0.011	± 0.005
$[-1.33, -1.00]$	0.164	± 0.012	± 0.004
$[-1.00, -0.67]$	0.245	± 0.013	± 0.004
$[-0.67, -0.33]$	0.314	± 0.015	± 0.007
$[-0.33, 0.00]$	0.400	± 0.016	± 0.004
$[0.00, 0.33]$	0.392	± 0.016	± 0.004
$[0.33, 0.67]$	0.349	± 0.015	± 0.009
$[0.67, 1.00]$	0.244	± 0.013	± 0.010
$[1.00, 1.33]$	0.209	± 0.013	± 0.005
$[1.33, 1.67]$	0.129	± 0.011	± 0.003
$[1.67, 2.00]$	0.0815	± 0.0093	± 0.0028
$[2.00, 3.00]$	0.0361	± 0.0076	± 0.0035

Table 4: Normalized differential cross-sections for $\Delta|\eta|$ in the $e\mu$ channel presented with statistical and systematic uncertainties.

Bin of $\Delta y $	$\frac{1}{\sigma} \frac{d\sigma}{d\Delta y }$ (\pm stat. \pm syst.)		
$[-5.00, -0.71]$	0.0435	± 0.0029	± 0.0017
$[-0.71, 0.00]$	0.437	± 0.016	± 0.013
$[0.00, 0.71]$	0.420	± 0.025	± 0.015
$[0.71, 5.00]$	0.0470	± 0.0032	± 0.0024

Table 5: Normalized differential cross-sections for $\Delta|y|$ in the $e\mu$ channel presented with statistical and systematic uncertainties.

Channel	$A_C^{\ell\ell}$	$A_C^{t\bar{t}}$
ee	$0.101 \pm 0.052 \pm 0.021$	$0.025 \pm 0.069 \pm 0.027$
$e\mu$	$0.009 \pm 0.019 \pm 0.009$	$0.007 \pm 0.032 \pm 0.018$
$\mu\mu$	$0.047 \pm 0.030 \pm 0.012$	$0.043 \pm 0.045 \pm 0.013$
Combined	$0.024 \pm 0.015 \pm 0.009$	$0.021 \pm 0.025 \pm 0.017$
SM, NLO QCD+EW [10]	0.0070 ± 0.0003 (scale)	0.0123 ± 0.0005 (scale)

Table 6: Results for the lepton-based asymmetry $A_C^{\ell\ell}$ and the $t\bar{t}$ asymmetry $A_C^{t\bar{t}}$ after correcting for detector, resolution and acceptance effects. The values in the ee , $e\mu$ and $\mu\mu$ channels as well as the combined value are presented with their statistical and systematic uncertainties.

lipses corresponding to 1σ and 2σ combined statistical and systematic uncertainties of the

	$A_C^{\ell\ell}$	$A_C^{t\bar{t}}$
χ^2	3.1	0.4
Probability (in %)	21	81
Weights ($ee/e\mu/\mu\mu$ in %)	7 / 68 / 25	9 / 57 / 34

Table 7: Information about the combination of the three channels using the best linear unbiased estimator method: χ^2 and probability of the combination, as well as the weight of each channel.

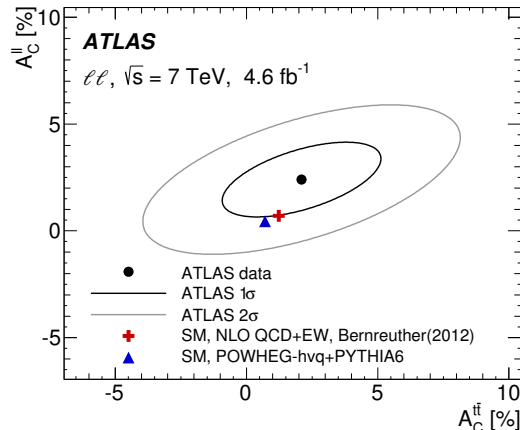


Figure 7: Comparison of the inclusive $A_C^{\ell\ell}$ and $A_C^{t\bar{t}}$ measurement values to the theory predictions (SM NLO QCD+EW prediction [10] and the prediction of the POWHEG-hvq + PYTHIA6 generator). Ellipses corresponding to 1σ and 2σ combined statistical and systematic uncertainties of the measurement, including the correlation between $A_C^{\ell\ell}$ and $A_C^{t\bar{t}}$, are also shown.

measurement, including the correlation between $A_C^{\ell\ell}$ and $A_C^{t\bar{t}}$, are also shown. The statistical correlation between $A_C^{\ell\ell}$ and $A_C^{t\bar{t}}$ is evaluated to be $37\pm 5\%$ using pseudo-experiments based on simulation. The systematic uncertainties are treated as 100% correlated. The resulting correlation between $A_C^{\ell\ell}$ and $A_C^{t\bar{t}}$ is about 55%. The measured values are both consistent with the theory predictions within the uncertainties. The measured $A_C^{t\bar{t}}$ values are consistent with but less precise than measurements in the single-lepton decay channel by the ATLAS [18] and CMS [19] collaborations. The measurements of $A_C^{\ell\ell}$ and $A_C^{t\bar{t}}$ are also consistent with the CMS collaboration measurements in the dilepton decay channel [20].

The inclusive measurement of $A_C^{\ell\ell}$ and $A_C^{t\bar{t}}$ is furthermore compared to two models of physics beyond the Standard Model (BSM) [9] that could be invoked to explain an anomalous forward-backward asymmetry at the Tevatron, such as reported by the CDF experiment [24]. Two models with a new colour octet particle exchanged in the s-channel are considered. In the model with the light octet, the new particle mass is below the $t\bar{t}$ production threshold. The model with the heavy octet uses the octet mass beyond the reach of the LHC. The new particles would not be visible as resonances in the $m_{t\bar{t}}$ spectrum at the

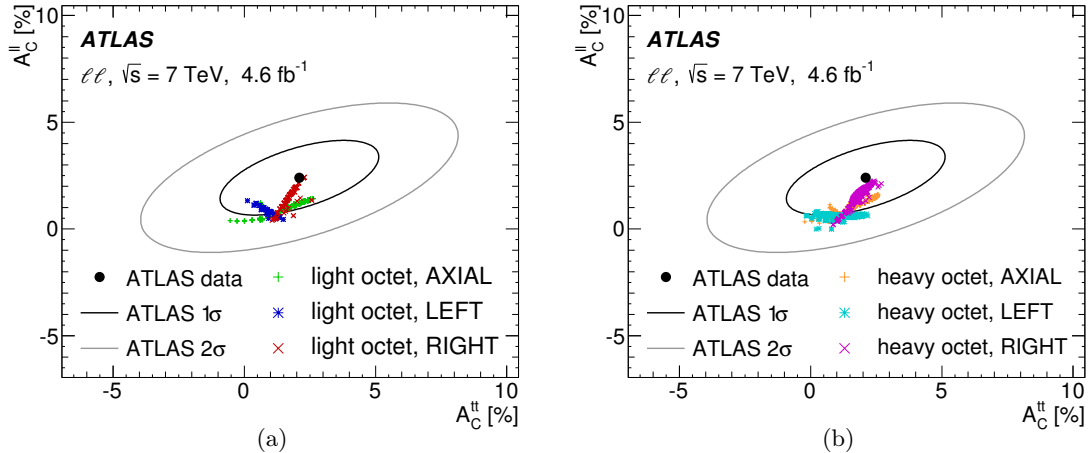


Figure 8: Comparison of the measured inclusive $A_C^{\ell\ell}$ and $A_C^{t\bar{t}}$ values to two benchmark BSM models, one a light octet with mass below $t\bar{t}$ production threshold (left) and one with a heavy octet with mass beyond LHC reach (right), for various couplings as described in the legend.

Tevatron or at the LHC. The light octet is assumed to have a mass of $m = 250$ GeV and a width of $\Gamma = 0.2m$. For the heavy octet, the corrections to $t\bar{t}$ production are independent of the mass but instead depend on the ratio of coupling to mass, which is assumed to be $1/\text{TeV}$. In figure 8 the measured $A_C^{\ell\ell}$ and $A_C^{t\bar{t}}$ values are compared to the light (figure 8(a)) and heavy (figure 8(b)) colour octet model predictions in order to assess whether any of the BSM predictions can be excluded. Models with left-handed, right-handed and axial coupling to the up, down and top quarks are shown. The considered couplings to the quarks are such that the global fit to $t\bar{t}$ observables at the Tevatron and the LHC, including total cross-sections, various asymmetries, the top polarisation and spin correlations, is consistent with the measurements within two standard deviations [9]. The LHC asymmetry measurements in the dilepton decay channel are excluded from the fit. While the models span a sizeable range of values in the $A_C^{\ell\ell}$ and $A_C^{t\bar{t}}$ plane in figure 8, their predictions are consistent with the measured value within the present uncertainties. Thus the potential BSM contributions cannot be excluded beyond the reach of the previous Tevatron and LHC measurements. Future $A_C^{\ell\ell}$ and $A_C^{t\bar{t}}$ measurements with a larger dataset could however further constrain the allowed couplings of the colour octet models if both statistical and systematic uncertainties can be reduced further.

9 Conclusion

Measurements of the $t\bar{t}$ charge asymmetry in the dilepton channel are presented. The measurements are performed using data corresponding to an integrated luminosity of 4.6 fb^{-1} of pp collisions at $\sqrt{s} = 7$ TeV collected by the ATLAS detector at the LHC. Selected events are required to have exactly two charged leptons (electron or muon), large miss-

ing transverse momentum and at least two jets. Both the lepton-based asymmetry $A_C^{\ell\ell}$ and the $t\bar{t}$ asymmetry $A_C^{t\bar{t}}$ are extracted in three channels: ee , $e\mu$ and $\mu\mu$. The measurement of $A_C^{t\bar{t}}$ requires the kinematic reconstruction of the $t\bar{t}$ system, which is performed using the neutrino weighting technique. Agreement between predictions and data is checked after selection and kinematic reconstruction. Good agreement is obtained for all the kinematic observables studied. The $\ell\ell$ $\Delta|\eta|$ and $t\bar{t}$ $\Delta|y|$ distributions and inclusive asymmetries are corrected for detector and acceptance effects. Corrections are applied using bin-by-bin corrections for $A_C^{\ell\ell}$ and fully bayesian unfolding for $A_C^{t\bar{t}}$. The distributions of lepton $\Delta|\eta|$ and $t\bar{t}$ $\Delta|y|$ after the detector smearing corrections are provided for the $e\mu$ channel. Good agreement between the corrected values and predictions of the Monte Carlo generator models is observed in these distributions. The combined values of lepton-based inclusive asymmetry $A_C^{\ell\ell}$ and $t\bar{t}$ inclusive asymmetry $A_C^{t\bar{t}}$ are measured to be $A_C^{\ell\ell} = 0.024 \pm 0.015$ (stat.) ± 0.009 (syst.) and $A_C^{t\bar{t}} = 0.021 \pm 0.025$ (stat.) ± 0.017 (syst.). The measured values are in agreement with previous LHC measurements and with the Standard Model prediction [10]: $A_C^{\ell\ell} = 0.0070 \pm 0.0003$ (scale) and $A_C^{t\bar{t}} = 0.0123 \pm 0.0005$ (scale). The measurements are limited by statistical uncertainties. The predictions of benchmark light and heavy colour octet models with parameters selected such that the models are consistent with previous LHC and Tevatron data [9] are found to be consistent with the measured asymmetries.

Acknowledgements

We thank CERN for the very successful operation of the LHC, as well as the support staff from our institutions without whom ATLAS could not be operated efficiently.

We acknowledge the support of ANPCyT, Argentina; YerPhI, Armenia; ARC, Australia; BMFWF and FWF, Austria; ANAS, Azerbaijan; SSTC, Belarus; CNPq and FAPESP, Brazil; NSERC, NRC and CFI, Canada; CERN; CONICYT, Chile; CAS, MOST and NSFC, China; COLCIENCIAS, Colombia; MSMT CR, MPO CR and VSC CR, Czech Republic; DNRF, DNSRC and Lundbeck Foundation, Denmark; EPLANET, ERC and NSRF, European Union; IN2P3-CNRS, CEA-DSM/IRFU, France; GNSF, Georgia; BMBF, DFG, HGF, MPG and AvH Foundation, Germany; GSRT and NSRF, Greece; RGC, Hong Kong SAR, China; ISF, MINERVA, GIF, I-CORE and Benoziyo Center, Israel; INFN, Italy; MEXT and JSPS, Japan; CNRST, Morocco; FOM and NWO, Netherlands; BRF and RCN, Norway; MNiSW and NCN, Poland; GRICES and FCT, Portugal; MNE/IFA, Romania; MES of Russia and NRC KI, Russian Federation; JINR; MSTB, Serbia; MSSR, Slovakia; ARRS and MIZŠ, Slovenia; DST/NRF, South Africa; MINECO, Spain; SRC and Wallenberg Foundation, Sweden; SER, SNSF and Cantons of Bern and Geneva, Switzerland; NSC, Taiwan; TAEK, Turkey; STFC, the Royal Society and Leverhulme Trust, United Kingdom; DOE and NSF, United States of America.

The crucial computing support from all WLCG partners is acknowledged gratefully, in particular from CERN and the ATLAS Tier-1 facilities at TRIUMF (Canada), NDGF (Denmark, Norway, Sweden), CC-IN2P3 (France), KIT/GridKA (Germany), INFN-CNAF

(Italy), NL-T1 (Netherlands), PIC (Spain), ASGC (Taiwan), RAL (UK) and BNL (USA) and in the Tier-2 facilities worldwide.

References

- [1] F. Abe et al., CDF Collaboration, *Observation of top quark production in $p\bar{p}$ collisions*, *Phys. Rev. Lett.* **74** (1995) 2626 [arXiv:hep-ex/9503002].
- [2] A. Abachi et al., D0 Collaboration, *Observation of the top quark*, *Phys. Rev. Lett.* **74** (1995) 2632 [arXiv:hep-ex/9503003].
- [3] R. Frederix and F. Maltoni, *Top pair invariant mass distribution: A Window on new physics*, *JHEP* **01** (2009) 047 [arXiv:0712.2355].
- [4] V. Barger, T. Han and D. G. E. Walker, *Top Quark Pairs at High Invariant Mass: A Model-Independent Discriminator of New Physics at the LHC*, *Phys. Rev. Lett.* **100** (2008) 031801 [arXiv:hep-ph/0612016].
- [5] J. A. Aguilar-Saavedra, *Effective four-fermion operators in top physics: A Roadmap*, *Nucl. Phys.* **B 843** (2011) 638 [arXiv:1008.3562].
- [6] C. Zhang and S. Willenbrock, *Effective-Field-Theory Approach to Top-Quark Production and Decay*, *Phys. Rev.* **D 83** (2011) 034006 [arXiv:1008.3869].
- [7] C. T. Hill, *Topcolor assisted technicolor*, *Phys. Lett.* **B 345** (1995) 483 [arXiv:hep-ph/9411426].
- [8] J. Cao, G. Liu and J. M. Yang, *Probing topcolor-assisted technicolor from like-sign top pair production at CERN LHC*, *Phys. Rev.* **D 70** (2004) 114035 [arXiv:hep-ph/0409334].
- [9] J. A. Aguilar-Saavedra, *Portrait of a colour octet*, *JHEP* **08** (2014) 172 [arXiv:1405.5826].
- [10] W. Bernreuther and Z.-G. Si, *Top quark and leptonic charge asymmetries for the Tevatron and LHC*, *Phys. Rev.* **D 86** (2012) 034026 [arXiv:1205.6580].
- [11] M. Czakon, P. Fiedler, and A. Mitov, *Resolving the Tevatron top quark forward-backward asymmetry puzzle* [arXiv:1411.3007].
- [12] J. S. Brodsky et al., *Application of the Principle of Maximum Conformality to the Top-Quark Charge Asymmetry at the LHC*, *Phys. Rev.* **D 90** (2014) 114034 [arXiv:1410.1607].
- [13] P. H. Frampton and S. L. Glashow, *Chiral Color: An Alternative to the Standard Model*, *Phys. Lett.* **B 190** (1987) 157.
- [14] P. Ferrario and G. Rodrigo, *Massive color-octet bosons and the charge asymmetries of top quarks at hadron colliders*, *Phys. Rev.* **D 78** (2008) 094018 [arXiv:0809.3354].
- [15] J. A. Aguilar-Saavedra and M. Perez-Victoria, *Probing the Tevatron $t\bar{t}$ asymmetry at LHC*, *JHEP* **05** (2011) 034 [arXiv:1103.2765].
- [16] A. Falkowski et al., *Data driving the top quark forward-backward asymmetry with a lepton-based handle*, *Phys. Rev.* **D 87** (2013) 034039 [arXiv:1212.4003].
- [17] J. A. Aguilar-Saavedra et al., *Asymmetries in top quark pair production*, (2014) [arXiv:1406.1798].
- [18] ATLAS Collaboration, *Measurement of the top quark pair production charge asymmetry in proton-proton collisions at $\sqrt{s} = 7$ TeV using the ATLAS detector*, *JHEP* **02** (2014) 107 [arXiv:1311.6724].
- [19] CMS Collaboration, *Inclusive and differential measurements of the $t\bar{t}$ charge asymmetry in proton-proton collisions at 7 TeV*, *Phys. Lett.* **B 717** (2012) 129 [arXiv:1207.0065].

- [20] CMS Collaboration, *Measurements of the $t\bar{t}$ charge asymmetry using the dilepton decay channel in pp collisions at $\sqrt{s} = 7$ TeV*, *JHEP* **04** (2014) 191 [arXiv:1402.3803].
- [21] ATLAS and CMS Collaborations, *Combination of ATLAS and CMS $t\bar{t}$ charge asymmetry measurements using LHC proton-proton collisions at $\sqrt{s} = 7$ TeV*, ATLAS-CONF-2014-012, CMS-PAS-TOP-14-006, <https://cds.cern.ch/record/1670535> (2014).
- [22] T. Aaltonen et al., CDF Collaboration, *Evidence for a Mass Dependent Forward-Backward Asymmetry in Top Quark Pair Production*, *Phys. Rev. D* **83** (2011) 112003 [arXiv:1101.0034].
- [23] V. M. Abazov et al., D0 Collaboration, *Forward-backward asymmetry in top quark-antiquark production*, *Phys. Rev. D* **84** (2011) 112005 [arXiv:1107.4995].
- [24] T. Aaltonen et al., CDF Collaboration, *Measurement of the top quark forward-backward production asymmetry and its dependence on event kinematic properties*, *Phys. Rev. D* **87** (2013) 092002 [arXiv:1211.1003].
- [25] T. Aaltonen et al., CDF Collaboration, *Measurement of the leptonic asymmetry in $t\bar{t}$ events produced in $p\bar{p}$ collisions at $\sqrt{s} = 1.96$ TeV*, *Phys. Rev.* **88** (2013) 072003 [arXiv:1308.1120].
- [26] T. Aaltonen et al., CDF Collaboration, *Measurement of the inclusive leptonic asymmetry in top-quark pairs that decay to two charged leptons at CDF*, *Phys. Rev. Lett.* **113** (2014) 042001 [arXiv:1404.3698].
- [27] V. M. Abazov et al., D0 Collaboration, *Measurement of the forward-backward asymmetry in the distribution of leptons in $t\bar{t}$ events in the lepton+jets channel*, *Phys. Rev. D* **90** (2014) 072001 [arXiv:1403.1294].
- [28] V. M. Abazov et al., D0 Collaboration, *Measurement of the forward-backward asymmetry in top quark-antiquark production in $p\bar{p}$ collisions using the lepton+jets channel*, *Phys. Rev. D* **90** (2014) 072011 [arXiv:1405.0421].
- [29] ATLAS Collaboration, *The ATLAS Experiment at the CERN Large Hadron Collider*, *JINST* **3** (2008) S08003.
- [30] S. Frixione, P. Nason and C. Oleari, *Matching NLO QCD computations with Parton Shower simulations: the POWHEG method*, *JHEP* **11** (2007) 070 [arXiv:0709.2092].
- [31] P. Nason, *A New method for combining NLO QCD with shower Monte Carlo algorithms*, *JHEP* **11** (2004) 040.
- [32] S. Frixione, G. Ridolfi and P. Nason, *A Positive-weight next-to-leading-order Monte Carlo for heavy flavour hadroproduction*, *JHEP* **09** (2007) 126 [arXiv:0707.3088].
- [33] H. L. Lai et al., *New parton distributions for collider physics*, *Phys. Rev. D* **82** (2010) 074024 [arXiv:1007.2241].
- [34] T. Sjöstrand, S. Mrenna and P. Z. Skands, *PYTHIA 6.4 Physics and Manual*, *JHEP* **05** (2006) 026 [arXiv:hep-ph/0603175].
- [35] J. Pumplin et al., *New generation of parton distributions with uncertainties from global QCD analysis*, *JHEP* **07** (2002) 012 [arXiv:hep-ph/0201195].
- [36] P. Z. Skands, *Tuning Monte Carlo Generators: The Perugia Tunes*, *Phys. Rev. D* **82** (2010) 074018 [arXiv:1005.3457].

- [37] M. Cacciari et al., *Top-pair production at hadron colliders with next-to-next-to-leading logarithmic soft-gluon resummation*, *Phys. Lett. B* **710** (2012) 612 [arXiv:1111.5869].
- [38] P. Baernreuther, M. Czakon and A. Mitov, *Percent Level Precision Physics at the Tevatron: First Genuine NNLO QCD Corrections to $q\bar{q} \rightarrow t\bar{t} + X$* , *Phys. Rev. Lett.* **109** (2012) 132001 [arXiv:1204.5201].
- [39] M. Czakon and A. Mitov, *NNLO corrections to top-pair production at hadron colliders: the all-fermionic scattering channels*, *JHEP* **12** (2012) 054 [arXiv:1207.0236].
- [40] M. Czakon and A. Mitov, *NNLO corrections to top pair production at hadron colliders: the quark-gluon reaction*, *JHEP* **01** (2013) 080 [arXiv:1210.6832].
- [41] M. Czakon, P. Fiedler and A. Mitov, *Total Top-Quark Pair-Production Cross Section at Hadron Colliders Through $O(\alpha_S^4)$* , *Phys. Rev. Lett.* **110** (2013) 252004 [arXiv:1303.6254].
- [42] M. Beneke et al., *Hadronic top-quark pair production with NNLL threshold resummation*, *Nucl. Phys. B* **855** (2012) 695 [arXiv:1109.1536].
- [43] M. Czakon and A. Mitov, *Top++: A Program for the Calculation of the Top-Pair Cross-Section at Hadron Colliders*, *Comput. Phys. Commun.* **185** (2014) 2930 [arXiv:1112.5675].
- [44] M Botje et al., *The PDF4LHC Working Group Interim Recommendations*, (2011) [arXiv:1101.0538].
- [45] A. D. Martin et al., *Parton distributions for the LHC*, *Eur. Phys. J. C* **63** (2009) 189 [arXiv:0901.0002].
- [46] A. D. Martin et al., *Uncertainties on α_S in global PDF analyses and implications for predicted hadronic cross sections*, *Eur. Phys. J. C* **64** (2009) 653 [arXiv:0905.3531].
- [47] J. Gao et al., *The CT10 NNLO Global Analysis of QCD*, *Phys. Rev. D* **89** (2014) 033009 [arXiv:1302.6246].
- [48] R. D. Ball et al., *Parton distributions with LHC data*, *Nucl. Phys. B* **867** (2013) 244 [arXiv:1207.1303].
- [49] M. Aliev et al., *HATHOR: HAdronic Top and Heavy quarks crOss section calculatoR*, *Comput. Phys. Commun.* **182** (2011) 1034 [arXiv:1007.1327].
- [50] S. Frixione and B. R. Webber, *Matching NLO QCD computations and parton shower simulations*, *JHEP* **06** (2002) 029 [arXiv:hep-ph/0204244].
- [51] S. Frixione et al., *Single-top hadroproduction in association with a W boson*, *JHEP* **07** (2008) 029 [arXiv:0805.3067].
- [52] G. Marchesini et al., *HERWIG 5.1 - a Monte Carlo event generator for simulating hadron emission reactions with interfering gluons*, *Comput. Phys. Commun.* **67** (1992) 465.
- [53] G. Corcella et al., *HERWIG 6: An Event generator for hadron emission reactions with interfering gluons (including supersymmetric processes)*, *JHEP* **01** (2001) 010 [arXiv:hep-ph/0011363].
- [54] J. M. Butterworth et al., *Multiparton interactions in photoproduction at HERA*, *Z. Phys. C* **72** (1996) 637 [arXiv:hep-ph/9601371].
- [55] ATLAS Collaboration, *New ATLAS event generator tunes to 2010 data*, ATL-PHYS-PUB-2011-008, <http://cdsweb.cern.ch/record/1345343> (2011).

- [56] M. L. Mangano et al., *ALPGEN, a generator for hard multiparton processes in hadronic collisions*, *JHEP* **07** (2003) 001 [arXiv:hep-ex/0206293].
- [57] N. Kidonakis, *Two-loop soft anomalous dimensions for single top quark associated production with a W- or H-*, *Phys. Rev. D* **82** (2010) 054018 [arXiv:1005.4451].
- [58] J. M. Campbell and R. K. Ellis, *An Update on vector boson pair production at hadron colliders*, *Phys. Rev. D* **60** (1999) 113006 [arXiv:hep-ph/9905386].
- [59] C. Anastasiou et al., *High precision QCD at hadron colliders: Electroweak gauge boson rapidity distributions at NNLO*, *Phys. Rev. D* **69** (2004) 094008 [arXiv:hep-ph/0312266].
- [60] R. Hamberg, W. L. van Neerven and T. Matsuura, *A Complete calculation of the order α_s^2 correction to the Drell-Yan K factor*, *Nucl. Phys. B* **359** (1991) 343, Erratum-ibid. **B 644** (2002) 403.
- [61] ATLAS Collaboration, *The ATLAS Simulation Infrastructure*, *Eur. Phys. J. C* **70** (2010) 823 [arXiv:1005.4568].
- [62] S. Agostinelli et al., *GEANT4: A simulation toolkit*, *Nucl. Instrum. Meth. A* **506** (2003) 250.
- [63] ATLAS Collaboration, *The simulation principle and performance of the ATLAS fast calorimeter simulation FastCaloSim*, ATL-PHYS-PUB-2010-013, <http://cdsweb.cern.ch/record/1300517> (2010).
- [64] ATLAS Collaboration, *Improved luminosity determination in pp collisions at $\sqrt{s} = 7$ TeV using the ATLAS detector at the LHC*, *Eur. Phys. J. C* **73** (2013) 2518 [arXiv:1302.4393].
- [65] ATLAS Collaboration, *Electron reconstruction and identification efficiency measurements with the ATLAS detector using the 2011 LHC proton-proton collision data*, *Eur. Phys. J. C* **74** (2014) 2941 [arXiv:1404.2240].
- [66] ATLAS Collaboration, *Measurement of the muon reconstruction performance of the ATLAS detector using 2011 and 2012 LHC proton-proton collision data*, *Eur. Phys. J. C* **74** (2014) 3130 [arXiv:1407.3935].
- [67] M. Cacciari, G. P. Salam and G. Soyez, *The anti-kt jet clustering algorithm*, *JHEP* **04** (2008) 063 [arXiv:0802.1189].
- [68] ATLAS Collaboration, *Calorimeter Clustering Algorithms: Description and Performance*, ATL-LARG-PUB-2008-002, <https://cds.cern.ch/record/1099735> (2010).
- [69] ATLAS Collaboration, *Jet energy measurement and its systematic uncertainty in proton-proton collisions at $\sqrt{s} = 7$ TeV with the ATLAS detector*, *Eur. Phys. J. C* **75** (2015) 17 [arXiv:1406.0076].
- [70] ATLAS Collaboration, *Performance of Missing Transverse Momentum Reconstruction in Proton-Proton Collisions at 7 TeV with ATLAS*, *Eur. Phys. J. C* **72** (2012) 1844 [arXiv:1108.5602].
- [71] ATLAS Collaboration, *Measurement of the top quark-pair production cross section with ATLAS in pp collisions at $\sqrt{s} = 7$ TeV*, *Eur. Phys. J. C* **71** (2011) 1577 [arXiv:1012.1792].
- [72] B. Abbott et al., D0 Collaboration, *Measurement of the top quark mass using dilepton events*, *Phys. Rev. Lett.* **80** (1998) 2063 [arXiv:hep-ex/9706014].
- [73] G. Choudalakis, *Fully Bayesian Unfolding* [arXiv:1201.4612].
- [74] ATLAS Collaboration, *Jet energy resolution in proton-proton collisions at $\sqrt{s} = 7$ TeV recorded in 2010 with the ATLAS detector*, *Eur. Phys. J. C* **73** (2013) 2306 [arXiv:1210.6210].

- [75] L. Lyons, D. Gibaut and P. Clifford, *How to Combine Correlated Estimates of a Single Physical Quantity*, *Nucl. Instrum. Meth.* **A 270** (1988) 110.
- [76] A. Valassi, *Combining correlated measurements of several different physical quantities*, *Nucl. Instrum. Meth.* **A 500** (2003) 391.

A Additional tables

Additional information about the normalized differential cross-sections in the $e\mu$ channel are provided in this appendix.

The detail of the systematic uncertainties in each bin of the distributions are reported in tables 8 and 9.

Bin of $\Delta \eta $	[-3., -2.]	[-2., -1.67]	[-1.67, -1.33]	[-1.33, -1.]	[-1., -0.67]	[-0.67, -0.33]	[-0.33, 0.]
Central value	0.0440	0.106	0.126	0.164	0.245	0.314	0.400
Stat.	0.0077	0.011	0.011	0.012	0.013	0.015	0.016
Lepton reconstruction	0.0023	0.003	0.005	0.003	0.003	0.005	0.003
Jet reconstruction	0.0005	0.001	-	0.002	-	0.002	0.001
E_T^{miss}	-	-	-	-	-	-	-
Signal modelling	n/r	n/r	n/r	n/r	n/r	n/r	n/r
PDF	n/r	n/r	n/r	n/r	n/r	n/r	n/r
Background	-	0.001	0.001	-	0.001	0.002	0.002
NP and fake	0.0005	0.002	0.001	-	0.001	0.004	0.001
Total systematics	0.0025	0.004	0.005	0.004	0.004	0.007	0.004
Total uncertainty	0.0081	0.011	0.012	0.013	0.014	0.016	0.017

Bin of $\Delta \eta $	[0., 0.33]	[0.33, 0.67]	[0.67, 1.]	[1., 1.33]	[1.33, 1.67]	[1.67, 2.]	[2., 3.]
Central value	0.392	0.349	0.244	0.209	0.129	0.0815	0.0361
Stat.	0.016	0.015	0.013	0.013	0.011	0.0093	0.0076
Lepton reconstruction	0.003	0.009	0.009	0.003	0.003	0.0019	0.0032
Jet reconstruction	0.001	0.001	0.002	0.002	-	0.0012	0.0003
E_T^{miss}	-	-	-	-	-	-	-
Signal modelling	n/r	n/r	n/r	n/r	n/r	n/r	n/r
PDF	n/r	n/r	n/r	n/r	n/r	n/r	n/r
Background	0.002	-	-	0.001	0.001	0.0009	-
NP and fake	0.001	0.001	0.002	0.003	0.001	0.0012	0.0013
Total systematics	0.004	0.009	0.010	0.005	0.003	0.0028	0.0035
Total uncertainty	0.017	0.018	0.017	0.014	0.011	0.0097	0.0084

Table 8: Systematic uncertainties in each bin of the $\Delta|\eta|$ distribution in the $e\mu$ channel. Hyphens are used when the uncertainties are lower than 0.0005. The signal modelling and the PDF uncertainty, (labeled as n/r) are limited by the statistical fluctuations in the simulated samples and are thus not reported in the table.

The statistical correlations between the different bins of each distribution are reported in tables 10 and 11. They were estimated using bootstrapping.

Bin of $\Delta y $	$[-5.00, -0.71]$	$[-0.71, 0.00]$	$[0.00, 0.71]$	$[0.71, 5.00]$
Central value	0.0435	0.437	0.420	0.0470
Stat.	0.0029	0.016	0.025	0.0032
Lepton reconstruction	0.0009	0.006	0.010	0.0016
Jet reconstruction	0.0007	0.011	0.009	0.0012
E_T^{miss}	0.0002	0.003	0.007	0.0009
Signal modelling	n/r	n/r	n/r	n/r
PDF	n/r	n/r	n/r	n/r
Background	0.0003	0.001	0.001	0.0002
NP and fake	0.0011	0.001	0.004	0.0007
Total systematics	0.0017	0.013	0.015	0.0024
Total uncertainty	0.0034	0.021	0.029	0.0040

Table 9: Systematic uncertainties in each bin of the $\Delta|y|$ distribution in the $e\mu$ channel. The signal modelling and the PDF uncertainty, (labeled as n/r) are limited by the statistical fluctuations in the simulated samples and are thus not reported in the table.

	1	2	3	4	5	6	7	8	9	10	11	12	13	14
1	+1.00	-0.49	-0.02	-0.03	-0.02	+0.01	-0.03	+0.02	+0.06	-0.06	-0.01	+0.03	-0.02	+0.03
2	-0.49	+1.00	-0.50	-0.04	+0.02	+0.00	+0.00	+0.01	-0.04	+0.05	-0.02	-0.01	+0.01	-0.03
3	-0.02	-0.50	+1.00	-0.47	+0.00	+0.02	-0.03	-0.02	-0.03	+0.03	+0.03	+0.01	-0.02	-0.00
4	-0.03	-0.04	-0.47	+1.00	-0.49	-0.04	-0.00	+0.04	+0.03	-0.05	+0.03	-0.03	+0.03	-0.01
5	-0.02	+0.02	+0.00	-0.49	+1.00	-0.52	+0.06	-0.04	-0.01	+0.03	-0.05	+0.00	-0.04	+0.06
6	+0.01	+0.00	+0.02	-0.04	-0.52	+1.00	-0.54	+0.04	-0.02	+0.01	+0.01	-0.00	+0.02	-0.01
7	-0.03	+0.00	-0.03	-0.00	+0.06	-0.54	+1.00	-0.54	-0.00	-0.00	-0.00	+0.04	-0.02	+0.01
8	+0.02	+0.01	-0.02	+0.04	-0.04	+0.04	-0.54	+1.00	-0.53	+0.02	+0.02	-0.05	+0.00	-0.02
9	+0.06	-0.04	-0.03	+0.03	-0.01	-0.02	-0.00	-0.53	+1.00	-0.52	+0.01	+0.00	+0.03	-0.02
10	-0.06	+0.05	+0.03	-0.05	+0.03	+0.01	-0.00	+0.02	-0.52	+1.00	-0.52	+0.02	-0.02	+0.01
11	-0.01	-0.02	+0.03	+0.03	-0.05	+0.01	-0.00	+0.02	+0.01	-0.52	+1.00	-0.49	+0.03	-0.03
12	+0.03	-0.01	+0.01	-0.03	+0.00	-0.00	+0.04	-0.05	+0.00	+0.02	-0.49	+1.00	-0.56	+0.02
13	-0.02	+0.01	-0.02	+0.03	-0.04	+0.02	-0.02	+0.00	+0.03	-0.02	+0.03	-0.56	+1.00	-0.54
14	+0.03	-0.03	-0.00	-0.01	+0.06	-0.01	+0.01	-0.02	-0.02	+0.01	-0.03	+0.02	-0.54	+1.00

Table 10: Statistical bin-bin correlations within the $\Delta|\eta|$ distribution in the $e\mu$ channel. The bin numbers are used instead of the bin boundaries. Bin 1 corresponds to $[-3.00, -2.00]$ and bin 14 to $[2.00, 3.00]$.

	1	2	3	4
1	+1.00	-0.63	+0.38	-0.38
2	-0.63	+1.00	-0.79	+0.37
3	+0.38	-0.79	+1.00	-0.61
4	-0.38	+0.37	-0.61	+1.00

Table 11: Statistical bin-bin correlations within the $\Delta|y|$ distribution in the $e\mu$ channel. The bin numbers are used instead of the bin boundaries. Bin 1 corresponds to $[-5.00, -0.71]$ and bin 4 to $[0.71, 5.00]$.

The ATLAS Collaboration

G. Aad⁸⁵, B. Abbott¹¹³, J. Abdallah¹⁵², S. Abdel Khalek¹¹⁷, O. Abdinov¹¹, R. Aben¹⁰⁷, B. Abi¹¹⁴, M. Abolins⁹⁰, O.S. AbouZeid¹⁵⁹, H. Abramowicz¹⁵⁴, H. Abreu¹⁵³, R. Abreu³⁰, Y. Abulaiti^{147a,147b}, B.S. Acharya^{165a,165b,a}, L. Adamczyk^{38a}, D.L. Adams²⁵, J. Adelman¹⁷⁷, S. Adomeit¹⁰⁰, T. Adye¹³¹, T. Agatonovic-Jovin^{13a}, J.A. Aguilar-Saavedra^{126a,126f}, M. Agustoni¹⁷, S.P. Ahlen²², F. Ahmadov^{65,b}, G. Aielli^{134a,134b}, H. Akerstedt^{147a,147b}, T.P.A. Åkesson⁸¹, G. Akimoto¹⁵⁶, A.V. Akimov⁹⁶, G.L. Alberghi^{20a,20b}, J. Albert¹⁷⁰, S. Albrand⁵⁵, M.J. Alconada Verzini⁷¹, M. Aleksa³⁰, I.N. Aleksandrov⁶⁵, C. Alexa^{26a}, G. Alexander¹⁵⁴, G. Alexandre⁴⁹, T. Alexopoulos¹⁰, M. Alhroob¹¹³, G. Alimonti^{91a}, L. Alio⁸⁵, J. Alison³¹, B.M.M. Allbrooke¹⁸, L.J. Allison⁷², P.P. Allport⁷⁴, A. Aloisio^{104a,104b}, A. Alonso³⁶, F. Alonso⁷¹, C. Alpigiani⁷⁶, A. Altheimer³⁵, B. Alvarez Gonzalez⁹⁰, M.G. Alviggi^{104a,104b}, K. Amako⁶⁶, Y. Amaral Coutinho^{24a}, C. Amelung²³, D. Amidei⁸⁹, S.P. Amor Dos Santos^{126a,126c}, A. Amorim^{126a,126b}, S. Amoroso⁴⁸, N. Amram¹⁵⁴, G. Amundsen²³, C. Anastopoulos¹⁴⁰, L.S. Ancu⁴⁹, N. Andari³⁰, T. Andeen³⁵, C.F. Anders^{58b}, G. Anders³⁰, K.J. Anderson³¹, A. Andreazza^{91a,91b}, V. Andrei^{58a}, X.S. Anduaga⁷¹, S. Angelidakis⁹, I. Angelozzi¹⁰⁷, P. Anger⁴⁴, A. Angerami³⁵, F. Anghinolfi³⁰, A.V. Anisenkov^{109,c}, N. Anjos¹², A. Annovi⁴⁷, A. Antonaki⁹, M. Antonelli⁴⁷, A. Antonov⁹⁸, J. Antos^{145b}, F. Anulli^{133a}, M. Aoki⁶⁶, L. Aperio Bella¹⁸, R. Apolle^{120,d}, G. Arabidze⁹⁰, I. Aracena¹⁴⁴, Y. Arai⁶⁶, J.P. Araque^{126a}, A.T.H. Arce⁴⁵, F.A. Arduh⁷¹, J-F. Arguin⁹⁵, S. Argyropoulos⁴², M. Arik^{19a}, A.J. Armbruster³⁰, O. Arnaez³⁰, V. Arnal⁸², H. Arnold⁴⁸, M. Arratia²⁸, O. Arslan²¹, A. Artamonov⁹⁷, G. Artoni²³, S. Asai¹⁵⁶, N. Asbah⁴², A. Ashkenazi¹⁵⁴, B. Åsman^{147a,147b}, L. Asquith⁶, K. Assamagan²⁵, R. Astalos^{145a}, M. Atkinson¹⁶⁶, N.B. Atlay¹⁴², B. Auerbach⁶, K. Augsten¹²⁸, M. Aurousseau^{146b}, G. Avolio³⁰, B. Axen¹⁵, G. Azuelos^{95,e}, Y. Azuma¹⁵⁶, M.A. Baak³⁰, A.E. Baas^{58a}, C. Bacci^{135a,135b}, H. Bachacou¹³⁷, K. Bachas¹⁵⁵, M. Backes³⁰, M. Backhaus³⁰, J. Backus Mayes¹⁴⁴, E. Badescu^{26a}, P. Bagiacchi^{133a,133b}, P. Bagnaia^{133a,133b}, Y. Bai^{33a}, T. Bain³⁵, J.T. Baines¹³¹, O.K. Baker¹⁷⁷, P. Balek¹²⁹, F. Balli¹³⁷, E. Banas³⁹, Sw. Banerjee¹⁷⁴, A.A.E. Bannoura¹⁷⁶, H.S. Bansil¹⁸, L. Barak¹⁷³, S.P. Baranov⁹⁶, E.L. Barberio⁸⁸, D. Barberis^{50a,50b}, M. Barbero⁸⁵, T. Barillari¹⁰¹, M. Barisonzi¹⁷⁶, T. Barklow¹⁴⁴, N. Barlow²⁸, S.L. Barnes⁸⁴, B.M. Barnett¹³¹, R.M. Barnett¹⁵, Z. Barnovska⁵, A. Baroncelli^{135a}, G. Barone⁴⁹, A.J. Barr¹²⁰, F. Barreiro⁸², J. Barreiro Guimarães da Costa⁵⁷, R. Bartoldus¹⁴⁴, A.E. Barton⁷², P. Bartos^{145a}, V. Bartsch¹⁵⁰, A. Bassalat¹¹⁷, A. Basye¹⁶⁶, R.L. Bates⁵³, S.J. Batista¹⁵⁹, J.R. Batley²⁸, M. Battaglia¹³⁸, M. Battistin³⁰, F. Bauer¹³⁷, H.S. Bawa^{144,f}, M.D. Beattie⁷², T. Beau⁸⁰, P.H. Beauchemin¹⁶², R. Beccherle^{124a,124b}, P. Bechtel²¹, H.P. Beck¹⁷, K. Becker¹⁷⁶, S. Becker¹⁰⁰, M. Beckingham¹⁷¹, C. Becot¹¹⁷, A.J. Beddall^{19c}, A. Beddall^{19c}, S. Bedikian¹⁷⁷, V.A. Bednyakov⁶⁵, C.P. Bee¹⁴⁹, L.J. Beemster¹⁰⁷, T.A. Beermann¹⁷⁶, M. Begel²⁵, K. Behr¹²⁰, C. Belanger-Champagne⁸⁷, P.J. Bell⁴⁹, W.H. Bell⁴⁹, G. Bella¹⁵⁴, L. Bellagamba^{20a}, A. Bellerive²⁹, M. Bellomo⁸⁶, K. Belotskiy⁹⁸, O. Beltramello³⁰, O. Benary¹⁵⁴, D. Bencheikroun^{136a}, K. Bendtz^{147a,147b}, N. Benekos¹⁶⁶, Y. Benhammou¹⁵⁴, E. Benhar Nocchioli⁴⁹, J.A. Benitez Garcia^{160b}, D.P. Benjamin⁴⁵, J.R. Bensinger²³, S. Bentvelsen¹⁰⁷, D. Berge¹⁰⁷, E. Bergeaas Kuutmann¹⁶⁷, N. Berger⁵,

F. Berghaus¹⁷⁰, J. Beringer¹⁵, C. Bernard²², P. Bernat⁷⁸, C. Bernius¹¹⁰,
 F.U. Bernlochner²¹, T. Berry⁷⁷, P. Berta¹²⁹, C. Bertella⁸³, G. Bertoli^{147a,147b},
 F. Bertolucci^{124a,124b}, C. Bertsche¹¹³, D. Bertsche¹¹³, M.I. Besana^{91a}, G.J. Besjes¹⁰⁶,
 O. Bessidskaia Bylund^{147a,147b}, M. Bessner⁴², N. Besson¹³⁷, C. Betancourt⁴⁸,
 S. Bethke¹⁰¹, W. Bhimji⁴⁶, R.M. Bianchi¹²⁵, L. Bianchini²³, M. Bianco³⁰, O. Biebel¹⁰⁰,
 S.P. Bieniek⁷⁸, K. Bierwagen⁵⁴, J. Biesiada¹⁵, M. Biglietti^{135a}, J. Bilbao De Mendizabal⁴⁹,
 H. Bilokon⁴⁷, M. Bindi⁵⁴, S. Binet¹¹⁷, A. Bingul^{19c}, C. Bini^{133a,133b}, C.W. Black¹⁵¹,
 J.E. Black¹⁴⁴, K.M. Black²², D. Blackburn¹³⁹, R.E. Blair⁶, J.-B. Blanchard¹³⁷,
 T. Blazek^{145a}, I. Bloch⁴², C. Blocker²³, W. Blum^{83,*}, U. Blumenschein⁵⁴, G.J. Bobbink¹⁰⁷,
 V.S. Bobrovnikov^{109,c}, S.S. Bocchetta⁸¹, A. Bocci⁴⁵, C. Bock¹⁰⁰, C.R. Boddy¹²⁰,
 M. Boehler⁴⁸, T.T. Boek¹⁷⁶, J.A. Bogaerts³⁰, A.G. Bogdanchikov¹⁰⁹, A. Bogouch^{92,*},
 C. Bohm^{147a}, V. Boisvert⁷⁷, T. Bold^{38a}, V. Boldea^{26a}, A.S. Boldyrev⁹⁹, M. Bomben⁸⁰,
 M. Bona⁷⁶, M. Boonekamp¹³⁷, A. Borisov¹³⁰, G. Borissov⁷², M. Borri⁸⁴, S. Borroni⁴²,
 J. Bortfeldt¹⁰⁰, V. Bortolotto^{60a}, K. Bos¹⁰⁷, D. Boscherini^{20a}, M. Bosman¹²,
 H. Boterenbrood¹⁰⁷, J. Boudreau¹²⁵, J. Bouffard², E.V. Bouhova-Thacker⁷²,
 D. Boumediene³⁴, C. Bourdarios¹¹⁷, N. Bousson¹¹⁴, S. Boutouil^{136d}, A. Boveia³¹,
 J. Boyd³⁰, I.R. Boyko⁶⁵, I. Bozic^{13a}, J. Bracinik¹⁸, A. Brandt⁸, G. Brandt¹⁵,
 O. Brandt^{58a}, U. Bratzler¹⁵⁷, B. Brau⁸⁶, J.E. Brau¹¹⁶, H.M. Braun^{176,*},
 S.F. Brazzale^{165a,165c}, B. Brelief¹⁵⁹, K. Brendlinger¹²², A.J. Brennan⁸⁸, R. Brenner¹⁶⁷,
 S. Bressler¹⁷³, K. Bristow^{146c}, T.M. Bristow⁴⁶, D. Britton⁵³, F.M. Brochu²⁸, I. Brock²¹,
 R. Brock⁹⁰, J. Bronner¹⁰¹, G. Brooijmans³⁵, T. Brooks⁷⁷, W.K. Brooks^{32b}, J. Brosamer¹⁵,
 E. Brost¹¹⁶, J. Brown⁵⁵, P.A. Bruckman de Renstrom³⁹, D. Bruncko^{145b}, R. Bruneliere⁴⁸,
 S. Brunet⁶¹, A. Bruni^{20a}, G. Bruni^{20a}, M. Bruschi^{20a}, L. Bryngemark⁸¹, T. Buanes¹⁴,
 Q. Buat¹⁴³, F. Bucci⁴⁹, P. Buchholz¹⁴², A.G. Buckley⁵³, S.I. Buda^{26a}, I.A. Budagov⁶⁵,
 F. Buehrer⁴⁸, L. Bugge¹¹⁹, M.K. Bugge¹¹⁹, O. Bulekov⁹⁸, A.C. Bundock⁷⁴,
 H. Burckhart³⁰, S. Burdin⁷⁴, B. Burghgrave¹⁰⁸, S. Burke¹³¹, I. Burmeister⁴³, E. Busato³⁴,
 D. B"uscher⁴⁸, V. B"uscher⁸³, P. Bussey⁵³, C.P. Buszello¹⁶⁷, B. Butler⁵⁷, J.M. Butler²²,
 A.I. Butt³, C.M. Buttar⁵³, J.M. Butterworth⁷⁸, P. Butti¹⁰⁷, W. Buttinger²⁸, A. Buzatu⁵³,
 M. Byszewski¹⁰, S. Cabrera Urb"an¹⁶⁸, D. Caforio^{20a,20b}, O. Cakir^{4a}, P. Calafiura¹⁵,
 A. Calandri¹³⁷, G. Calderini⁸⁰, P. Calfayan¹⁰⁰, R. Calkins¹⁰⁸, L.P. Caloba^{24a}, D. Calvet³⁴,
 S. Calvet³⁴, R. Camacho Toro⁴⁹, S. Camarda⁴², D. Cameron¹¹⁹, L.M. Caminada¹⁵,
 R. Caminal Armadans¹², S. Campana³⁰, M. Campanelli⁷⁸, A. Campoverde¹⁴⁹,
 V. Canale^{104a,104b}, A. Canepa^{160a}, M. Cano Bret⁷⁶, J. Cantero⁸², R. Cantrill^{126a},
 T. Cao⁴⁰, M.D.M. Capeans Garrido³⁰, I. Caprini^{26a}, M. Caprini^{26a}, M. Capua^{37a,37b},
 R. Caputo⁸³, R. Cardarelli^{134a}, T. Carli³⁰, G. Carlino^{104a}, L. Carminati^{91a,91b},
 S. Caron¹⁰⁶, E. Carquin^{32a}, G.D. Carrillo-Montoya^{146c}, J.R. Carter²⁸, J. Carvalho^{126a,126c},
 D. Casadei⁷⁸, M.P. Casado¹², M. Casolino¹², E. Castaneda-Miranda^{146b}, A. Castelli¹⁰⁷,
 V. Castillo Gimenez¹⁶⁸, N.F. Castro^{126a}, P. Catastini⁵⁷, A. Catinaccio³⁰, J.R. Catmore¹¹⁹,
 A. Cattai³⁰, G. Cattani^{134a,134b}, J. Caudron⁸³, V. Cavaliere¹⁶⁶, D. Cavalli^{91a},
 M. Cavalli-Sforza¹², V. Cavasinni^{124a,124b}, F. Ceradini^{135a,135b}, B.C. Cerio⁴⁵, K. Cerny¹²⁹,
 A.S. Cerqueira^{24b}, A. Cerri¹⁵⁰, L. Cerrito⁷⁶, F. Cerutti¹⁵, M. Cerv³⁰, A. Cervelli¹⁷,
 S.A. Cetin^{19b}, A. Chafaq^{136a}, D. Chakraborty¹⁰⁸, I. Chalupkova¹²⁹, P. Chang¹⁶⁶,
 B. Chapleau⁸⁷, J.D. Chapman²⁸, D. Charfeddine¹¹⁷, D.G. Charlton¹⁸, C.C. Chau¹⁵⁹,

C.A. Chavez Barajas¹⁵⁰, S. Cheatham¹⁵³, A. Chegwiddden⁹⁰, S. Chekanov⁶,
 S.V. Chekulaev^{160a}, G.A. Chelkov^{65,g}, M.A. Chelstowska⁸⁹, C. Chen⁶⁴, H. Chen²⁵,
 K. Chen¹⁴⁹, L. Chen^{33d,h}, S. Chen^{33c}, X. Chen^{33f}, Y. Chen⁶⁷, H.C. Cheng⁸⁹, Y. Cheng³¹,
 A. Cheplakov⁶⁵, R. Cherkaoui El Moursli^{136e}, V. Chernyatin^{25,*}, E. Cheu⁷,
 L. Chevalier¹³⁷, V. Chiarella⁴⁷, G. Chiefari^{104a,104b}, J.T. Childers⁶, A. Chilingarov⁷²,
 G. Chiodini^{73a}, A.S. Chisholm¹⁸, R.T. Chislett⁷⁸, A. Chitan^{26a}, M.V. Chizhov⁶⁵,
 S. Chouridou⁹, B.K.B. Chow¹⁰⁰, D. Chromek-Burckhart³⁰, M.L. Chu¹⁵², J. Chudoba¹²⁷,
 J.J. Chwastowski³⁹, L. Chytka¹¹⁵, G. Ciapetti^{133a,133b}, A.K. Ciftci^{4a}, R. Ciftci^{4a},
 D. Cinca⁵³, V. Cindro⁷⁵, A. Ciocio¹⁵, Z.H. Citron¹⁷³, M. Citterio^{91a}, M. Ciubancan^{26a},
 A. Clark⁴⁹, P.J. Clark⁴⁶, R.N. Clarke¹⁵, W. Cleland¹²⁵, J.C. Clemens⁸⁵,
 C. Clement^{147a,147b}, Y. Coadou⁸⁵, M. Cobal^{165a,165c}, A. Coccaro¹³⁹, J. Cochran⁶⁴,
 L. Coffey²³, J.G. Cogan¹⁴⁴, B. Cole³⁵, S. Cole¹⁰⁸, A.P. Colijn¹⁰⁷, J. Collot⁵⁵,
 T. Colombo^{58c}, G. Compostella¹⁰¹, P. Conde Muino^{126a,126b}, E. Coniavitis⁴⁸,
 S.H. Connell^{146b}, I.A. Connelly⁷⁷, S.M. Consonni^{91a,91b}, V. Consorti⁴⁸,
 S. Constantinescu^{26a}, C. Conta^{121a,121b}, G. Conti⁵⁷, F. Conventi^{104a,i}, M. Cooke¹⁵,
 B.D. Cooper⁷⁸, A.M. Cooper-Sarkar¹²⁰, N.J. Cooper-Smith⁷⁷, K. Copic¹⁵,
 T. Cornelissen¹⁷⁶, M. Corradi^{20a}, F. Corriveau^{87,j}, A. Corso-Radu¹⁶⁴,
 A. Cortes-Gonzalez¹², G. Cortiana¹⁰¹, G. Costa^{91a}, M.J. Costa¹⁶⁸, D. Costanzo¹⁴⁰,
 D. Côté⁸, G. Cottin²⁸, G. Cowan⁷⁷, B.E. Cox⁸⁴, K. Cranmer¹¹⁰, G. Cree²⁹,
 S. Crépe-Renaudin⁵⁵, F. Crescioli⁸⁰, W.A. Cribbs^{147a,147b}, M. Crispin Ortuzar¹²⁰,
 M. Cristinziani²¹, V. Croft¹⁰⁶, G. Crosetti^{37a,37b}, T. Cuhadar Donszelmann¹⁴⁰,
 J. Cummings¹⁷⁷, M. Curatolo⁴⁷, C. Cuthbert¹⁵¹, H. Czirr¹⁴², P. Czodrowski³,
 S. D'Auria⁵³, M. D'Onofrio⁷⁴, M.J. Da Cunha Sargedas De Sousa^{126a,126b}, C. Da Via⁸⁴,
 W. Dabrowski^{38a}, A. Dafinca¹²⁰, T. Dai⁸⁹, O. Dale¹⁴, F. Dallaire⁹⁵, C. Dallapiccola⁸⁶,
 M. Dam³⁶, A.C. Daniells¹⁸, M. Dano Hoffmann¹³⁷, V. Dao⁴⁸, G. Darbo^{50a}, S. Darmora⁸,
 J. Dassoulas⁷⁴, A. Dattagupta⁶¹, W. Davey²¹, C. David¹⁷⁰, T. Davidek¹²⁹, E. Davies^{120,d},
 M. Davies¹⁵⁴, O. Davignon⁸⁰, A.R. Davison⁷⁸, P. Davison⁷⁸, Y. Davygora^{58a}, E. Dawe¹⁴³,
 I. Dawson¹⁴⁰, R.K. Daya-Ishmukhametova⁸⁶, K. De⁸, R. de Asmundis^{104a},
 S. De Castro^{20a,20b}, S. De Cecco⁸⁰, N. De Groot¹⁰⁶, P. de Jong¹⁰⁷, H. De la Torre⁸²,
 F. De Lorenzi⁶⁴, L. De Nooij¹⁰⁷, D. De Pedis^{133a}, A. De Salvo^{133a}, U. De Sanctis¹⁵⁰,
 A. De Santo¹⁵⁰, J.B. De Vivie De Regie¹¹⁷, W.J. Dearnaley⁷², R. Debbé²⁵,
 C. Debenedetti¹³⁸, B. Dechenaux⁵⁵, D.V. Dedovich⁶⁵, I. Deigaard¹⁰⁷, J. Del Peso⁸²,
 T. Del Prete^{124a,124b}, F. Deliot¹³⁷, C.M. Delitzsch⁴⁹, M. Deliyergiyev⁷⁵, A. Dell'Acqua³⁰,
 L. Dell'Asta²², M. Dell'Orso^{124a,124b}, M. Della Pietra^{104a,i}, D. della Volpe⁴⁹,
 M. Delmastro⁵, P.A. Delsart⁵⁵, C. Deluca¹⁰⁷, D.A. DeMarco¹⁵⁹, S. Demers¹⁷⁷,
 M. Demichev⁶⁵, A. Demilly⁸⁰, S.P. Denisov¹³⁰, D. Derendarz³⁹, J.E. Derkaoui^{136d},
 F. Derue⁸⁰, P. Dervan⁷⁴, K. Desch²¹, C. Deterre⁴², P.O. Deviveiros³⁰, A. Dewhurst¹³¹,
 S. Dhaliwal¹⁰⁷, A. Di Ciaccio^{134a,134b}, L. Di Ciaccio⁵, A. Di Domenico^{133a,133b},
 C. Di Donato^{104a,104b}, A. Di Girolamo³⁰, B. Di Girolamo³⁰, A. Di Mattia¹⁵³,
 B. Di Micco^{135a,135b}, R. Di Nardo⁴⁷, A. Di Simone⁴⁸, R. Di Sipio^{20a,20b}, D. Di Valentino²⁹,
 F.A. Dias⁴⁶, M.A. Diaz^{32a}, E.B. Diehl⁸⁹, J. Dietrich¹⁶, T.A. Dietzsch^{58a}, S. Diglio⁸⁵,
 A. Dimitrievska^{13a}, J. Dingfelder²¹, P. Dita^{26a}, S. Dita^{26a}, F. Dittus³⁰, F. Djama⁸⁵,
 T. Djobava^{51b}, J.I. Djuvsland^{58a}, M.A.B. do Vale^{24c}, D. Dobos³⁰, C. Dogliani⁴⁹,

T. Doherty⁵³, T. Dohmae¹⁵⁶, J. Dolejsi¹²⁹, Z. Dolezal¹²⁹, B.A. Dolgoshein^{98,*},
 M. Donadelli^{24d}, S. Donati^{124a,124b}, P. Dondero^{121a,121b}, J. Donini³⁴, J. Dopke¹³¹,
 A. Doria^{104a}, M.T. Dova⁷¹, A.T. Doyle⁵³, M. Dris¹⁰, J. Dubbert⁸⁹, S. Dube¹⁵,
 E. Dubreuil³⁴, E. Duchovni¹⁷³, G. Duckeck¹⁰⁰, O.A. Ducu^{26a}, D. Duda¹⁷⁶, A. Dudarev³⁰,
 F. Dudziak⁶⁴, L. Duflo¹¹⁷, L. Duguid⁷⁷, M. Dührssen³⁰, M. Dunford^{58a},
 H. Duran Yildiz^{4a}, M. Düren⁵², A. Durglishvili^{51b}, D. Duschinger⁴⁴, M. Dwuznik^{38a},
 M. Dyndal^{38a}, J. Ebke¹⁰⁰, W. Edson², N.C. Edwards⁴⁶, W. Ehrenfeld²¹, T. Eifert³⁰,
 G. Eigen¹⁴, K. Einsweiler¹⁵, T. Ekelof¹⁶⁷, M. El Kacimi^{136c}, M. Ellert¹⁶⁷, S. Elles⁵,
 F. Ellinghaus⁸³, N. Ellis³⁰, J. Elmsheuser¹⁰⁰, M. Elsing³⁰, D. Emelianov¹³¹, Y. Enari¹⁵⁶,
 O.C. Endner⁸³, M. Endo¹¹⁸, R. Engelmann¹⁴⁹, J. Erdmann¹⁷⁷, A. Ereditato¹⁷,
 D. Eriksson^{147a}, G. Ernis¹⁷⁶, J. Ernst², M. Ernst²⁵, J. Ernwein¹³⁷, D. Errede¹⁶⁶,
 S. Errede¹⁶⁶, E. Ertel⁸³, M. Escalier¹¹⁷, H. Esch⁴³, C. Escobar¹²⁵, B. Esposito⁴⁷,
 A.I. Etienne¹³⁷, E. Etzion¹⁵⁴, H. Evans⁶¹, A. Ezhilov¹²³, L. Fabbri^{20a,20b}, G. Facini³¹,
 R.M. Fakhruddinov¹³⁰, S. Falciano^{133a}, R.J. Falla⁷⁸, J. Faltova¹²⁹, Y. Fang^{33a},
 M. Fanti^{91a,91b}, A. Farbin⁸, A. Farilla^{135a}, T. Farooque¹², S. Farrell¹⁵, S.M. Farrington¹⁷¹,
 P. Farthouat³⁰, F. Fassi^{136e}, P. Fassnacht³⁰, D. Fassouliotis⁹, A. Favareto^{50a,50b},
 L. Fayard¹¹⁷, P. Federic^{145a}, O.L. Fedin^{123,k}, W. Fedorko¹⁶⁹, S. Feigl³⁰, L. Felgioni⁸⁵,
 C. Feng^{33d}, E.J. Feng⁶, H. Feng⁸⁹, A.B. Fenyuk¹³⁰, S. Fernandez Perez³⁰, S. Ferrag⁵³,
 J. Ferrando⁵³, A. Ferrari¹⁶⁷, P. Ferrari¹⁰⁷, R. Ferrari^{121a}, D.E. Ferreira de Lima⁵³,
 A. Ferrer¹⁶⁸, D. Ferrere⁴⁹, C. Ferretti⁸⁹, A. Ferretto Parodi^{50a,50b}, M. Fiascaris³¹,
 F. Fiedler⁸³, A. Filipčič⁷⁵, M. Filipuzzi⁴², F. Filthaut¹⁰⁶, M. Fincke-Keeler¹⁷⁰,
 K.D. Finelli¹⁵¹, M.C.N. Fiolhais^{126a,126c}, L. Fiorini¹⁶⁸, A. Firan⁴⁰, A. Fischer²,
 J. Fischer¹⁷⁶, W.C. Fisher⁹⁰, E.A. Fitzgerald²³, M. Flechl⁴⁸, I. Fleck¹⁴², P. Fleischmann⁸⁹,
 S. Fleischmann¹⁷⁶, G.T. Fletcher¹⁴⁰, G. Fletcher⁷⁶, T. Flick¹⁷⁶, A. Floderus⁸¹,
 L.R. Flores Castillo^{60a}, M.J. Flowerdew¹⁰¹, A. Formica¹³⁷, A. Forti⁸⁴, D. Fortin^{160a},
 D. Fournier¹¹⁷, H. Fox⁷², S. Fracchia¹², P. Francavilla⁸⁰, M. Franchini^{20a,20b},
 S. Franchino³⁰, D. Francis³⁰, L. Franconi¹¹⁹, M. Franklin⁵⁷, M. Fraternali^{121a,121b},
 S.T. French²⁸, C. Friedrich⁴², F. Friedrich⁴⁴, D. Froidevaux³⁰, J.A. Frost²⁸,
 C. Fukunaga¹⁵⁷, E. Fullana Torregrosa⁸³, B.G. Fulsom¹⁴⁴, J. Fuster¹⁶⁸, C. Gabaldon⁵⁵,
 O. Gabizon¹⁷⁶, A. Gabrielli^{20a,20b}, A. Gabrielli^{133a,133b}, S. Gadatsch¹⁰⁷, S. Gadomski⁴⁹,
 G. Gagliardi^{50a,50b}, P. Gagnon⁶¹, C. Galea¹⁰⁶, B. Galhardo^{126a,126c}, E.J. Gallas¹²⁰,
 B.J. Gallop¹³¹, P. Gallus¹²⁸, G. Galster³⁶, K.K. Gan¹¹¹, J. Gao^{33b,h}, Y.S. Gao^{144,f},
 F.M. Garay Walls⁴⁶, F. Garbers¹⁷⁷, C. García¹⁶⁸, J.E. García Navarro¹⁶⁸,
 M. Garcia-Sciveres¹⁵, R.W. Gardner³¹, N. Garelli¹⁴⁴, V. Garonne³⁰, C. Gatti⁴⁷,
 G. Gaudio^{121a}, B. Gaur¹⁴², L. Gauthier⁹⁵, P. Gauzzi^{133a,133b}, I.L. Gavrilenko⁹⁶, C. Gay¹⁶⁹,
 G. Gaycken²¹, E.N. Gazis¹⁰, P. Ge^{33d}, Z. Gecse¹⁶⁹, C.N.P. Gee¹³¹, D.A.A. Geerts¹⁰⁷,
 Ch. Geich-Gimbel²¹, K. Gellerstedt^{147a,147b}, C. Gemme^{50a}, A. Gemmell⁵³, M.H. Genest⁵⁵,
 S. Gentile^{133a,133b}, M. George⁵⁴, S. George⁷⁷, D. Gerbaudo¹⁶⁴, A. Gershon¹⁵⁴,
 H. Ghazlane^{136b}, N. Ghodbane³⁴, B. Giacobbe^{20a}, S. Giagu^{133a,133b}, V. Giangiobbe¹²,
 P. Giannetti^{124a,124b}, F. Gianotti³⁰, B. Gibbard²⁵, S.M. Gibson⁷⁷, M. Gilchriese¹⁵,
 T.P.S. Gillam²⁸, D. Gillberg³⁰, G. Gilles³⁴, D.M. Gingrich^{3,e}, N. Giokaris⁹,
 M.P. Giordani^{165a,165c}, R. Giordano^{104a,104b}, F.M. Giorgi^{20a}, F.M. Giorgi¹⁶,
 P.F. Giraud¹³⁷, D. Giugni^{91a}, C. Giuliani⁴⁸, M. Giulini^{58b}, B.K. Gjelsten¹¹⁹,

S. Gkaitatzis¹⁵⁵, I. Gkialas^{155,l}, E.L. Gkoukousis¹¹⁷, L.K. Gladilin⁹⁹, C. Glasman⁸²,
 J. Glatzer³⁰, P.C.F. Glaysher⁴⁶, A. Glazov⁴², G.L. Glonti⁶², M. Goblirsch-Kolb¹⁰¹,
 J.R. Goddard⁷⁶, J. Godlewski³⁰, C. Goeringer⁸³, S. Goldfarb⁸⁹, T. Golling¹⁷⁷,
 D. Golubkov¹³⁰, A. Gomes^{126a,126b,126d}, L.S. Gomez Fajardo⁴², R. Gonalo^{126a},
 J. Goncalves Pinto Firmino Da Costa¹³⁷, L. Gonella²¹, S. Gonzalez de la Hoz¹⁶⁸,
 G. Gonzalez Parra¹², S. Gonzalez-Sevilla⁴⁹, L. Goossens³⁰, P.A. Gorbounov⁹⁷,
 H.A. Gordon²⁵, I. Gorelov¹⁰⁵, B. Gorini³⁰, E. Gorini^{73a,73b}, A. Gorišek⁷⁵, E. Gornicki³⁹,
 A.T. Goshaw⁴⁵, C. Gossling⁴³, M.I. Gostkin⁶⁵, M. Gouighri^{136a}, D. Goujdami^{136c},
 M.P. Goulette⁴⁹, A.G. Goussiou¹³⁹, C. Goy⁵, H.M.X. Grabas¹³⁸, L. Graber⁵⁴,
 I. Grabowska-Bold^{38a}, P. Grafstrom^{20a,20b}, K-J. Grahn⁴², J. Gramling⁴⁹, E. Gramstad¹¹⁹,
 S. Grancagnolo¹⁶, V. Grassi¹⁴⁹, V. Gratchev¹²³, H.M. Gray³⁰, E. Graziani^{135a},
 O.G. Grebenyuk¹²³, Z.D. Greenwood^{79,m}, K. Gregersen⁷⁸, I.M. Gregor⁴², P. Grenier¹⁴⁴,
 J. Griffiths⁸, A.A. Grillo¹³⁸, K. Grimm⁷², S. Grinstein^{12,n}, Ph. Gris³⁴, Y.V. Grishkevich⁹⁹,
 J.-F. Grivaz¹¹⁷, J.P. Grohs⁴⁴, A. Grohsjean⁴², E. Gross¹⁷³, J. Grosse-Knetter⁵⁴,
 G.C. Grossi^{134a,134b}, Z.J. Grout¹⁵⁰, L. Guan^{33b}, J. Guenther¹²⁸, F. Guescini⁴⁹,
 D. Guest¹⁷⁷, O. Gueta¹⁵⁴, C. Guicheney³⁴, E. Guido^{50a,50b}, T. Guillemin¹¹⁷, S. Guindon²,
 U. Gul⁵³, C. Gumpert⁴⁴, J. Guo³⁵, S. Gupta¹²⁰, P. Gutierrez¹¹³, N.G. Gutierrez Ortiz⁵³,
 C. Gutschew⁷⁸, N. Guttman¹⁵⁴, C. Guyot¹³⁷, C. Gwenlan¹²⁰, C.B. Gwilliam⁷⁴,
 A. Haas¹¹⁰, C. Haber¹⁵, H.K. Hadavand⁸, N. Haddad^{136e}, P. Haefner²¹, S. Hagebock²¹,
 Z. Hajduk³⁹, H. Hakobyan¹⁷⁸, M. Haleem⁴², D. Hall¹²⁰, G. Halladjian⁹⁰, G.D. Hallewell⁸⁵,
 K. Hamacher¹⁷⁶, P. Hamal¹¹⁵, K. Hamano¹⁷⁰, M. Hamer⁵⁴, A. Hamilton^{146a},
 S. Hamilton¹⁶², G.N. Hamity^{146c}, P.G. Hamnett⁴², L. Han^{33b}, K. Hanagaki¹¹⁸,
 K. Hanawa¹⁵⁶, M. Hance¹⁵, P. Hanke^{58a}, R. Hanna¹³⁷, J.B. Hansen³⁶, J.D. Hansen³⁶,
 P.H. Hansen³⁶, K. Hara¹⁶¹, A.S. Hard¹⁷⁴, T. Harenberg¹⁷⁶, F. Hariri¹¹⁷, S. Harkusha⁹²,
 D. Harper⁸⁹, R.D. Harrington⁴⁶, O.M. Harris¹³⁹, P.F. Harrison¹⁷¹, F. Hartjes¹⁰⁷,
 M. Hasegawa⁶⁷, S. Hasegawa¹⁰³, Y. Hasegawa¹⁴¹, A. Hasib¹¹³, S. Hassani¹³⁷, S. Haug¹⁷,
 M. Hauschild³⁰, R. Hauser⁹⁰, M. Havranek¹²⁷, C.M. Hawkes¹⁸, R.J. Hawkings³⁰,
 A.D. Hawkins⁸¹, T. Hayashi¹⁶¹, D. Hayden⁹⁰, C.P. Hays¹²⁰, J.M. Hays⁷⁶, H.S. Hayward⁷⁴,
 S.J. Haywood¹³¹, S.J. Head¹⁸, T. Heck⁸³, V. Hedberg⁸¹, L. Heelan⁸, S. Heim¹²²,
 T. Heim¹⁷⁶, B. Heinemann¹⁵, L. Heinrich¹¹⁰, J. Hejbal¹²⁷, L. Helary²², C. Heller¹⁰⁰,
 M. Heller³⁰, S. Hellman^{147a,147b}, D. Hellmich²¹, C. Helsen³⁰, J. Henderson¹²⁰,
 R.C.W. Henderson⁷², Y. Heng¹⁷⁴, C. Hengler⁴², A. Henrichs¹⁷⁷,
 A.M. Henriques Correia³⁰, S. Henrot-Versille¹¹⁷, G.H. Herbert¹⁶,
 Y. Hernandez Jimenez¹⁶⁸, R. Herrberg-Schubert¹⁶, G. Herten⁴⁸, R. Hertenberger¹⁰⁰,
 L. Hervas³⁰, G.G. Hesketh⁷⁸, N.P. Hessey¹⁰⁷, R. Hickling⁷⁶, E. Higon-Rodriguez¹⁶⁸,
 E. Hill¹⁷⁰, J.C. Hill²⁸, K.H. Hiller⁴², S.J. Hillier¹⁸, I. Hinchliffe¹⁵, E. Hines¹²²,
 M. Hirose¹⁵⁸, D. Hirschbuehl¹⁷⁶, J. Hobbs¹⁴⁹, N. Hod¹⁰⁷, M.C. Hodgkinson¹⁴⁰,
 P. Hodgson¹⁴⁰, A. Hoecker³⁰, M.R. Hoferkamp¹⁰⁵, F. Hoenig¹⁰⁰, D. Hoffmann⁸⁵,
 M. Hohlfeld⁸³, T.R. Holmes¹⁵, T.M. Hong¹²², L. Hooft van Huysduynen¹¹⁰,
 W.H. Hopkins¹¹⁶, Y. Horii¹⁰³, A.J. Horton¹⁴³, J-Y. Hostachy⁵⁵, S. Hou¹⁵²,
 A. Hoummada^{136a}, J. Howard¹²⁰, J. Howarth⁴², M. Hrabovsky¹¹⁵, I. Hristova¹⁶,
 J. Hrivnac¹¹⁷, T. Hryn'ova⁵, A. Hrynevich⁹³, C. Hsu^{146c}, P.J. Hsu⁸³, S.-C. Hsu¹³⁹,
 D. Hu³⁵, X. Hu⁸⁹, Y. Huang⁴², Z. Hubacek³⁰, F. Hubaut⁸⁵, F. Huegging²¹,

T.B. Huffman¹²⁰, E.W. Hughes³⁵, G. Hughes⁷², M. Huhtinen³⁰, T.A. Hülsing⁸³,
 M. Hurwitz¹⁵, N. Huseynov^{65,b}, J. Huston⁹⁰, J. Huth⁵⁷, G. Iacobucci⁴⁹, G. Iakovidis¹⁰,
 I. Ibragimov¹⁴², L. Iconomidou-Fayard¹¹⁷, E. Ideal¹⁷⁷, Z. Idrissi^{136e}, P. Iengo^{104a},
 O. Igonkina¹⁰⁷, T. Iizawa¹⁷², Y. Ikegami⁶⁶, K. Ikematsu¹⁴², M. Ikeno⁶⁶, Y. Ilchenko^{31,o},
 D. Iliadis¹⁵⁵, N. Ilic¹⁵⁹, Y. Inamaru⁶⁷, T. Ince¹⁰¹, P. Ioannou⁹, M. Iodice^{135a},
 K. Iordanidou⁹, V. Ippolito⁵⁷, A. Irles Quiles¹⁶⁸, C. Isaksson¹⁶⁷, M. Ishino⁶⁸,
 M. Ishitsuka¹⁵⁸, R. Ishmukhametov¹¹¹, C. Issever¹²⁰, S. Istin^{19a}, J.M. Iturbe Ponce⁸⁴,
 R. Iuppa^{134a,134b}, J. Ivarsson⁸¹, W. Iwanski³⁹, H. Iwasaki⁶⁶, J.M. Izen⁴¹, V. Izzo^{104a},
 B. Jackson¹²², M. Jackson⁷⁴, P. Jackson¹, M.R. Jaekel³⁰, V. Jain², K. Jakobs⁴⁸,
 S. Jakobsen³⁰, T. Jakoubek¹²⁷, J. Jakubek¹²⁸, D.O. Jamin¹⁵², D.K. Jana⁷⁹, E. Jansen⁷⁸,
 H. Jansen³⁰, J. Janssen²¹, M. Janus¹⁷¹, G. Jarlskog⁸¹, N. Javadov^{65,b}, T. Javürek⁴⁸,
 L. Jeanty¹⁵, J. Jejelava^{51a,p}, G.-Y. Jeng¹⁵¹, D. Jennens⁸⁸, P. Jenni^{48,q}, J. Jentzsch⁴³,
 C. Jeske¹⁷¹, S. Jézéquel⁵, H. Ji¹⁷⁴, J. Jia¹⁴⁹, Y. Jiang^{33b}, M. Jimenez Belenguer⁴²,
 S. Jin^{33a}, A. Jinaru^{26a}, O. Jinnouchi¹⁵⁸, M.D. Joergensen³⁶, K.E. Johansson^{147a,147b},
 P. Johansson¹⁴⁰, K.A. Johns⁷, K. Jon-And^{147a,147b}, G. Jones¹⁷¹, R.W.L. Jones⁷²,
 T.J. Jones⁷⁴, J. Jongmanns^{58a}, P.M. Jorge^{126a,126b}, K.D. Joshi⁸⁴, J. Jovicevic¹⁴⁸, X. Ju¹⁷⁴,
 C.A. Jung⁴³, P. Jussel⁶², A. Juste Rozas^{12,n}, M. Kaci¹⁶⁸, A. Kaczmarska³⁹, M. Kado¹¹⁷,
 H. Kagan¹¹¹, M. Kagan¹⁴⁴, E. Kajomovitz⁴⁵, C.W. Kalderon¹²⁰, S. Kama⁴⁰,
 A. Kamenshchikov¹³⁰, N. Kanaya¹⁵⁶, M. Kaneda³⁰, S. Kaneti²⁸, V.A. Kantserov⁹⁸,
 J. Kanzaki⁶⁶, B. Kaplan¹¹⁰, A. Kapliy³¹, D. Kar⁵³, K. Karakostas¹⁰, N. Karastathis¹⁰,
 M.J. Kareem⁵⁴, M. Karnevskiy⁸³, S.N. Karpov⁶⁵, Z.M. Karpova⁶⁵, K. Karthik¹¹⁰,
 V. Kartvelishvili⁷², A.N. Karyukhin¹³⁰, L. Kashif¹⁷⁴, G. Kasieczka^{58b}, R.D. Kass¹¹¹,
 A. Kastanas¹⁴, Y. Kataoka¹⁵⁶, A. Katre⁴⁹, J. Katzy⁴², V. Kaushik⁷, K. Kawagoe⁷⁰,
 T. Kawamoto¹⁵⁶, G. Kawamura⁵⁴, S. Kazama¹⁵⁶, V.F. Kazanin¹⁰⁹, M.Y. Kazarinov⁶⁵,
 R. Keeler¹⁷⁰, R. Kehoe⁴⁰, M. Keil⁵⁴, J.S. Keller⁴², J.J. Kempster⁷⁷, H. Keoshkerian⁵,
 O. Kepka¹²⁷, B.P. Kerševan⁷⁵, S. Kersten¹⁷⁶, K. Kessoku¹⁵⁶, J. Keung¹⁵⁹, R.A. Keyes⁸⁷,
 F. Khalil-zada¹¹, H. Khandanyan^{147a,147b}, A. Khanov¹¹⁴, A. Kharlamov¹⁰⁹,
 A. Khodinov⁹⁸, A. Khomich^{58a}, T.J. Khoo²⁸, G. Khorauli²¹, V. Khovanskiy⁹⁷,
 E. Khramov⁶⁵, J. Khubua^{51b}, H.Y. Kim⁸, H. Kim^{147a,147b}, S.H. Kim¹⁶¹, N. Kimura¹⁷²,
 O. Kind¹⁶, B.T. King⁷⁴, M. King¹⁶⁸, R.S.B. King¹²⁰, S.B. King¹⁶⁹, J. Kirk¹³¹,
 A.E. Kiryunin¹⁰¹, T. Kishimoto⁶⁷, D. Kisielewska^{38a}, F. Kiss⁴⁸, K. Kiuchi¹⁶¹,
 E. Kladiva^{145b}, M. Klein⁷⁴, U. Klein⁷⁴, K. Kleinknecht⁸³, P. Klimek^{147a,147b},
 A. Klimentov²⁵, R. Klingenberg⁴³, J.A. Klinger⁸⁴, T. Klioutchnikova³⁰, P.F. Klok¹⁰⁶,
 E.-E. Kluge^{58a}, P. Kluit¹⁰⁷, S. Kluth¹⁰¹, E. Kneringer⁶², E.B.F.G. Knoops⁸⁵, A. Knue⁵³,
 D. Kobayashi¹⁵⁸, T. Kobayashi¹⁵⁶, M. Kobel⁴⁴, M. Kocian¹⁴⁴, P. Kodys¹²⁹, T. Koffas²⁹,
 E. Koffeman¹⁰⁷, L.A. Kogan¹²⁰, S. Kohlmann¹⁷⁶, Z. Kohout¹²⁸, T. Kohriki⁶⁶, T. Koi¹⁴⁴,
 H. Kolanoski¹⁶, I. Koletsou⁵, J. Koll⁹⁰, A.A. Komar^{96,*}, Y. Komori¹⁵⁶, T. Kondo⁶⁶,
 N. Kondrashova⁴², K. Köneke⁴⁸, A.C. König¹⁰⁶, S. König⁸³, T. Kono^{66,r},
 R. Konoplich^{110,s}, N. Konstantinidis⁷⁸, R. Kopeliainsky¹⁵³, S. Koperny^{38a}, L. Köpke⁸³,
 A.K. Kopp⁴⁸, K. Korcyl³⁹, K. Kordas¹⁵⁵, A. Korn⁷⁸, A.A. Korol^{109,c}, I. Korolkov¹²,
 E.V. Korolkova¹⁴⁰, V.A. Korotkov¹³⁰, O. Kortner¹⁰¹, S. Kortner¹⁰¹, V.V. Kostyukhin²¹,
 V.M. Kotov⁶⁵, A. Kotwal⁴⁵, A. Kourkouveli-Charalampidi¹⁵⁵, C. Kourkouvelis⁹,
 V. Kouskoura²⁵, A. Koutsman^{160a}, R. Kowalewski¹⁷⁰, T.Z. Kowalski^{38a}, W. Kozanecki¹³⁷,

A.S. Kozhin¹³⁰, V.A. Kramarenko⁹⁹, G. Kramberger⁷⁵, D. Krasnopevtsev⁹⁸,
 M.W. Krasny⁸⁰, A. Krasznahorkay³⁰, J.K. Kraus²¹, A. Kravchenko²⁵, S. Kreiss¹¹⁰,
 M. Kretz^{58c}, J. Kretzschmar⁷⁴, K. Kreutzfeldt⁵², P. Krieger¹⁵⁹, K. Kroeninger⁵⁴,
 H. Kroha¹⁰¹, J. Kroll¹²², J. Kroseberg²¹, J. Krstic^{13a}, U. Kruchonak⁶⁵, H. Krüger²¹,
 T. Kruker¹⁷, N. Krumnack⁶⁴, Z.V. Krumshteyn⁶⁵, A. Kruse¹⁷⁴, M.C. Kruse⁴⁵,
 M. Kruskal²², T. Kubota⁸⁸, H. Kucuk⁷⁸, S. Kuday^{4c}, S. Kuehn⁴⁸, A. Kugel^{58c}, A. Kuhl¹³⁸,
 T. Kuhl⁴², V. Kukhtin⁶⁵, Y. Kulchitsky⁹², S. Kuleshov^{32b}, M. Kuna^{133a,133b}, T. Kunigo⁶⁸,
 A. Kupco¹²⁷, H. Kurashige⁶⁷, Y.A. Kurochkin⁹², R. Kurumida⁶⁷, V. Kus¹²⁷,
 E.S. Kuwertz¹⁴⁸, M. Kuze¹⁵⁸, J. Kvita¹¹⁵, D. Kyriazopoulos¹⁴⁰, A. La Rosa⁴⁹,
 L. La Rotonda^{37a,37b}, C. Lacasta¹⁶⁸, F. Lacava^{133a,133b}, J. Lacey²⁹, H. Lacker¹⁶,
 D. Lacour⁸⁰, V.R. Lacuesta¹⁶⁸, E. Ladygin⁶⁵, R. Lafaye⁵, B. Laforge⁸⁰, T. Lagouri¹⁷⁷,
 S. Lai⁴⁸, H. Laier^{58a}, L. Lambourne⁷⁸, S. Lammers⁶¹, C.L. Lampen⁷, W. Lampl⁷,
 E. Lançon¹³⁷, U. Landgraf⁴⁸, M.P.J. Landon⁷⁶, V.S. Lang^{58a}, A.J. Lankford¹⁶⁴,
 F. Lanni²⁵, K. Lantzsch³⁰, S. Laplace⁸⁰, C. Lapoire²¹, J.F. Laporte¹³⁷, T. Lari^{91a},
 F. Lasagni Manghi^{20a,20b}, M. Lassnig³⁰, P. Laurelli⁴⁷, W. Lavrijsen¹⁵, A.T. Law¹³⁸,
 P. Laycock⁷⁴, O. Le Dortz⁸⁰, E. Le Guirriec⁸⁵, E. Le Menedeu¹², T. LeCompte⁶,
 F. Ledroit-Guillon⁵⁵, C.A. Lee^{146b}, H. Lee¹⁰⁷, S.C. Lee¹⁵², L. Lee¹, G. Lefebvre⁸⁰,
 M. Lefebvre¹⁷⁰, F. Legger¹⁰⁰, C. Leggett¹⁵, A. Lehan⁷⁴, G. Lehmann Miotto³⁰, X. Lei⁷,
 W.A. Light²⁹, A. Leisos¹⁵⁵, A.G. Leister¹⁷⁷, M.A.L. Leite^{24d}, R. Leitner¹²⁹,
 D. Lellouch¹⁷³, B. Lemmer⁵⁴, K.J.C. Leney⁷⁸, T. Lenz²¹, G. Lenzen¹⁷⁶, B. Lenzi³⁰,
 R. Leone⁷, S. Leone^{124a,124b}, C. Leonidopoulos⁴⁶, S. Leontsinis¹⁰, C. Leroy⁹⁵,
 C.G. Lester²⁸, C.M. Lester¹²², M. Levchenko¹²³, J. Levêque⁵, D. Levin⁸⁹,
 L.J. Levinson¹⁷³, M. Levy¹⁸, A. Lewis¹²⁰, G.H. Lewis¹¹⁰, A.M. Leyko²¹, M. Leyton⁴¹,
 B. Li^{33b,t}, B. Li⁸⁵, H. Li¹⁴⁹, H.L. Li³¹, L. Li⁴⁵, L. Li^{33e}, S. Li⁴⁵, Y. Li^{33c,u}, Z. Liang¹³⁸,
 H. Liao³⁴, B. Liberti^{134a}, P. Lichard³⁰, K. Lie¹⁶⁶, J. Liebal²¹, W. Liebig¹⁴, C. Limbach²¹,
 A. Limosani¹⁵¹, S.C. Lin^{152,v}, T.H. Lin⁸³, F. Linde¹⁰⁷, B.E. Lindquist¹⁴⁹,
 J.T. Linnemann⁹⁰, E. Lipeles¹²², A. Lipniacka¹⁴, M. Lisovyi⁴², T.M. Liss¹⁶⁶,
 D. Lissauer²⁵, A. Lister¹⁶⁹, A.M. Litke¹³⁸, B. Liu¹⁵², D. Liu¹⁵², J.B. Liu^{33b}, K. Liu^{33b,w},
 L. Liu⁸⁹, M. Liu⁴⁵, M. Liu^{33b}, Y. Liu^{33b}, M. Livan^{121a,121b}, A. Lleres⁵⁵,
 J. Llorente Merino⁸², S.L. Lloyd⁷⁶, F. Lo Sterzo¹⁵², E. Lobodzinska⁴², P. Loch⁷,
 W.S. Lockman¹³⁸, F.K. Loebinger⁸⁴, A.E. Loevschall-Jensen³⁶, A. Loginov¹⁷⁷, T. Lohse¹⁶,
 K. Lohwasser⁴², M. Lokajicek¹²⁷, V.P. Lombardo⁵, B.A. Long²², J.D. Long⁸⁹,
 R.E. Long⁷², L. Lopes^{126a}, D. Lopez Mateos⁵⁷, B. Lopez Paredes¹⁴⁰, I. Lopez Paz¹²,
 J. Lorenz¹⁰⁰, N. Lorenzo Martinez⁶¹, M. Losada¹⁶³, P. Loscutoff¹⁵, X. Lou⁴¹,
 A. Lounis¹¹⁷, J. Love⁶, P.A. Love⁷², A.J. Lowe^{144,f}, F. Lu^{33a}, N. Lu⁸⁹, H.J. Lubatti¹³⁹,
 C. Luci^{133a,133b}, A. Lucotte⁵⁵, F. Luehring⁶¹, W. Lukas⁶², L. Luminari^{133a},
 O. Lundberg^{147a,147b}, B. Lund-Jensen¹⁴⁸, M. Lungwitz⁸³, D. Lynn²⁵, R. Lysak¹²⁷,
 E. Lytken⁸¹, H. Ma²⁵, L.L. Ma^{33d}, G. Maccarrone⁴⁷, A. Macchiolo¹⁰¹,
 J. Machado Miguens^{126a,126b}, D. Macina³⁰, D. Madaffari⁸⁵, R. Madar⁴⁸, H.J. Maddocks⁷²,
 W.F. Mader⁴⁴, A. Madsen¹⁶⁷, M. Maeno⁸, T. Maeno²⁵, A. Maevskiy⁹⁹, E. Magradze⁵⁴,
 K. Mahboubi⁴⁸, J. Mahlstedt¹⁰⁷, S. Mahmoud⁷⁴, C. Maiani¹³⁷, C. Maidantchik^{24a},
 A.A. Maier¹⁰¹, A. Maio^{126a,126b,126d}, S. Majewski¹¹⁶, Y. Makida⁶⁶, N. Makovec¹¹⁷,
 P. Mal^{137,x}, B. Malaescu⁸⁰, Pa. Malecki³⁹, V.P. Maleev¹²³, F. Malek⁵⁵, U. Mallik⁶³,

D. Malon⁶, C. Malone¹⁴⁴, S. Maltezos¹⁰, V.M. Malyshev¹⁰⁹, S. Malyukov³⁰,
 J. Mamuzic^{13b}, B. Mandelli³⁰, L. Mandelli^{91a}, I. Mandić⁷⁵, R. Mandrysch⁶³,
 J. Maneira^{126a,126b}, A. Manfredini¹⁰¹, L. Manhaes de Andrade Filho^{24b},
 J.A. Manjarres Ramos^{160b}, A. Mann¹⁰⁰, P.M. Manning¹³⁸, A. Manousakis-Katsikakis⁹,
 B. Mansoulie¹³⁷, R. Mantifel⁸⁷, L. Mapelli³⁰, L. March^{146c}, J.F. Marchand²⁹,
 G. Marchiori⁸⁰, M. Marcisovsky¹²⁷, C.P. Marino¹⁷⁰, M. Marjanovic^{13a}, F. Marroquin^{24a},
 S.P. Marsden⁸⁴, Z. Marshall¹⁵, L.F. Marti¹⁷, S. Marti-Garcia¹⁶⁸, B. Martin³⁰,
 B. Martin⁹⁰, T.A. Martin¹⁷¹, V.J. Martin⁴⁶, B. Martin dit Latour¹⁴, H. Martinez¹³⁷,
 M. Martinez^{12,n}, S. Martin-Haugh¹³¹, A.C. Martyniuk⁷⁸, M. Marx¹³⁹, F. Marzano^{133a},
 A. Marzin³⁰, L. Masetti⁸³, T. Mashimo¹⁵⁶, R. Mashinistov⁹⁶, J. Masik⁸⁴,
 A.L. Maslennikov^{109,c}, I. Massa^{20a,20b}, L. Massa^{20a,20b}, N. Massol⁵, P. Mastrandrea¹⁴⁹,
 A. Mastroberardino^{37a,37b}, T. Masubuchi¹⁵⁶, P. Mättig¹⁷⁶, J. Mattmann⁸³, J. Maurer^{26a},
 S.J. Maxfield⁷⁴, D.A. Maximov^{109,c}, R. Mazini¹⁵², L. Mazzaferro^{134a,134b},
 G. Mc Goldrick¹⁵⁹, S.P. Mc Kee⁸⁹, A. McCarn⁸⁹, R.L. McCarthy¹⁴⁹, T.G. McCarthy²⁹,
 N.A. McCubbin¹³¹, K.W. McFarlane^{56,*}, J.A. Mcfayden⁷⁸, G. Mchedlidze⁵⁴,
 S.J. McMahon¹³¹, R.A. McPherson^{170,j}, J. Mechnich¹⁰⁷, M. Medinnis⁴², S. Meehan³¹,
 S. Mehlhase¹⁰⁰, A. Mehta⁷⁴, K. Meier^{58a}, C. Meineck¹⁰⁰, B. Meirose⁴¹, C. Melachrinou³¹,
 B.R. Mellado Garcia^{146c}, F. Meloni¹⁷, A. Mengarelli^{20a,20b}, S. Menke¹⁰¹, E. Meoni¹⁶²,
 K.M. Mercurio⁵⁷, S. Mergelmeyer²¹, N. Meric¹³⁷, P. Mermod⁴⁹, L. Merola^{104a,104b},
 C. Meroni^{91a}, F.S. Merritt³¹, H. Merritt¹¹¹, A. Messina^{30,y}, J. Metcalfe²⁵, A.S. Mete¹⁶⁴,
 C. Meyer⁸³, C. Meyer¹²², J-P. Meyer¹³⁷, J. Meyer³⁰, R.P. Middleton¹³¹, S. Migas⁷⁴,
 S. Miglioranzì^{165a,165c}, L. Mijović²¹, G. Mikenberg¹⁷³, M. Mikestikova¹²⁷, M. Mikuž⁷⁵,
 A. Milic³⁰, D.W. Miller³¹, C. Mills⁴⁶, A. Milov¹⁷³, D.A. Milstead^{147a,147b},
 A.A. Minaenko¹³⁰, Y. Minami¹⁵⁶, I.A. Minashvili⁶⁵, A.I. Mincer¹¹⁰, B. Mindur^{38a},
 M. Mineev⁶⁵, Y. Ming¹⁷⁴, L.M. Mir¹², G. Mirabelli^{133a}, T. Mitani¹⁷², J. Mitrevski¹⁰⁰,
 V.A. Mitsou¹⁶⁸, A. Miucci⁴⁹, P.S. Miyagawa¹⁴⁰, J.U. Mjörnmark⁸¹, T. Moa^{147a,147b},
 K. Mochizuki⁸⁵, S. Mohapatra³⁵, W. Mohr⁴⁸, S. Molander^{147a,147b}, R. Moles-Valls¹⁶⁸,
 K. Mönig⁴², C. Monini⁵⁵, J. Monk³⁶, E. Monnier⁸⁵, J. Montejo Berlingen¹²,
 F. Monticelli⁷¹, S. Monzani^{133a,133b}, R.W. Moore³, N. Morange⁶³, D. Moreno¹⁶³,
 M. Moreno Llácer⁵⁴, P. Morettini^{50a}, M. Morgenstern⁴⁴, M. Morii⁵⁷, V. Morisbak¹¹⁹,
 S. Moritz⁸³, A.K. Morley¹⁴⁸, G. Mornacchi³⁰, J.D. Morris⁷⁶, A. Morton⁴², L. Morvaj¹⁰³,
 H.G. Moser¹⁰¹, M. Mosidze^{51b}, J. Moss¹¹¹, K. Motohashi¹⁵⁸, R. Mount¹⁴⁴,
 E. Mountricha²⁵, S.V. Mouraviev^{96,*}, E.J.W. Moyses⁸⁶, S. Muanza⁸⁵, R.D. Mudd¹⁸,
 F. Mueller^{58a}, J. Mueller¹²⁵, K. Mueller²¹, T. Mueller²⁸, T. Mueller⁸³,
 D. Muenstermann⁴⁹, Y. Munwes¹⁵⁴, J.A. Murillo Quijada¹⁸, W.J. Murray^{171,131},
 H. Musheghyan⁵⁴, E. Musto¹⁵³, A.G. Myagkov^{130,z}, M. Myska¹²⁸, O. Nackenhorst⁵⁴,
 J. Nadal⁵⁴, K. Nagai¹²⁰, R. Nagai¹⁵⁸, Y. Nagai⁸⁵, K. Nagano⁶⁶, A. Nagarkar¹¹¹,
 Y. Nagasaka⁵⁹, K. Nagata¹⁶¹, M. Nagel¹⁰¹, A.M. Nairz³⁰, Y. Nakahama³⁰,
 K. Nakamura⁶⁶, T. Nakamura¹⁵⁶, I. Nakano¹¹², H. Namasivayam⁴¹, G. Nanava²¹,
 R.F. Naranjo Garcia⁴², R. Narayan^{58b}, T. Nattermann²¹, T. Naumann⁴², G. Navarro¹⁶³,
 R. Nayyar⁷, H.A. Neal⁸⁹, P.Yu. Nechaeva⁹⁶, T.J. Neep⁸⁴, P.D. Nef¹⁴⁴, A. Negri^{121a,121b},
 G. Negri³⁰, M. Negrini^{20a}, S. Nektarijevic⁴⁹, C. Nellist¹¹⁷, A. Nelson¹⁶⁴, T.K. Nelson¹⁴⁴,
 S. Nemecek¹²⁷, P. Nemethy¹¹⁰, A.A. Nepomuceno^{24a}, M. Nessi^{30,aa}, M.S. Neubauer¹⁶⁶,

M. Neumann¹⁷⁶, R.M. Neves¹¹⁰, P. Nevski²⁵, P.R. Newman¹⁸, D.H. Nguyen⁶,
R.B. Nickerson¹²⁰, R. Nicolaidou¹³⁷, B. Nicquevert³⁰, J. Nielsen¹³⁸, N. Nikiforou³⁵,
A. Nikiforov¹⁶, V. Nikolaenko^{130,z}, I. Nikolic-Audit⁸⁰, K. Nikolics⁴⁹, K. Nikolopoulos¹⁸,
P. Nilsson²⁵, Y. Ninomiya¹⁵⁶, A. Nisati^{133a}, R. Nisius¹⁰¹, T. Nobe¹⁵⁸, L. Nodulman⁶,
M. Nomachi¹¹⁸, I. Nomidis²⁹, S. Norberg¹¹³, M. Nordberg³⁰, O. Novgorodova⁴⁴,
S. Nowak¹⁰¹, M. Nozaki⁶⁶, L. Nozka¹¹⁵, K. Ntekas¹⁰, G. Nunes Hanninger⁸⁸,
T. Nunnemann¹⁰⁰, E. Nurse⁷⁸, F. Nuti⁸⁸, B.J. O'Brien⁴⁶, F. O'grady⁷, D.C. O'Neil¹⁴³,
V. O'Shea⁵³, F.G. Oakham^{29,e}, H. Oberlack¹⁰¹, T. Obermann²¹, J. Ocariz⁸⁰, A. Ochi⁶⁷,
M.I. Ochoa⁷⁸, S. Oda⁷⁰, S. Odaka⁶⁶, H. Ogren⁶¹, A. Oh⁸⁴, S.H. Oh⁴⁵, C.C. Ohm¹⁵,
H. Ohman¹⁶⁷, H. Oide³⁰, W. Okamura¹¹⁸, H. Okawa¹⁶¹, Y. Okumura³¹, T. Okuyama¹⁵⁶,
A. Olariu^{26a}, A.G. Olchevski⁶⁵, S.A. Olivares Pino⁴⁶, D. Oliveira Damazio²⁵,
E. Oliver Garcia¹⁶⁸, A. Olszewski³⁹, J. Olszowska³⁹, A. Onofre^{126a,126e}, P.U.E. Onyisi^{31,o},
C.J. Oram^{160a}, M.J. Oreglia³¹, Y. Oren¹⁵⁴, D. Orestano^{135a,135b}, N. Orlando^{73a,73b},
C. Oropeza Barrera⁵³, R.S. Orr¹⁵⁹, B. Osculati^{50a,50b}, R. Ospanov¹²²,
G. Otero y Garzon²⁷, H. Otono⁷⁰, M. Ouchrif^{136d}, E.A. Ouellette¹⁷⁰, F. Ould-Saada¹¹⁹,
A. Ouraou¹³⁷, K.P. Oussoren¹⁰⁷, Q. Ouyang^{33a}, A. Ovcharova¹⁵, M. Owen⁸⁴,
V.E. Ozcan^{19a}, N. Ozturk⁸, K. Pachal¹²⁰, A. Pacheco Pages¹², C. Padilla Aranda¹²,
M. Pagáčová⁴⁸, S. Pagan Griso¹⁵, E. Paganis¹⁴⁰, C. Pahl¹⁰¹, F. Paige²⁵, P. Pais⁸⁶,
K. Pajchel¹¹⁹, G. Palacino^{160b}, S. Palestini³⁰, M. Palka^{38b}, D. Pallin³⁴, A. Palma^{126a,126b},
J.D. Palmer¹⁸, Y.B. Pan¹⁷⁴, E. Panagiotopoulou¹⁰, J.G. Panduro Vazquez⁷⁷, P. Pani¹⁰⁷,
N. Panikashvili⁸⁹, S. Panitkin²⁵, D. Pantea^{26a}, L. Paolozzi^{134a,134b},
Th.D. Papadopoulou¹⁰, K. Papageorgiou^{155,l}, A. Paramonov⁶, D. Paredes Hernandez¹⁵⁵,
M.A. Parker²⁸, F. Parodi^{50a,50b}, J.A. Parsons³⁵, U. Parzefall⁴⁸, E. Pasqualucci^{133a},
S. Passaggio^{50a}, A. Passeri^{135a}, F. Pastore^{135a,135b,*}, Fr. Pastore⁷⁷, G. Pásztor²⁹,
S. Patarraia¹⁷⁶, N.D. Patel¹⁵¹, J.R. Pater⁸⁴, S. Patricelli^{104a,104b}, T. Pauly³⁰, J. Pearce¹⁷⁰,
L.E. Pedersen³⁶, M. Pedersen¹¹⁹, S. Pedraza Lopez¹⁶⁸, R. Pedro^{126a,126b},
S.V. Peleganchuk¹⁰⁹, D. Pelikan¹⁶⁷, H. Peng^{33b}, B. Penning³¹, J. Penwell⁶¹,
D.V. Perepelitsa²⁵, E. Perez Codina^{160a}, M.T. Pérez García-Estañ¹⁶⁸, L. Perini^{91a,91b},
H. Pernegger³⁰, S. Perrella^{104a,104b}, R. Perrino^{73a}, R. Peschke⁴², V.D. Peshekhonov⁶⁵,
K. Peters³⁰, R.F.Y. Peters⁸⁴, B.A. Petersen³⁰, T.C. Petersen³⁶, E. Petit⁴²,
A. Petridis^{147a,147b}, C. Petridou¹⁵⁵, E. Petrolu^{133a}, F. Petrucci^{135a,135b}, N.E. Pettersson¹⁵⁸,
R. Pezoa^{32b}, P.W. Phillips¹³¹, G. Piacquadio¹⁴⁴, E. Pianori¹⁷¹, A. Picazio⁴⁹, E. Piccaro⁷⁶,
M. Piccinini^{20a,20b}, R. Piegai²⁷, D.T. Pignotti¹¹¹, J.E. Pilcher³¹, A.D. Pilkington⁷⁸,
J. Pina^{126a,126b,126d}, M. Pinamonti^{165a,165c,ab}, A. Pinder¹²⁰, J.L. Pinfold³, A. Pingel³⁶,
B. Pinto^{126a}, S. Pires⁸⁰, M. Pitt¹⁷³, C. Pizio^{91a,91b}, L. Plazak^{145a}, M.-A. Pleier²⁵,
V. Pleskot¹²⁹, E. Plotnikova⁶⁵, P. Plucinski^{147a,147b}, D. Pluth⁶⁴, S. Poddar^{58a},
F. Podlyski³⁴, R. Poettgen⁸³, L. Poggioli¹¹⁷, D. Pohl²¹, M. Pohl⁴⁹, G. Polesello^{121a},
A. Policicchio^{37a,37b}, R. Polifka¹⁵⁹, A. Polini^{20a}, C.S. Pollard⁴⁵, V. Polychronakos²⁵,
K. Pommès³⁰, L. Pontecorvo^{133a}, B.G. Pope⁹⁰, G.A. Popeneciu^{26b}, D.S. Popovic^{13a},
A. Poppleton³⁰, X. Portell Bueso¹², S. Pospisil¹²⁸, K. Potamianos¹⁵, I.N. Potrap⁶⁵,
C.J. Potter¹⁵⁰, C.T. Potter¹¹⁶, G. Poulard³⁰, J. Poveda⁶¹, V. Pozdnyakov⁶⁵,
P. Pralavorio⁸⁵, A. Pranko¹⁵, S. Prasad³⁰, R. Pravahan⁸, S. Prell⁶⁴, D. Price⁸⁴, J. Price⁷⁴,
L.E. Price⁶, D. Prieur¹²⁵, M. Primavera^{73a}, M. Proissl⁴⁶, K. Prokofiev⁴⁷, F. Prokoshin^{32b},

E. Protopapadaki¹³⁷, S. Protopopescu²⁵, J. Proudfoot⁶, M. Przybycien^{38a},
 H. Przysiesniak⁵, E. Ptacek¹¹⁶, D. Puddu^{135a,135b}, E. Poeschel⁸⁶, D. Puldon¹⁴⁹,
 M. Purohit^{25,ac}, P. Puzo¹¹⁷, J. Qian⁸⁹, G. Qin⁵³, Y. Qin⁸⁴, A. Quadt⁵⁴, D.R. Quarrie¹⁵,
 W.B. Quayle^{165a,165b}, M. Queitsch-Maitland⁸⁴, D. Quilty⁵³, A. Qureshi^{160b}, V. Radeka²⁵,
 V. Radescu⁴², S.K. Radhakrishnan¹⁴⁹, P. Radloff¹¹⁶, P. Rados⁸⁸, F. Ragusa^{91a,91b},
 G. Rahal¹⁷⁹, S. Rajagopalan²⁵, M. Rammensee³⁰, C. Rangel-Smith¹⁶⁷, K. Rao¹⁶⁴,
 F. Rauscher¹⁰⁰, T.C. Rave⁴⁸, T. Ravenscroft⁵³, M. Raymond³⁰, A.L. Read¹¹⁹,
 N.P. Readioff⁷⁴, D.M. Rebuzzi^{121a,121b}, A. Redelbach¹⁷⁵, G. Redlinger²⁵, R. Reece¹³⁸,
 K. Reeves⁴¹, L. Rehnisch¹⁶, H. Reisin²⁷, M. Relich¹⁶⁴, C. Rembser³⁰, H. Ren^{33a},
 Z.L. Ren¹⁵², A. Renaud¹¹⁷, M. Rescigno^{133a}, S. Resconi^{91a}, O.L. Rezanova^{109,c},
 P. Reznicek¹²⁹, R. Rezvani⁹⁵, R. Richter¹⁰¹, M. Ridel⁸⁰, P. Rieck¹⁶, J. Rieger⁵⁴,
 M. Rijssenbeek¹⁴⁹, A. Rimoldi^{121a,121b}, L. Rinaldi^{20a}, E. Ritsch⁶², I. Riu¹²,
 F. Rizatdinova¹¹⁴, E. Rizvi⁷⁶, S.H. Robertson^{87,j}, A. Robichaud-Veronneau⁸⁷,
 D. Robinson²⁸, J.E.M. Robinson⁸⁴, A. Robson⁵³, C. Roda^{124a,124b}, L. Rodrigues³⁰,
 S. Roe³⁰, O. Røhne¹¹⁹, S. Rolli¹⁶², A. Romaniouk⁹⁸, M. Romano^{20a,20b},
 E. Romero Adam¹⁶⁸, N. Rompotis¹³⁹, M. Ronzani⁴⁸, L. Roos⁸⁰, E. Ros¹⁶⁸, S. Rosati^{133a},
 K. Rosbach⁴⁹, M. Rose⁷⁷, P. Rose¹³⁸, P.L. Rosendahl¹⁴, O. Rosenthal¹⁴²,
 V. Rossetti^{147a,147b}, E. Rossi^{104a,104b}, L.P. Rossi^{50a}, R. Rosten¹³⁹, M. Rotaru^{26a},
 I. Roth¹⁷³, J. Rothberg¹³⁹, D. Rousseau¹¹⁷, C.R. Royon¹³⁷, A. Rozanov⁸⁵, Y. Rozen¹⁵³,
 X. Ruan^{146c}, F. Rubbo¹², I. Rubinskiy⁴², V.I. Rud⁹⁹, C. Rudolph⁴⁴, M.S. Rudolph¹⁵⁹,
 F. Rühr⁴⁸, A. Ruiz-Martinez³⁰, Z. Rurikova⁴⁸, N.A. Rusakovich⁶⁵, A. Ruschke¹⁰⁰,
 H.L. Russell¹³⁹, J.P. Rutherford⁷, N. Ruthmann⁴⁸, Y.F. Ryabov¹²³, M. Rybar¹²⁹,
 G. Rybkin¹¹⁷, N.C. Ryder¹²⁰, A.F. Saavedra¹⁵¹, G. Sabato¹⁰⁷, S. Sacerdoti²⁷,
 A. Saddique³, I. Sadeh¹⁵⁴, H.F-W. Sadrozinski¹³⁸, R. Sadykov⁶⁵, F. Safai Tehrani^{133a},
 H. Sakamoto¹⁵⁶, Y. Sakurai¹⁷², G. Salamanna^{135a,135b}, A. Salamon^{134a}, M. Saleem¹¹³,
 D. Salek¹⁰⁷, P.H. Sales De Bruin¹³⁹, D. Salihagic¹⁰¹, A. Salnikov¹⁴⁴, J. Salt¹⁶⁸,
 D. Salvatore^{37a,37b}, F. Salvatore¹⁵⁰, A. Salvucci¹⁰⁶, A. Salzburger³⁰, D. Sampsonidis¹⁵⁵,
 A. Sanchez^{104a,104b}, J. Sánchez¹⁶⁸, V. Sanchez Martinez¹⁶⁸, H. Sandaker¹⁴,
 R.L. Sandbach⁷⁶, H.G. Sander⁸³, M.P. Sanders¹⁰⁰, M. Sandhoff¹⁷⁶, T. Sandoval²⁸,
 C. Sandoval¹⁶³, R. Sandstroem¹⁰¹, D.P.C. Sankey¹³¹, A. Sansoni⁴⁷, C. Santoni³⁴,
 R. Santonico^{134a,134b}, H. Santos^{126a}, I. Santoyo Castillo¹⁵⁰, K. Sapp¹²⁵, A. Saponov⁶⁵,
 J.G. Saraiva^{126a,126d}, B. Sarrazin²¹, G. Sartiso¹⁷⁶, O. Sasaki⁶⁶, Y. Sasaki¹⁵⁶,
 G. Sauvage^{5,*}, E. Sauvan⁵, P. Savard^{159,e}, D.O. Savu³⁰, C. Sawyer¹²⁰, L. Sawyer^{79,m},
 D.H. Saxon⁵³, J. Saxon¹²², C. Sbarra^{20a}, A. Sbrizzi^{20a,20b}, T. Scanlon⁷⁸,
 D.A. Scannicchio¹⁶⁴, M. Scarcella¹⁵¹, V. Scarfone^{37a,37b}, J. Schaarschmidt¹⁷³,
 P. Schacht¹⁰¹, D. Schaefer³⁰, R. Schaefer⁴², S. Schaepe²¹, S. Schaetzel^{58b}, U. Schäfer⁸³,
 A.C. Schaffer¹¹⁷, D. Schaile¹⁰⁰, R.D. Schamberger¹⁴⁹, V. Scharf^{58a}, V.A. Schegelsky¹²³,
 D. Scheirich¹²⁹, M. Schernau¹⁶⁴, M.I. Scherzer³⁵, C. Schiavi^{50a,50b}, J. Schieck¹⁰⁰,
 C. Schillo⁴⁸, M. Schioppa^{37a,37b}, S. Schlenker³⁰, E. Schmidt⁴⁸, K. Schmieden³⁰,
 C. Schmitt⁸³, S. Schmitt^{58b}, B. Schneider¹⁷, Y.J. Schnellbach⁷⁴, U. Schnoor⁴⁴,
 L. Schoeffel¹³⁷, A. Schoening^{58b}, B.D. Schoenrock⁹⁰, A.L.S. Schorlemmer⁵⁴, M. Schott⁸³,
 D. Schouten^{160a}, J. Schovancova²⁵, S. Schramm¹⁵⁹, M. Schreyer¹⁷⁵, C. Schroeder⁸³,
 N. Schuh⁸³, M.J. Schultens²¹, H.-C. Schultz-Coulon^{58a}, H. Schulz¹⁶, M. Schumacher⁴⁸,

B.A. Schumm¹³⁸, Ph. Schune¹³⁷, C. Schwanenberger⁸⁴, A. Schwartzman¹⁴⁴,
 T.A. Schwarz⁸⁹, Ph. Schwegler¹⁰¹, Ph. Schwemling¹³⁷, R. Schwienhorst⁹⁰,
 J. Schwindling¹³⁷, T. Schwindt²¹, M. Schwoerer⁵, F.G. Sciacca¹⁷, E. Scifo¹¹⁷, G. Sciolla²³,
 F. Scuri^{124a,124b}, F. Scutti²¹, J. Searcy⁸⁹, G. Sedov⁴², E. Sedykh¹²³, P. Seema²¹,
 S.C. Seidel¹⁰⁵, A. Seiden¹³⁸, F. Seifert¹²⁸, J.M. Seixas^{24a}, G. Sekhniaidze^{104a},
 S.J. Sekula⁴⁰, K.E. Selbach⁴⁶, D.M. Seliverstov^{123,*}, G. Sellers⁷⁴,
 N. Semprini-Cesari^{20a,20b}, C. Serfon³⁰, L. Serin¹¹⁷, L. Serkin⁵⁴, T. Serre⁸⁵, R. Seuster^{160a},
 H. Severini¹¹³, T. Sfiligoj⁷⁵, F. Sforza¹⁰¹, A. Sfyrla³⁰, E. Shabalina⁵⁴, M. Shamim¹¹⁶,
 L.Y. Shan^{33a}, R. Shang¹⁶⁶, J.T. Shank²², M. Shapiro¹⁵, P.B. Shatalov⁹⁷, K. Shaw^{165a,165b},
 C.Y. Shehu¹⁵⁰, P. Sherwood⁷⁸, L. Shi^{152,ad}, S. Shimizu⁶⁷, C.O. Shimmin¹⁶⁴,
 M. Shimojima¹⁰², M. Shiyakova⁶⁵, A. Shmeleva⁹⁶, D. Shoaleh Saadi⁹⁵, M.J. Shochet³¹,
 D. Short¹²⁰, S. Shrestha⁶⁴, E. Shulga⁹⁸, M.A. Shupe⁷, S. Shushkevich⁴², P. Sicho¹²⁷,
 O. Sidiropoulou¹⁵⁵, D. Sidorov¹¹⁴, A. Sidoti^{133a}, F. Siegert⁴⁴, Dj. Sijacki^{13a},
 J. Silva^{126a,126d}, Y. Silver¹⁵⁴, D. Silverstein¹⁴⁴, S.B. Silverstein^{147a}, V. Simak¹²⁸,
 O. Simard⁵, Lj. Simic^{13a}, S. Simion¹¹⁷, E. Simioni⁸³, B. Simmons⁷⁸, D. Simon³⁴,
 R. Simoniello^{91a,91b}, P. Sinervo¹⁵⁹, N.B. Sinev¹¹⁶, G. Siragusa¹⁷⁵, A. Sircar⁷⁹,
 A.N. Sisakyan^{65,*}, S.Yu. Sivoklokov⁹⁹, J. Sjölin^{147a,147b}, T.B. Sjursen¹⁴, H.P. Skottowe⁵⁷,
 P. Skubic¹¹³, M. Slater¹⁸, T. Slavicek¹²⁸, M. Slawinska¹⁰⁷, K. Sliwa¹⁶², V. Smakhtin¹⁷³,
 B.H. Smart⁴⁶, L. Smestad¹⁴, S.Yu. Smirnov⁹⁸, Y. Smirnov⁹⁸, L.N. Smirnova^{99,ae},
 O. Smirnova⁸¹, K.M. Smith⁵³, M. Smizanska⁷², K. Smolek¹²⁸, A.A. Snesarev⁹⁶,
 G. Snidero⁷⁶, S. Snyder²⁵, R. Sobie^{170,j}, F. Socher⁴⁴, A. Soffer¹⁵⁴, D.A. Soh^{152,ad},
 C.A. Solans³⁰, M. Solar¹²⁸, J. Solc¹²⁸, E.Yu. Soldatov⁹⁸, U. Soldevila¹⁶⁸,
 A.A. Solodkov¹³⁰, A. Soloshenko⁶⁵, O.V. Solovyanov¹³⁰, V. Solovyev¹²³, P. Sommer⁴⁸,
 H.Y. Song^{33b}, N. Soni¹, A. Sood¹⁵, A. Sopczak¹²⁸, B. Sopko¹²⁸, V. Sopko¹²⁸, V. Sorin¹²,
 M. Sosebee⁸, R. Soualah^{165a,165c}, P. Soueid⁹⁵, A.M. Soukharev^{109,c}, D. South⁴²,
 S. Spagnolo^{73a,73b}, F. Spanò⁷⁷, W.R. Spearman⁵⁷, F. Spettel¹⁰¹, R. Spighi^{20a}, G. Spigo³⁰,
 L.A. Spiller⁸⁸, M. Spousta¹²⁹, T. Spreitzer¹⁵⁹, R.D. St. Denis^{53,*}, S. Staerz⁴⁴,
 J. Stahlman¹²², R. Stamen^{58a}, S. Stamm¹⁶, E. Stanecka³⁹, R.W. Stanek⁶, C. Stanescu^{135a},
 M. Stanescu-Bellu⁴², M.M. Stanitzki⁴², S. Stapnes¹¹⁹, E.A. Starchenko¹³⁰, J. Stark⁵⁵,
 P. Staroba¹²⁷, P. Starovoitov⁴², R. Staszewski³⁹, P. Stavina^{145a,*}, P. Steinberg²⁵,
 B. Stelzer¹⁴³, H.J. Stelzer³⁰, O. Stelzer-Chilton^{160a}, H. Stenzel⁵², S. Stern¹⁰¹,
 G.A. Stewart⁵³, J.A. Stillings²¹, M.C. Stockton⁸⁷, M. Stoebe⁸⁷, G. Stoicea^{26a}, P. Stolte⁵⁴,
 S. Stonjek¹⁰¹, A.R. Stradling⁸, A. Straessner⁴⁴, M.E. Stramaglia¹⁷, J. Strandberg¹⁴⁸,
 S. Strandberg^{147a,147b}, A. Strandlie¹¹⁹, E. Strauss¹⁴⁴, M. Strauss¹¹³, P. Strizenec^{145b},
 R. Ströhmer¹⁷⁵, D.M. Strom¹¹⁶, R. Stroynowski⁴⁰, A. Strubig¹⁰⁶, S.A. Stucci¹⁷,
 B. Stugu¹⁴, N.A. Styles⁴², D. Su¹⁴⁴, J. Su¹²⁵, R. Subramaniam⁷⁹, A. Succurro¹²,
 Y. Sugaya¹¹⁸, C. Suhr¹⁰⁸, M. Suk¹²⁸, V.V. Sulin⁹⁶, S. Sultansoy^{4d}, T. Sumida⁶⁸, S. Sun⁵⁷,
 X. Sun^{33a}, J.E. Sundermann⁴⁸, K. Suruliz¹⁵⁰, G. Susinno^{37a,37b}, M.R. Sutton¹⁵⁰,
 Y. Suzuki⁶⁶, M. Svatos¹²⁷, S. Swedish¹⁶⁹, M. Swiatlowski¹⁴⁴, I. Sykora^{145a}, T. Sykora¹²⁹,
 D. Ta⁹⁰, C. Taccini^{135a,135b}, K. Tackmann⁴², J. Taenzer¹⁵⁹, A. Taffard¹⁶⁴, R. Tafirout^{160a},
 N. Taiblum¹⁵⁴, H. Takai²⁵, R. Takashima⁶⁹, H. Takeda⁶⁷, T. Takeshita¹⁴¹, Y. Takubo⁶⁶,
 M. Talby⁸⁵, A.A. Talyshev^{109,c}, J.Y.C. Tam¹⁷⁵, K.G. Tan⁸⁸, J. Tanaka¹⁵⁶, R. Tanaka¹¹⁷,
 S. Tanaka¹³², S. Tanaka⁶⁶, A.J. Tanasijczuk¹⁴³, B.B. Tannenwald¹¹¹, N. Tannoury²¹,

S. Tapprogge⁸³, S. Tarem¹⁵³, F. Tarrade²⁹, G.F. Tartarelli^{91a}, P. Tas¹²⁹, M. Tasevsky¹²⁷,
 T. Tashiro⁶⁸, E. Tassi^{37a,37b}, A. Tavares Delgado^{126a,126b}, Y. Tayalati^{136d}, F.E. Taylor⁹⁴,
 G.N. Taylor⁸⁸, W. Taylor^{160b}, F.A. Teischinger³⁰, M. Teixeira Dias Castanheira⁷⁶,
 P. Teixeira-Dias⁷⁷, K.K. Temming⁴⁸, H. Ten Kate³⁰, P.K. Teng¹⁵², J.J. Teoh¹¹⁸,
 S. Terada⁶⁶, K. Terashi¹⁵⁶, J. Terron⁸², S. Terzo¹⁰¹, M. Testa⁴⁷, R.J. Teuscher^{159,j},
 J. Therhaag²¹, T. Theveneaux-Pelzer³⁴, J.P. Thomas¹⁸, J. Thomas-Wilsker⁷⁷,
 E.N. Thompson³⁵, P.D. Thompson¹⁸, P.D. Thompson¹⁵⁹, R.J. Thompson⁸⁴,
 A.S. Thompson⁵³, L.A. Thomsen³⁶, E. Thomson¹²², M. Thomson²⁸, W.M. Thong⁸⁸,
 R.P. Thun^{89,*}, F. Tian³⁵, M.J. Tibbetts¹⁵, V.O. Tikhomirov^{96,af}, Yu.A. Tikhonov^{109,c},
 S. Timoshenko⁹⁸, E. Tiouchichine⁸⁵, P. Tipton¹⁷⁷, S. Tisserant⁸⁵, T. Todorov⁵,
 S. Todorova-Nova¹²⁹, J. Tojo⁷⁰, S. Tokár^{145a}, K. Tokushuku⁶⁶, K. Tollefson⁹⁰, E. Tolley⁵⁷,
 L. Tomlinson⁸⁴, M. Tomoto¹⁰³, L. Tompkins³¹, K. Toms¹⁰⁵, N.D. Topilin⁶⁵,
 E. Torrence¹¹⁶, H. Torres¹⁴³, E. Torró Pastor¹⁶⁸, J. Toth^{85,ag}, F. Touchard⁸⁵,
 D.R. Tovey¹⁴⁰, H.L. Tran¹¹⁷, T. Trefzger¹⁷⁵, L. Tremblet³⁰, A. Tricoli³⁰, I.M. Trigger^{160a},
 S. Trincaz-Duvoid⁸⁰, M.F. Tripiana¹², W. Trischuk¹⁵⁹, B. Trocmé⁵⁵, C. Troncon^{91a},
 M. Trottier-McDonald¹⁵, M. Trovatelli^{135a,135b}, P. True⁹⁰, M. Trzebinski³⁹, A. Trzupke³⁹,
 C. Tsarouchas³⁰, J.C-L. Tseng¹²⁰, P.V. Tsiarehka⁹², D. Tsiou¹³⁷, G. Tsipolitis¹⁰,
 N. Tsirintanis⁹, S. Tsiskaridze¹², V. Tsiskaridze⁴⁸, E.G. Tskhadadze^{51a}, I.I. Tsukerman⁹⁷,
 V. Tsulaia¹⁵, S. Tsuno⁶⁶, D. Tsybychev¹⁴⁹, A. Tudorache^{26a}, V. Tudorache^{26a},
 A.N. Tuna¹²², S.A. Tupputi^{20a,20b}, S. Turchikhin^{99,ae}, D. Turecek¹²⁸, I. Turk Cakir^{4c},
 R. Turra^{91a,91b}, A.J. Turvey⁴⁰, P.M. Tuts³⁵, A. Tykhonov⁴⁹, M. Tylmad^{147a,147b},
 M. Tyndel¹³¹, K. Uchida²¹, I. Ueda¹⁵⁶, R. Ueno²⁹, M. Ughetto⁸⁵, M. Ugland¹⁴,
 M. Uhlenbrock²¹, F. Ukegawa¹⁶¹, G. Unal³⁰, A. Undrus²⁵, G. Unel¹⁶⁴, F.C. Ungaro⁴⁸,
 Y. Unno⁶⁶, C. Unverdorben¹⁰⁰, J. Urban^{145b}, D. Urbaniec³⁵, P. Urquijo⁸⁸, G. Usai⁸,
 A. Usanova⁶², L. Vacavant⁸⁵, V. Vacek¹²⁸, B. Vachon⁸⁷, N. Valencic¹⁰⁷,
 S. Valentineti^{20a,20b}, A. Valero¹⁶⁸, L. Valery³⁴, S. Valkar¹²⁹, E. Valladolid Gallego¹⁶⁸,
 S. Vallecorsa⁴⁹, J.A. Valls Ferrer¹⁶⁸, W. Van Den Wollenberg¹⁰⁷, P.C. Van Der Deijl¹⁰⁷,
 R. van der Geer¹⁰⁷, H. van der Graaf¹⁰⁷, R. Van Der Leeuw¹⁰⁷, D. van der Ster³⁰,
 N. van Eldik³⁰, P. van Gemmeren⁶, J. Van Nieuwkoop¹⁴³, I. van Vulpen¹⁰⁷,
 M.C. van Woerden³⁰, M. Vanadia^{133a,133b}, W. Vandelli³⁰, R. Vanguri¹²², A. Vaniachine⁶,
 P. Vankov⁴², F. Vannucci⁸⁰, G. Vardanyan¹⁷⁸, R. Vari^{133a}, E.W. Varnes⁷, T. Varol⁸⁶,
 D. Varouchas⁸⁰, A. Vartapetian⁸, K.E. Varvell¹⁵¹, F. Vazeille³⁴, T. Vazquez Schroeder⁵⁴,
 J. Veatch⁷, F. Veloso^{126a,126c}, T. Velz²¹, S. Veneziano^{133a}, A. Ventura^{73a,73b}, D. Ventura⁸⁶,
 M. Venturi¹⁷⁰, N. Venturi¹⁵⁹, A. Venturini²³, V. Vercesi^{121a}, M. Verducci^{133a,133b},
 W. Verkerke¹⁰⁷, J.C. Vermeulen¹⁰⁷, A. Vest⁴⁴, M.C. Vetterli^{143,e}, O. Viazlo⁸¹,
 I. Vichou¹⁶⁶, T. Vickey^{146c,ah}, O.E. Vickey Boeriu^{146c}, G.H.A. Viehhauser¹²⁰, S. Viel¹⁶⁹,
 R. Vigne³⁰, M. Villa^{20a,20b}, M. Villaplana Perez^{91a,91b}, E. Vilucchi⁴⁷, M.G. Vincter²⁹,
 V.B. Vinogradov⁶⁵, J. Virzi¹⁵, I. Vivarelli¹⁵⁰, F. Vives Vaque³, S. Vlachos¹⁰,
 D. Vladoiu¹⁰⁰, M. Vlasak¹²⁸, A. Vogel²¹, M. Vogel^{32a}, P. Vokac¹²⁸, G. Volpi^{124a,124b},
 M. Volpi⁸⁸, H. von der Schmitt¹⁰¹, H. von Radziewski⁴⁸, E. von Toerne²¹, V. Vorobel¹²⁹,
 K. Vorobev⁹⁸, M. Vos¹⁶⁸, R. Voss³⁰, J.H. Vosseveld⁷⁴, N. Vranjes¹³⁷,
 M. Vranjes Milosavljevic^{13a}, V. Vrba¹²⁷, M. Vreeswijk¹⁰⁷, T. Vu Anh⁴⁸, R. Vuillermet³⁰,
 I. Vukotic³¹, Z. Vykydal¹²⁸, P. Wagner²¹, W. Wagner¹⁷⁶, H. Wahlberg⁷¹, S. Wahrmund⁴⁴,

J. Wakabayashi¹⁰³, J. Walder⁷², R. Walker¹⁰⁰, W. Walkowiak¹⁴², R. Wall¹⁷⁷, P. Waller⁷⁴, B. Walsh¹⁷⁷, C. Wang^{152,ai}, C. Wang⁴⁵, F. Wang¹⁷⁴, H. Wang¹⁵, H. Wang⁴⁰, J. Wang⁴², J. Wang^{33a}, K. Wang⁸⁷, R. Wang¹⁰⁵, S.M. Wang¹⁵², T. Wang²¹, X. Wang¹⁷⁷, C. Wanotayaroj¹¹⁶, A. Warburton⁸⁷, C.P. Ward²⁸, D.R. Wardrope⁷⁸, M. Warsinsky⁴⁸, A. Washbrook⁴⁶, C. Wasicki⁴², P.M. Watkins¹⁸, A.T. Watson¹⁸, I.J. Watson¹⁵¹, M.F. Watson¹⁸, G. Watts¹³⁹, S. Watts⁸⁴, B.M. Waugh⁷⁸, S. Webb⁸⁴, M.S. Weber¹⁷, S.W. Weber¹⁷⁵, J.S. Webster³¹, A.R. Weidberg¹²⁰, B. Weinert⁶¹, J. Weingarten⁵⁴, C. Weiser⁴⁸, H. Weits¹⁰⁷, P.S. Wells³⁰, T. Wenaus²⁵, D. Wendland¹⁶, Z. Weng^{152,ad}, T. Wengler³⁰, S. Wenig³⁰, N. Vermes²¹, M. Werner⁴⁸, P. Werner³⁰, M. Wessels^{58a}, J. Wetter¹⁶², K. Whalen²⁹, A. White⁸, M.J. White¹, R. White^{32b}, S. White^{124a,124b}, D. Whiteson¹⁶⁴, D. Wicke¹⁷⁶, F.J. Wickens¹³¹, W. Wiedenmann¹⁷⁴, M. Wielers¹³¹, P. Wienemann²¹, C. Wiglesworth³⁶, L.A.M. Wiik-Fuchs²¹, P.A. Wijeratne⁷⁸, A. Wildauer¹⁰¹, M.A. Wildt^{42,aj}, H.G. Wilkens³⁰, H.H. Williams¹²², S. Williams²⁸, C. Willis⁹⁰, S. Willocq⁸⁶, A. Wilson⁸⁹, J.A. Wilson¹⁸, I. Wingerter-Seez⁵, F. Winklmeier¹¹⁶, B.T. Winter²¹, M. Wittgen¹⁴⁴, T. Wittig⁴³, J. Wittkowski¹⁰⁰, S.J. Wollstadt⁸³, M.W. Wolter³⁹, H. Wolters^{126a,126c}, B.K. Wosiek³⁹, J. Wotschack³⁰, M.J. Woudstra⁸⁴, K.W. Wozniak³⁹, M. Wright⁵³, M. Wu⁵⁵, S.L. Wu¹⁷⁴, X. Wu⁴⁹, Y. Wu⁸⁹, E. Wulf³⁵, T.R. Wyatt⁸⁴, B.M. Wynne⁴⁶, S. Xella³⁶, M. Xiao¹³⁷, D. Xu^{33a}, L. Xu^{33b,ak}, B. Yabsley¹⁵¹, S. Yacoob^{146b,al}, R. Yakabe⁶⁷, M. Yamada⁶⁶, H. Yamaguchi¹⁵⁶, Y. Yamaguchi¹¹⁸, A. Yamamoto⁶⁶, S. Yamamoto¹⁵⁶, T. Yamamura¹⁵⁶, T. Yamanaka¹⁵⁶, K. Yamauchi¹⁰³, Y. Yamazaki⁶⁷, Z. Yan²², H. Yang^{33e}, H. Yang¹⁷⁴, Y. Yang¹¹¹, S. Yanush⁹³, L. Yao^{33a}, W.-M. Yao¹⁵, Y. Yasu⁶⁶, E. Yatsenko⁴², K.H. Yau Wong²¹, J. Ye⁴⁰, S. Ye²⁵, I. Yeletsikh⁶⁵, A.L. Yen⁵⁷, E. Yildirim⁴², M. Yilmaz^{4b}, R. Yoosoofmiya¹²⁵, K. Yorita¹⁷², R. Yoshida⁶, K. Yoshihara¹⁵⁶, C. Young¹⁴⁴, C.J.S. Young³⁰, S. Youssef²², D.R. Yu¹⁵, J. Yu⁸, J.M. Yu⁸⁹, J. Yu¹¹⁴, L. Yuan⁶⁷, A. Yurkewicz¹⁰⁸, I. Yusuf^{28,am}, B. Zabinski³⁹, R. Zaidan⁶³, A.M. Zaitsev^{130,z}, A. Zaman¹⁴⁹, S. Zambito²³, L. Zanello^{133a,133b}, D. Zanzi⁸⁸, C. Zeitnitz¹⁷⁶, M. Zeman¹²⁸, A. Zemla^{38a}, K. Zengel²³, O. Zenin¹³⁰, T. Ženiš^{145a}, D. Zerwas¹¹⁷, G. Zevi della Porta⁵⁷, D. Zhang⁸⁹, F. Zhang¹⁷⁴, H. Zhang⁹⁰, J. Zhang⁶, L. Zhang¹⁵², R. Zhang^{33b}, X. Zhang^{33d}, Z. Zhang¹¹⁷, Y. Zhao^{33d}, Z. Zhao^{33b}, A. Zhemchugov⁶⁵, J. Zhong¹²⁰, B. Zhou⁸⁹, L. Zhou³⁵, N. Zhou¹⁶⁴, C.G. Zhu^{33d}, H. Zhu^{33a}, J. Zhu⁸⁹, Y. Zhu^{33b}, X. Zhuang^{33a}, K. Zhukov⁹⁶, A. Zibell¹⁷⁵, D. Zieminska⁶¹, N.I. Zimine⁶⁵, C. Zimmermann⁸³, R. Zimmermann²¹, S. Zimmermann²¹, S. Zimmermann⁴⁸, Z. Zinonos⁵⁴, M. Ziolkowski¹⁴², G. Zobernig¹⁷⁴, A. Zoccoli^{20a,20b}, M. zur Nedden¹⁶, G. Zurzolo^{104a,104b}, V. Zutshi¹⁰⁸, L. Zwalinski³⁰.

¹ Department of Physics, University of Adelaide, Adelaide, Australia

² Physics Department, SUNY Albany, Albany NY, United States of America

³ Department of Physics, University of Alberta, Edmonton AB, Canada

⁴ (a) Department of Physics, Ankara University, Ankara; (b) Department of Physics, Gazi University, Ankara; (c) Istanbul Aydin University, Istanbul; (d) Division of Physics, TOBB University of Economics and Technology, Ankara, Turkey

⁵ LAPP, CNRS/IN2P3 and Université de Savoie, Annecy-le-Vieux, France

⁶ High Energy Physics Division, Argonne National Laboratory, Argonne IL, United States

of America

⁷ Department of Physics, University of Arizona, Tucson AZ, United States of America

⁸ Department of Physics, The University of Texas at Arlington, Arlington TX, United States of America

⁹ Physics Department, University of Athens, Athens, Greece

¹⁰ Physics Department, National Technical University of Athens, Zografou, Greece

¹¹ Institute of Physics, Azerbaijan Academy of Sciences, Baku, Azerbaijan

¹² Institut de Física d'Altes Energies and Departament de Física de la Universitat Autònoma de Barcelona, Barcelona, Spain

¹³ ^(a) Institute of Physics, University of Belgrade, Belgrade; ^(b) Vinca Institute of Nuclear Sciences, University of Belgrade, Belgrade, Serbia

¹⁴ Department for Physics and Technology, University of Bergen, Bergen, Norway

¹⁵ Physics Division, Lawrence Berkeley National Laboratory and University of California, Berkeley CA, United States of America

¹⁶ Department of Physics, Humboldt University, Berlin, Germany

¹⁷ Albert Einstein Center for Fundamental Physics and Laboratory for High Energy Physics, University of Bern, Bern, Switzerland

¹⁸ School of Physics and Astronomy, University of Birmingham, Birmingham, United Kingdom

¹⁹ ^(a) Department of Physics, Bogazici University, Istanbul; ^(b) Department of Physics, Dogus University, Istanbul; ^(c) Department of Physics Engineering, Gaziantep University, Gaziantep, Turkey

²⁰ ^(a) INFN Sezione di Bologna; ^(b) Dipartimento di Fisica e Astronomia, Università di Bologna, Bologna, Italy

²¹ Physikalisches Institut, University of Bonn, Bonn, Germany

²² Department of Physics, Boston University, Boston MA, United States of America

²³ Department of Physics, Brandeis University, Waltham MA, United States of America

²⁴ ^(a) Universidade Federal do Rio De Janeiro COPPE/EE/IF, Rio de Janeiro; ^(b) Electrical Circuits Department, Federal University of Juiz de Fora (UFJF), Juiz de Fora; ^(c) Federal University of Sao Joao del Rei (UFSJ), Sao Joao del Rei; ^(d) Instituto de Física, Universidade de Sao Paulo, Sao Paulo, Brazil

²⁵ Physics Department, Brookhaven National Laboratory, Upton NY, United States of America

²⁶ ^(a) National Institute of Physics and Nuclear Engineering, Bucharest; ^(b) National Institute for Research and Development of Isotopic and Molecular Technologies, Physics Department, Cluj Napoca; ^(c) University Politehnica Bucharest, Bucharest; ^(d) West University in Timisoara, Timisoara, Romania

²⁷ Departamento de Física, Universidad de Buenos Aires, Buenos Aires, Argentina

²⁸ Cavendish Laboratory, University of Cambridge, Cambridge, United Kingdom

²⁹ Department of Physics, Carleton University, Ottawa ON, Canada

³⁰ CERN, Geneva, Switzerland

³¹ Enrico Fermi Institute, University of Chicago, Chicago IL, United States of America

³² ^(a) Departamento de Física, Pontificia Universidad Católica de Chile, Santiago; ^(b)

Departamento de Física, Universidad Técnica Federico Santa María, Valparaíso, Chile
³³ ^(a) Institute of High Energy Physics, Chinese Academy of Sciences, Beijing; ^(b) Department of Modern Physics, University of Science and Technology of China, Anhui; ^(c) Department of Physics, Nanjing University, Jiangsu; ^(d) School of Physics, Shandong University, Shandong; ^(e) Physics Department, Shanghai Jiao Tong University, Shanghai; ^(f) Physics Department, Tsinghua University, Beijing 100084, China
³⁴ Laboratoire de Physique Corpusculaire, Clermont Université and Université Blaise Pascal and CNRS/IN2P3, Clermont-Ferrand, France
³⁵ Nevis Laboratory, Columbia University, Irvington NY, United States of America
³⁶ Niels Bohr Institute, University of Copenhagen, Kobenhavn, Denmark
³⁷ ^(a) INFN Gruppo Collegato di Cosenza, Laboratori Nazionali di Frascati; ^(b) Dipartimento di Fisica, Università della Calabria, Rende, Italy
³⁸ ^(a) AGH University of Science and Technology, Faculty of Physics and Applied Computer Science, Krakow; ^(b) Marian Smoluchowski Institute of Physics, Jagiellonian University, Krakow, Poland
³⁹ The Henryk Niewodniczanski Institute of Nuclear Physics, Polish Academy of Sciences, Krakow, Poland
⁴⁰ Physics Department, Southern Methodist University, Dallas TX, United States of America
⁴¹ Physics Department, University of Texas at Dallas, Richardson TX, United States of America
⁴² DESY, Hamburg and Zeuthen, Germany
⁴³ Institut für Experimentelle Physik IV, Technische Universität Dortmund, Dortmund, Germany
⁴⁴ Institut für Kern- und Teilchenphysik, Technische Universität Dresden, Dresden, Germany
⁴⁵ Department of Physics, Duke University, Durham NC, United States of America
⁴⁶ SUPA - School of Physics and Astronomy, University of Edinburgh, Edinburgh, United Kingdom
⁴⁷ INFN Laboratori Nazionali di Frascati, Frascati, Italy
⁴⁸ Fakultät für Mathematik und Physik, Albert-Ludwigs-Universität, Freiburg, Germany
⁴⁹ Section de Physique, Université de Genève, Geneva, Switzerland
⁵⁰ ^(a) INFN Sezione di Genova; ^(b) Dipartimento di Fisica, Università di Genova, Genova, Italy
⁵¹ ^(a) E. Andronikashvili Institute of Physics, Iv. Javakhishvili Tbilisi State University, Tbilisi; ^(b) High Energy Physics Institute, Tbilisi State University, Tbilisi, Georgia
⁵² II Physikalisches Institut, Justus-Liebig-Universität Giessen, Giessen, Germany
⁵³ SUPA - School of Physics and Astronomy, University of Glasgow, Glasgow, United Kingdom
⁵⁴ II Physikalisches Institut, Georg-August-Universität, Göttingen, Germany
⁵⁵ Laboratoire de Physique Subatomique et de Cosmologie, Université Grenoble-Alpes, CNRS/IN2P3, Grenoble, France
⁵⁶ Department of Physics, Hampton University, Hampton VA, United States of America

- ⁵⁷ Laboratory for Particle Physics and Cosmology, Harvard University, Cambridge MA, United States of America
- ⁵⁸ ^(a) Kirchhoff-Institut für Physik, Ruprecht-Karls-Universität Heidelberg, Heidelberg; ^(b) Physikalisches Institut, Ruprecht-Karls-Universität Heidelberg, Heidelberg; ^(c) ZITI Institut für technische Informatik, Ruprecht-Karls-Universität Heidelberg, Mannheim, Germany
- ⁵⁹ Faculty of Applied Information Science, Hiroshima Institute of Technology, Hiroshima, Japan
- ⁶⁰ ^(a) Department of Physics, The Chinese University of Hong Kong, Shatin, N.T., Hong Kong; ^(b) Department of Physics, The University of Hong Kong, Hong Kong; ^(c) Department of Physics, The Hong Kong University of Science and Technology, Clear Water Bay, Kowloon, Hong Kong, China
- ⁶¹ Department of Physics, Indiana University, Bloomington IN, United States of America
- ⁶² Institut für Astro- und Teilchenphysik, Leopold-Franzens-Universität, Innsbruck, Austria
- ⁶³ University of Iowa, Iowa City IA, United States of America
- ⁶⁴ Department of Physics and Astronomy, Iowa State University, Ames IA, United States of America
- ⁶⁵ Joint Institute for Nuclear Research, JINR Dubna, Dubna, Russia
- ⁶⁶ KEK, High Energy Accelerator Research Organization, Tsukuba, Japan
- ⁶⁷ Graduate School of Science, Kobe University, Kobe, Japan
- ⁶⁸ Faculty of Science, Kyoto University, Kyoto, Japan
- ⁶⁹ Kyoto University of Education, Kyoto, Japan
- ⁷⁰ Department of Physics, Kyushu University, Fukuoka, Japan
- ⁷¹ Instituto de Física La Plata, Universidad Nacional de La Plata and CONICET, La Plata, Argentina
- ⁷² Physics Department, Lancaster University, Lancaster, United Kingdom
- ⁷³ ^(a) INFN Sezione di Lecce; ^(b) Dipartimento di Matematica e Fisica, Università del Salento, Lecce, Italy
- ⁷⁴ Oliver Lodge Laboratory, University of Liverpool, Liverpool, United Kingdom
- ⁷⁵ Department of Physics, Jožef Stefan Institute and University of Ljubljana, Ljubljana, Slovenia
- ⁷⁶ School of Physics and Astronomy, Queen Mary University of London, London, United Kingdom
- ⁷⁷ Department of Physics, Royal Holloway University of London, Surrey, United Kingdom
- ⁷⁸ Department of Physics and Astronomy, University College London, London, United Kingdom
- ⁷⁹ Louisiana Tech University, Ruston LA, United States of America
- ⁸⁰ Laboratoire de Physique Nucléaire et de Hautes Energies, UPMC and Université Paris-Diderot and CNRS/IN2P3, Paris, France
- ⁸¹ Fysiska institutionen, Lunds universitet, Lund, Sweden
- ⁸² Departamento de Física Teórica C-15, Universidad Autónoma de Madrid, Madrid, Spain

- ⁸³ Institut für Physik, Universität Mainz, Mainz, Germany
- ⁸⁴ School of Physics and Astronomy, University of Manchester, Manchester, United Kingdom
- ⁸⁵ CPPM, Aix-Marseille Université and CNRS/IN2P3, Marseille, France
- ⁸⁶ Department of Physics, University of Massachusetts, Amherst MA, United States of America
- ⁸⁷ Department of Physics, McGill University, Montreal QC, Canada
- ⁸⁸ School of Physics, University of Melbourne, Victoria, Australia
- ⁸⁹ Department of Physics, The University of Michigan, Ann Arbor MI, United States of America
- ⁹⁰ Department of Physics and Astronomy, Michigan State University, East Lansing MI, United States of America
- ⁹¹ ^(a) INFN Sezione di Milano; ^(b) Dipartimento di Fisica, Università di Milano, Milano, Italy
- ⁹² B.I. Stepanov Institute of Physics, National Academy of Sciences of Belarus, Minsk, Republic of Belarus
- ⁹³ National Scientific and Educational Centre for Particle and High Energy Physics, Minsk, Republic of Belarus
- ⁹⁴ Department of Physics, Massachusetts Institute of Technology, Cambridge MA, United States of America
- ⁹⁵ Group of Particle Physics, University of Montreal, Montreal QC, Canada
- ⁹⁶ P.N. Lebedev Institute of Physics, Academy of Sciences, Moscow, Russia
- ⁹⁷ Institute for Theoretical and Experimental Physics (ITEP), Moscow, Russia
- ⁹⁸ National Research Nuclear University MEPhI, Moscow, Russia
- ⁹⁹ D.V.Skobel'tsyn Institute of Nuclear Physics, M.V.Lomonosov Moscow State University, Moscow, Russia
- ¹⁰⁰ Fakultät für Physik, Ludwig-Maximilians-Universität München, München, Germany
- ¹⁰¹ Max-Planck-Institut für Physik (Werner-Heisenberg-Institut), München, Germany
- ¹⁰² Nagasaki Institute of Applied Science, Nagasaki, Japan
- ¹⁰³ Graduate School of Science and Kobayashi-Maskawa Institute, Nagoya University, Nagoya, Japan
- ¹⁰⁴ ^(a) INFN Sezione di Napoli; ^(b) Dipartimento di Fisica, Università di Napoli, Napoli, Italy
- ¹⁰⁵ Department of Physics and Astronomy, University of New Mexico, Albuquerque NM, United States of America
- ¹⁰⁶ Institute for Mathematics, Astrophysics and Particle Physics, Radboud University Nijmegen/Nikhef, Nijmegen, Netherlands
- ¹⁰⁷ Nikhef National Institute for Subatomic Physics and University of Amsterdam, Amsterdam, Netherlands
- ¹⁰⁸ Department of Physics, Northern Illinois University, DeKalb IL, United States of America
- ¹⁰⁹ Budker Institute of Nuclear Physics, SB RAS, Novosibirsk, Russia
- ¹¹⁰ Department of Physics, New York University, New York NY, United States of America

- 111 Ohio State University, Columbus OH, United States of America
- 112 Faculty of Science, Okayama University, Okayama, Japan
- 113 Homer L. Dodge Department of Physics and Astronomy, University of Oklahoma, Norman OK, United States of America
- 114 Department of Physics, Oklahoma State University, Stillwater OK, United States of America
- 115 Palacký University, RCPTM, Olomouc, Czech Republic
- 116 Center for High Energy Physics, University of Oregon, Eugene OR, United States of America
- 117 LAL, Université Paris-Sud and CNRS/IN2P3, Orsay, France
- 118 Graduate School of Science, Osaka University, Osaka, Japan
- 119 Department of Physics, University of Oslo, Oslo, Norway
- 120 Department of Physics, Oxford University, Oxford, United Kingdom
- 121 ^(a) INFN Sezione di Pavia; ^(b) Dipartimento di Fisica, Università di Pavia, Pavia, Italy
- 122 Department of Physics, University of Pennsylvania, Philadelphia PA, United States of America
- 123 Petersburg Nuclear Physics Institute, Gatchina, Russia
- 124 ^(a) INFN Sezione di Pisa; ^(b) Dipartimento di Fisica E. Fermi, Università di Pisa, Pisa, Italy
- 125 Department of Physics and Astronomy, University of Pittsburgh, Pittsburgh PA, United States of America
- 126 ^(a) Laboratório de Instrumentação e Física Experimental de Partículas - LIP, Lisboa; ^(b) Faculdade de Ciências, Universidade de Lisboa, Lisboa; ^(c) Department of Physics, University of Coimbra, Coimbra; ^(d) Centro de Física Nuclear da Universidade de Lisboa, Lisboa; ^(e) Departamento de Física, Universidade do Minho, Braga; ^(f) Departamento de Física Teórica y del Cosmos and CAFPE, Universidad de Granada, Granada (Spain); ^(g) Dep Física and CEFITEC of Faculdade de Ciências e Tecnologia, Universidade Nova de Lisboa, Caparica, Portugal
- 127 Institute of Physics, Academy of Sciences of the Czech Republic, Praha, Czech Republic
- 128 Czech Technical University in Prague, Praha, Czech Republic
- 129 Faculty of Mathematics and Physics, Charles University in Prague, Praha, Czech Republic
- 130 State Research Center Institute for High Energy Physics, Protvino, Russia
- 131 Particle Physics Department, Rutherford Appleton Laboratory, Didcot, United Kingdom
- 132 Ritsumeikan University, Kusatsu, Shiga, Japan
- 133 ^(a) INFN Sezione di Roma; ^(b) Dipartimento di Fisica, Sapienza Università di Roma, Roma, Italy
- 134 ^(a) INFN Sezione di Roma Tor Vergata; ^(b) Dipartimento di Fisica, Università di Roma Tor Vergata, Roma, Italy
- 135 ^(a) INFN Sezione di Roma Tre; ^(b) Dipartimento di Matematica e Fisica, Università Roma Tre, Roma, Italy

- 136 ^(a) Faculté des Sciences Ain Chock, Réseau Universitaire de Physique des Hautes Energies - Université Hassan II, Casablanca; ^(b) Centre National de l'Energie des Sciences Techniques Nucleaires, Rabat; ^(c) Faculté des Sciences Semlalia, Université Cadi Ayyad, LPHEA-Marrakech; ^(d) Faculté des Sciences, Université Mohamed Premier and LPTPM, Oujda; ^(e) Faculté des sciences, Université Mohammed V-Agdal, Rabat, Morocco
- 137 DSM/IRFU (Institut de Recherches sur les Lois Fondamentales de l'Univers), CEA Saclay (Commissariat à l'Energie Atomique et aux Energies Alternatives), Gif-sur-Yvette, France
- 138 Santa Cruz Institute for Particle Physics, University of California Santa Cruz, Santa Cruz CA, United States of America
- 139 Department of Physics, University of Washington, Seattle WA, United States of America
- 140 Department of Physics and Astronomy, University of Sheffield, Sheffield, United Kingdom
- 141 Department of Physics, Shinshu University, Nagano, Japan
- 142 Fachbereich Physik, Universität Siegen, Siegen, Germany
- 143 Department of Physics, Simon Fraser University, Burnaby BC, Canada
- 144 SLAC National Accelerator Laboratory, Stanford CA, United States of America
- 145 ^(a) Faculty of Mathematics, Physics & Informatics, Comenius University, Bratislava; ^(b) Department of Subnuclear Physics, Institute of Experimental Physics of the Slovak Academy of Sciences, Kosice, Slovak Republic
- 146 ^(a) Department of Physics, University of Cape Town, Cape Town; ^(b) Department of Physics, University of Johannesburg, Johannesburg; ^(c) School of Physics, University of the Witwatersrand, Johannesburg, South Africa
- 147 ^(a) Department of Physics, Stockholm University; ^(b) The Oskar Klein Centre, Stockholm, Sweden
- 148 Physics Department, Royal Institute of Technology, Stockholm, Sweden
- 149 Departments of Physics & Astronomy and Chemistry, Stony Brook University, Stony Brook NY, United States of America
- 150 Department of Physics and Astronomy, University of Sussex, Brighton, United Kingdom
- 151 School of Physics, University of Sydney, Sydney, Australia
- 152 Institute of Physics, Academia Sinica, Taipei, Taiwan
- 153 Department of Physics, Technion: Israel Institute of Technology, Haifa, Israel
- 154 Raymond and Beverly Sackler School of Physics and Astronomy, Tel Aviv University, Tel Aviv, Israel
- 155 Department of Physics, Aristotle University of Thessaloniki, Thessaloniki, Greece
- 156 International Center for Elementary Particle Physics and Department of Physics, The University of Tokyo, Tokyo, Japan
- 157 Graduate School of Science and Technology, Tokyo Metropolitan University, Tokyo, Japan
- 158 Department of Physics, Tokyo Institute of Technology, Tokyo, Japan
- 159 Department of Physics, University of Toronto, Toronto ON, Canada

- 160 (a) TRIUMF, Vancouver BC; (b) Department of Physics and Astronomy, York University, Toronto ON, Canada
- 161 Faculty of Pure and Applied Sciences, University of Tsukuba, Tsukuba, Japan
- 162 Department of Physics and Astronomy, Tufts University, Medford MA, United States of America
- 163 Centro de Investigaciones, Universidad Antonio Narino, Bogota, Colombia
- 164 Department of Physics and Astronomy, University of California Irvine, Irvine CA, United States of America
- 165 (a) INFN Gruppo Collegato di Udine, Sezione di Trieste, Udine; (b) ICTP, Trieste; (c) Dipartimento di Chimica, Fisica e Ambiente, Università di Udine, Udine, Italy
- 166 Department of Physics, University of Illinois, Urbana IL, United States of America
- 167 Department of Physics and Astronomy, University of Uppsala, Uppsala, Sweden
- 168 Instituto de Física Corpuscular (IFIC) and Departamento de Física Atómica, Molecular y Nuclear and Departamento de Ingeniería Electrónica and Instituto de Microelectrónica de Barcelona (IMB-CNM), University of Valencia and CSIC, Valencia, Spain
- 169 Department of Physics, University of British Columbia, Vancouver BC, Canada
- 170 Department of Physics and Astronomy, University of Victoria, Victoria BC, Canada
- 171 Department of Physics, University of Warwick, Coventry, United Kingdom
- 172 Waseda University, Tokyo, Japan
- 173 Department of Particle Physics, The Weizmann Institute of Science, Rehovot, Israel
- 174 Department of Physics, University of Wisconsin, Madison WI, United States of America
- 175 Fakultät für Physik und Astronomie, Julius-Maximilians-Universität, Würzburg, Germany
- 176 Fachbereich C Physik, Bergische Universität Wuppertal, Wuppertal, Germany
- 177 Department of Physics, Yale University, New Haven CT, United States of America
- 178 Yerevan Physics Institute, Yerevan, Armenia
- 179 Centre de Calcul de l'Institut National de Physique Nucléaire et de Physique des Particules (IN2P3), Villeurbanne, France
- ^a Also at Department of Physics, King's College London, London, United Kingdom
- ^b Also at Institute of Physics, Azerbaijan Academy of Sciences, Baku, Azerbaijan
- ^c Also at Novosibirsk State University, Novosibirsk, Russia
- ^d Also at Particle Physics Department, Rutherford Appleton Laboratory, Didcot, United Kingdom
- ^e Also at TRIUMF, Vancouver BC, Canada
- ^f Also at Department of Physics, California State University, Fresno CA, United States of America
- ^g Also at Tomsk State University, Tomsk, Russia
- ^h Also at CPPM, Aix-Marseille Université and CNRS/IN2P3, Marseille, France
- ⁱ Also at Università di Napoli Parthenope, Napoli, Italy
- ^j Also at Institute of Particle Physics (IPP), Canada
- ^k Also at Department of Physics, St. Petersburg State Polytechnical University, St.

Petersburg, Russia

^l Also at Department of Financial and Management Engineering, University of the Aegean, Chios, Greece

^m Also at Louisiana Tech University, Ruston LA, United States of America

ⁿ Also at Institutio Catalana de Recerca i Estudis Avancats, ICREA, Barcelona, Spain

^o Also at Department of Physics, The University of Texas at Austin, Austin TX, United States of America

^p Also at Institute of Theoretical Physics, Ilia State University, Tbilisi, Georgia

^q Also at CERN, Geneva, Switzerland

^r Also at O Chadai Academic Production, Ochanomizu University, Tokyo, Japan

^s Also at Manhattan College, New York NY, United States of America

^t Also at Institute of Physics, Academia Sinica, Taipei, Taiwan

^u Also at LAL, Université Paris-Sud and CNRS/IN2P3, Orsay, France

^v Also at Academia Sinica Grid Computing, Institute of Physics, Academia Sinica, Taipei, Taiwan

^w Also at Laboratoire de Physique Nucléaire et de Hautes Energies, UPMC and Université Paris-Diderot and CNRS/IN2P3, Paris, France

^x Also at School of Physical Sciences, National Institute of Science Education and Research, Bhubaneswar, India

^y Also at Dipartimento di Fisica, Sapienza Università di Roma, Roma, Italy

^z Also at Moscow Institute of Physics and Technology State University, Dolgoprudny, Russia

^{aa} Also at Section de Physique, Université de Genève, Geneva, Switzerland

^{ab} Also at International School for Advanced Studies (SISSA), Trieste, Italy

^{ac} Also at Department of Physics and Astronomy, University of South Carolina, Columbia SC, United States of America

^{ad} Also at School of Physics and Engineering, Sun Yat-sen University, Guangzhou, China

^{ae} Also at Faculty of Physics, M.V.Lomonosov Moscow State University, Moscow, Russia

^{af} Also at National Research Nuclear University MEPhI, Moscow, Russia

^{ag} Also at Institute for Particle and Nuclear Physics, Wigner Research Centre for Physics, Budapest, Hungary

^{ah} Also at Department of Physics, Oxford University, Oxford, United Kingdom

^{ai} Also at Department of Physics, Nanjing University, Jiangsu, China

^{aj} Also at Institut für Experimentalphysik, Universität Hamburg, Hamburg, Germany

^{ak} Also at Department of Physics, The University of Michigan, Ann Arbor MI, United States of America

^{al} Also at Discipline of Physics, University of KwaZulu-Natal, Durban, South Africa

^{am} Also at University of Malaya, Department of Physics, Kuala Lumpur, Malaysia

* Deceased